Characterization of recombinant Modified Vaccinia virus Ankara delivering immunomodulatory African swine fever virus proteins

von Lisa Maria Oberberger

Inaugural-Dissertation zur Erlangung der Doktorwürde
der Tierärztlichen Fakultät der Ludwig-Maximilians-Universität
München

Characterization of recombinant Modified Vaccinia virus Ankara delivering immunomodulatory African swine fever virus proteins

von Lisa Maria Oberberger

aus Straubing

München 2024

Aus dem Veterinärwisschenschaftlichen Department der Tierärztlichen

Fakultät der Ludwig-Maximilians-Universität München

Lehrstuhl für Virologie

Arbeit angefertigt unter der Leitung von:

Univ.-Prof. Dr. Markus Meißner

Mitbetreuung durch:

Dr. Robert Fux

Dr. Michael Lehmann

Dekan: Univ.-Prof. Dr. Reinhard K. Straubinger, Ph.D.

Berichterstatter: Univ.-Prof. Dr. Markus Meißner

Korreferent: Priv.-Doz. Karin Weber

Tag der Promotion: 06. Juli 2024

Für Gerti & Benny

Fantasie ist wichtiger als Wissen, denn Wissen ist begrenzt.

Zitat von Albert Einstein

TABLE OF CONTENTS

LIST OF ABBREVIATIONS

ASF	African swine fever
ASFV	African swine fever virus
ASFV-recMVAs	recombinant modified Vaccinia Virus Ankara with insertion of a target gene of African Swine Fever Virus
BSA	bovine serum albumin
CaN	calcineurin phosphatase
CBP	CREB-binding protein
cDNA	complementary DNA
CEF	chicken embryo fibroblasts
cGAMP	cyclic guanosine monophosphate - adenosine
cGAS	Cyclic GMP – AMP synthase
COX2	Cyclooxygenase 2
CVA	Chorioallantoic Vaccinia Virus Ankara
DAPI	4′,6-Diamidin-2-phenylindol
DMEM	Dulbecco´s modified Eagle´s medium
DNA	deoxyribonucleic acid
dsDNA	double-stranded DNA
dsRNA	double-stranded RNA
ED	extracellular domain
eIF2	eukaryotic initiation factor - 2
Endo H	endoglycosidase H
ER	endoplasmic reticulum
EV	enveloped virion
FBS	fetal bovine serum
GAG	glycosaminoglycans
GAPDH	Glyceraldehyde-3-phosphate dehydrogenase
gDNA	genomic deoxyribonucleic acid
GFP	green fluorescent protein
GOI	gene of interest
HAD	hemadsorption
HEK-293T	human embryonic kidney cells
HEK-TLR3	human embryonic kidney cells constitutively expressing
HEPES	N-(2-Hydroxyethyl)-piperazin-N′-(2-ethansulfonsäure)
hpi	hours post infection
HRP	horseradish peroxidase
IEV	immature enveloped virus
IFA	immunofluorescence assay
IFN	Interferon
IFNAR 1/2	Interferon α/β receptor
type I IFNs	Type I interferons

IFN-α	Interferon α
IFN-β	Interferon β
IκB	inhibitor of nuclear factor-kappa B
IKK	inhibitory kappa B kinase
IMV	immature virion
IPAM	immortalized porcine alveolar macrophages
IRF	Interferon regulatory factor
ISGs	Interferon stimulated genes
ISRE	Interferon-sensitive response element
J2 / IPEC-J2	intestinal porcine epihelial cell line – J2 (jejunal)
JAK1	Janus kinase 1
kb	kilobase
kbp	kilobase pair
kDa	kilo-Dalton
mCC	mCherry
LB	lysogeny broth
MDA5	melanoma differentiation-associated gene 5
MEM	minimum essential medium
min	minute
ml	milliliter
mM	milimolar
MOI	multiplicity of infection
MPS	Mononuclear phagocyte system
mRNA	messenger ribonucleic acid
MTOC	microtubule organizing center
MV	mature virion
MVA	Modified Vaccinia Virus Ankara
MyD88	myeloid differentiation primary response protein 88
NF-κB	nuclear factor kappa-light-chain-enhancer of activated B
ng	nanogram
NH/P68	African swine fever virus isolate NH/P68
NIH-3T3	embryonic mouse fibroblast cell line
Nt	N-terminal
PBMCs	peripheral blood mononuclear cells
PBS	phosphate buffered saline
PCR	polymerase chain reaction
PFU	plaque-forming units
p.i.	post infection
pIRF-3	phosphorylated interferon regulatory factor - 3
PK1 / LLC-PK1	pig kidney epithelial cells
PNGase F	Peptide: N-glycosidase F
pp62	polyprotein 62

pp220	polyprotein 220
PRR(s)	pattern recognition receptor(s)
qPCR	quantitative polymerase chain reaction
recMVA	recombinant Modified Vaccinia Virus Ankara
recMVA-A238L	recombinant Modified Vaccinia Virus Ankara expressing the protein A238L of the African Swine Fever Virus
recMVA-CD2v	recombinant Modified Vaccinia Virus Ankara expressing the protein CD2v of the African Swine Fever Virus
recMVA-DP96R	recombinant Modified Vaccinia Virus Ankara expressing the protein DP96R of the African Swine Fever Virus
recMVA-I329L	recombinant Modified Vaccinia Virus Ankara expressing the protein I329L of the African Swine Fever Virus
RIG-I	retinoic acid inducible gene I
RIP1	receptor interacting protein 1
RNA	ribonucleic acid
rpm	revolutions per minute
RPMI	Roswell Park Memorial Institute
SDS-PAGE	sodium dodecyl sulfate polyacrylamide gel electrophoresis
sec	second
STAT1/2	signal transducer and activator of transcription 1/2
STING	stimulator of interferon genes
TAE	Tris-acetate-EDTA
TBK-1	TANK-binding kinase 1
TBS	Tris-buffered saline
$TCID_{50}$	tissue culture infectious dose 50
TIR-domain	Toll/interleukin-1 receptor - domain
TLR	Toll-like receptor
Tm°	melting temperature
TNF	tumor necrosis factor
TRAF	tumor necrosis factor receptor-associated factor
TRIF	TIR-domain-containing adaptor-inducing IFN-β
TYK2	Tyrosine kinase 2
VV	Vaccinia virus
VVA	Vaccinia virus Ankara
WB	Western Blot
3D4/21	porcine alveolar macrophages
μg	microgram

I.   INTRODUCTION

Since decades, African swine fever virus (ASFV) is known as causative pathogen inhibiting the development of a stable pork industry in Africa. Warthogs as well as bushpigs serve as natural reservoir for ASFV infecting the domestic pig population. While natural hosts show an asymptomatic disease progression, domestic pigs and wild boars suffer an acute or peracute disease (Anderson et al., 1998; Mebus, 1988; Parker et al., 1969; Thomson et al., 1980). Due to global trade, African swine fever (ASF) was repeatedly introduced into different countries in the past, but severity of epidemic events reached new levels with the outbreak of African swine fever (ASF) in China, in 2018. With ongoing spread of the disease in European countries, wild boar populations and swine industry were threatened by ASF leading to huge economic loss for pig husbandries worldwide. The absence of a safe vaccine against ASFV limits countermeasures to trade restrictions and slaughter of infected animals, intensifying the economic pressure on pig farmers (Penrith & Vosloo, 2009).

The main problem for the development of safe and protective vaccines against ASFV is the complexity of the virus (Arias et al., 2017; Dixon et al., 2019). ASFV encodes more than 160 different proteins, and the majority of the investigated proteins is expressed to evade the host immune response during infection (Arias et al., 2017). The heterogenicity of the different ASFV genotypes additionally complicates the identification of potential vaccine candidates (Arias et al., 2017).

In this study we asked, whether Modified Vaccinia virus Ankara (MVA) might be an adequate expression vector to analyze ASFV encoded proteins, which may have immunomodulatory properties. Therefore, recombinant MVA viruses (recMVAs) encoding four different ASFV proteins were generated and characterized. Expression of the target proteins was verified in different cell lines and cellular distribution was depicted using a porcine alveolar macrophage cell line (3D4/21). These results constitute MVA as suitable vector to study the expression of ASFV encoded proteins. Moreover, a promising experimental setup was established on 3D4/21 cells, depicting MVA as suitable vector to investigate possible effects of ASFV encoded proteins on Poly(I:C) induced Interferon-β production, prospectively.

II.   LITERATURE REVIEW

1.   African Swine Fever Virus

1.1.   General information, Taxonomy and Epidemiology

ASFV is the only member of the genus Asfivirus, belonging to the family Asfarviridae and the class of Pokkesviricetes, the same class as for Poxviridae. It is the only known DNA arbovirus (arthropode born virus), replicating not only in porcine species, but also in *Ornithodorus* soft ticks. These ticks represent an important viral reservoir and are an integral component of the sylvatic cycle in endemic regions of East Africa. Infected soft ticks transfer ASFV to warthogs (*Phacochoerus africanus*) or bushpigs (*Potamochoerus larvatus*) causing persistent infection without severe clinical manifestation (Dixon et al., 2019; Gaudreault et al., 2020). In contrast, domestic pigs (*Sus scrofa domesticus*) can develop a variety of symptoms, depending on the genotype and virulence of the viral strain as well as on the host susceptibility (Blome et al., 2013; Gaudreault et al., 2020). Therefore, clinical symptoms of ASFV infection in wild boars (*Sus scrofa*) and domestic pigs range from subclinical and chronic manifestations to acute and peracute haemorrhagic disease (Blome et al., 2013; Gabriel et al., 2011; Leitão et al., 2001; Montgomery, 1921).

ASFV is a highly specialized DNA virus, establishing a high viral load in the host blood system (up to 10^9 TCID$_{50}$/ml) (Dixon et al., 2019). Consequently, most efficient way of infection within porcine population is via skin abrasions, cannibalism and feeding of contaminated carcasses or food waste (Fig. 1) (Gaudreault et al., 2020; Guinat et al., 2016; Probst et al., 2017). The high environmental stability of ASFV increases the risk of indirect infection and explains large geographic jumps during outbreaks (Dixon et al., 2019). Transport of chronically or subclinical infected pigs as well as the movement of clinically conspicuous animals enhances the spread of ASF (Gogin et al., 2013; Penrith et al., 2013; Zhou et al., 2018). However, infectious viral particles were detected in body fluids as well as in faeces of viraemic animals enabling transmission of ASFV by direct and indirect contact (Costard et al., 2013; Guinat et al., 2016). The numerous possible infection routes emphasize the global relevance of ASFV and was consistently depicted by outbreaks of the disease in the past.
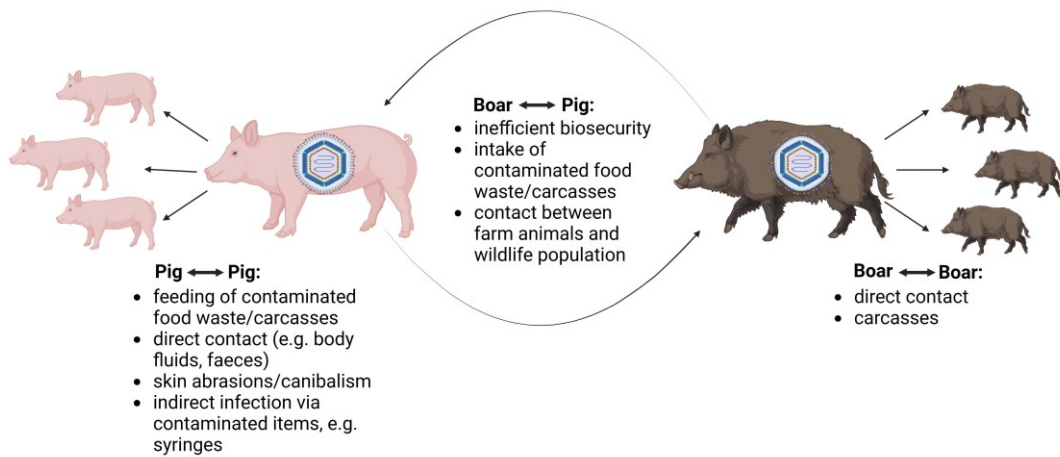
Fig. 1: ASFV infection cycle in Europe and Asia. Due to the high viral load in the bloodstream and in highly perfused organs, ASFV is predominantly transferred via food waste, carcasses, cannibalism and skin abrasions within pig population and wildlife population. Contaminated food waste and carcasses are also high-risk factors for ASFV transfer between domestic pigs and wild boars. Regarding to its global distribution, soft ticks do not account for viral transmission in Europe and Asia at this timepoint. Modified from (Gaudreault et al., 2020). Created with BioRender.com

In 1921, ASF emerged in domestic swine population in Kenya and was described as acute haemorrhagic disease with a mortality rate of 100% (Montgomery, 1921). In the following years ASFV spread over the whole continent. Repeated transmission of ASFV from porcine wildlife population to domestic pigs, inhibits the installation of a solid pork meat industry in Africa (Penrith & Vosloo, 2009). Contaminated food waste from Africa introduced ASF in Portugal in the 1960s, spreading to other European countries (Spain, France, Sardinia, Malta, Belgium, the Netherlands), the Caribbean and parts of South America. Eradication programs were successfully realised and even Sardinia, where ASF was endemic for 40 years, is lately classified as free from genotype I ASFV.

In 2007, ASFV has been reintroduced to Europe, starting in Georgia, spreading to Caucassus region and Russia. For various reasons eradication failed, leading to a massive spread of the disease in Europe in 2014. First cases were reported in Ukraine and Belarus. Estonia, Latvia, Lithuania and Poland followed. In 2018, ASFV arrived in the Czech Republic, Hungary, Romania and Bulgaria. The outbreak achieved its global peak with its spread to China. Since then, the Czech Republic and Belgium were the only countries recording successful eradication. However, Germany registered first cases of ASF in Brandenburg in 2020. Due to the global extent of the outbreak, comprehensive eradication failed. The lack of a protective vaccine led to movement and trade restrictions threatening the global pork meat industry. Cases of ASFV are still recorded in the European Union and

require a political renaissance of disease management.

1.2.   Pathogenesis

ASFV shows a strong tropism towards macrophages and monocytes and is able to replicate in cells of the mononuclear phagocyte system (MPS) (Gómez-Villamandos et al., 2013). In turn, infected macrophages show enhanced cytokine expression further attracting MPS cells and providing additional replication sites for ASFV (Carrasco et al., 2002; Gómez-Villamandos et al., 2013). After viral replication, necrosis is initiated and non-enveloped viral particles are released (Gómez-Villamandos et al., 2013; Gómez-Villamandos et al., 1995a; Sierra et al., 1989). Hemadsorption of erythrocytes to infected cells additionally contributes to rapid primary viremia (Sierra et al., 1991).

During secondary viremia, non-MPS cells, like endothelial cells lymphocytes, platelets and epithelial cells get infected, but additional virus replication is only described in hepatocytes as well as in epithelial cells and mesenchymal cells (Gómez-Villamandos et al., 2013). Massive chemokine expression of infected macrophages leads to apoptosis of non-MPS cells as well as lymphocytes and thrombocytes (Carrasco et al., 1996c; Gómez-Villamandos et al., 1995a; Oura et al., 1998). Extensive apoptosis causes severe lymphopenia, thrombocytopenia as well as endothelial cell damage, depicting bleedings and hemorrhagic lesions in host organs (Blome et al., 2013; Gómez-Villamandos et al., 2013). Though it remains unclear, if the thrombocytopenia is caused by apoptosis and peripheral consumption or by impairment of hematopoiesis (Blome et al., 2013).

Clinical symptoms of ASFV infection are predicated on the described pathological mechanisms. Regarding its various genotypes, moderate and virulent ASFV strains cause peracute or acute disease progression after an incubation time of 2 to 7 days (Mebus, 1988). In acute cases, symptoms may include anorexia, depression, high fever, (bloody) diarrhea, vomiting, respiratory symptoms, cyanosis, reddening of the skin at the acres and the ventral abdomen peaking in animal death 6 to 13 days p.i. (EFSA, 2009). Subacute or chronical infected pigs develop non-specific symptoms like recurring fever, weight loss, retardation of juvenile pigs, increased abortion rate in pregnant sows as well as respiratory symptoms and dyspnoea with a decreased mortality rate (EFSA, 2009).

1.3. Molecular structure and replication cycle

ASFV is a large, icosahedral DNA virus, with a size of more than 200nm. The linear double-stranded DNA is covalently closed by hairpin loops and is organized within a nucleoid together with a poly(A) polymerase and a capping enzyme (Fig. 2), necessary for autonomous early transcription of the virus within the cytoplasm of infected cells (Revilla et al., 2018). This internal core is surrounded by the core shell, mainly consisting of the polyprotein structures of pp220 and pp62 (Andrés et al., 2002; Andrés et al., 1997; Revilla et al., 2018). An inner lipid membrane, derived from the host cell endoplasmic reticulum, lines the viral core and is followed by the capsid giving the characteristic icosahedral appearance of the virions (Andrés et al., 1998). During budding process, the virions receive an outer lipid envelope, consisting of multiple layers containing 68 different viral proteins (Alejo et al., 2018). The functions of these proteins are not fully elucidated, but a protein with the molecular weight of 12kDa mediates virus attachment to the host cell surface (Carrascosa et al., 1991) and CD2v, a homologue to the CD2 T-cell surface antigen, causes hemadsorption to infected cells (Borca et al., 1998; Rodríguez et al., 1993).
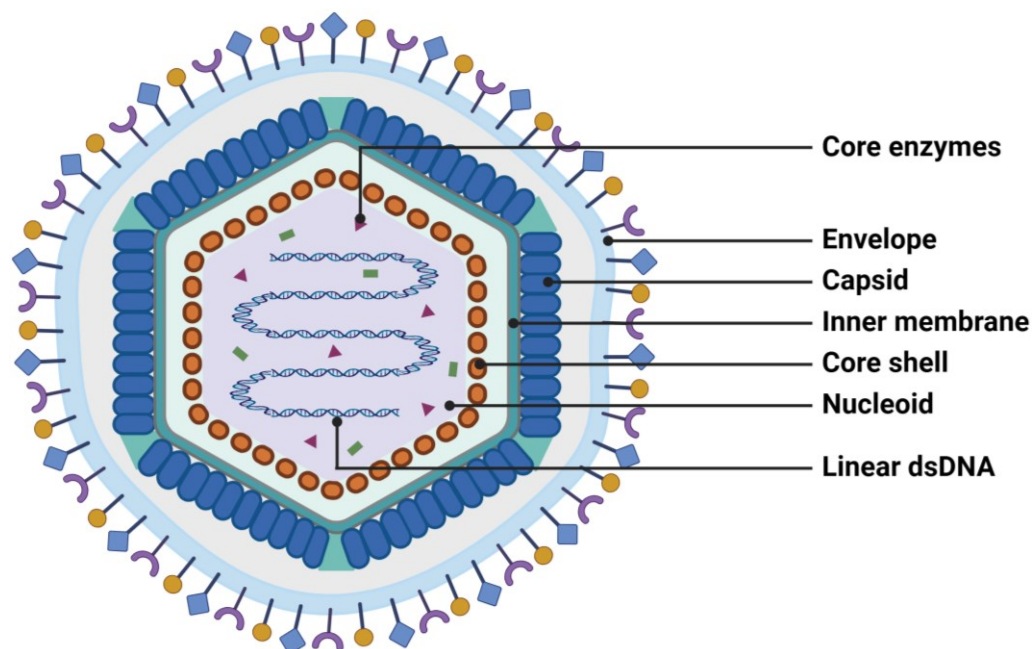

Fig. 2: Scheme of ASFV structure. The linear dsDNA is surrounded by the core shell. The inner membrane is accompanied by the capsid, mainly consisting of the structure protein p72. Modified from (Wang et al., 2021) and modified from the ViralZone, Swiss Institute of Bioinformatics, http://viralzone.expasy.org. Created with BioRender.com

Recently, two major endocytic pathways were identified (Fig. 3), granting the virus versatile cell entry possibilities. On the one hand, receptor dependent entry mechanisms are supported and ASFV is identified to exploit the clathrin-mediated endocytosis mechanism of eucaryotic cells (Galindo et al., 2015; Hernaez & Alonso, 2010). Though exact receptors for virus entry remain unknown. On the other hand, Sanchez et al. reveals that ASFV enters immortalized porcine alveolar macrophages (IPAMS) via macropinocytosis. Therefore, inhibition of macropinocytosis regulators and treatment of IPAMS with specific drugs, resulted in a distinct decrease of ASFV cell entry (Revilla et al., 2018; Sánchez et al., 2012). Each of the entry mechanisms allows ASFV to enter the endosomal pathway and to orchestrate endosomal maturation for capsid disassembly by activation of the PI3-Kinase (PI3K) pathway (Cuesta-Geijo et al., 2012; Galindo & Alonso, 2017; Sánchez et al., 2012). PI3K is essential for endosomal maturation as well as for organization of the endosomal traffic. Through this pathway, ASFV establishes successful early infection and grants the transport of virions to its replication site in the perinuclear area close to the microtubule organizing center (MTOC) (Alonso et al., 2001; Karger et al., 2019). For release of the core particle into the host-cell cytoplasm, the inner envelope of the virion fuses with the endosomal membrane. This process is mediated by the viral envelope protein pE248R that shows sequence homologies with proteins of the poxviral entry/fusion complex (Galindo & Alonso, 2017; Hernáez et al., 2016). After the virion is released into the cytoplasm, the partially uncoated viral particle is able to initiate immediate gene expression by a transcription machinery retained in the inner core (Kuznar et al., 1980; Salas et al., 1983). To enable viral DNA replication as well as intermediate and late gene expression, early genes are encoded within 4-6 hours post infection (Alejo et al., 2018; Cackett et al., 2020; Wang et al., 2021). This mechanism provides autonomous gene expression and mostly independent genome replication in cytoplasmic viral factories, similar to the poxvirus family (Hernaez et al., 2006). However, at an early stage ASFV replicates within the host cell nucleus and viral factories of ASFV require intact and solid microtubule filaments additionally stabilized by hyperacetylation (García-Beato et al., 1992; Quetglas et al., 2012; Rojo et al., 1999; Tabares & Sánchez Botija, 1979). About 12 hours p.i. ASFV exclusively replicates in viral factories, resulting in head-to-head concatemers that are cleaved in one unit length genomes before packaged into virus particles (Dixon et al., 2012; Enjuanes et al., 1976; Rojo et al., 1999). Virions remain in the viral

factory until successful assembly. For migration of mature virions to the plasma membrane of the host cell, the viral membrane protein p54 repeatedly hijacks the microtubule system by direct interaction with the motor protein dynein (Alonso et al., 2001; Jouvenet et al., 2004). At the cell surface ASFV leaves the cell by a budding process, receiving an additional lipid membrane as outer envelope (Breese & DeBoer, 1966). Certainly, budding cannot explain extensive apoptosis of infected cells during ASFV infection (Ramiro-Ibáñez et al., 1996). Therefore, Hernaez et al. depicted apoptotic processes in Vero cells via confocal microscopy resulting in complete cell destruction 18 hours p.i. (Hernaez et al., 2006). This observation outlines an important spreading strategy of ASFV, as both intracellular and extracellular viruses are infectious (Andrés et al., 2001; Galindo & Alonso, 2017).
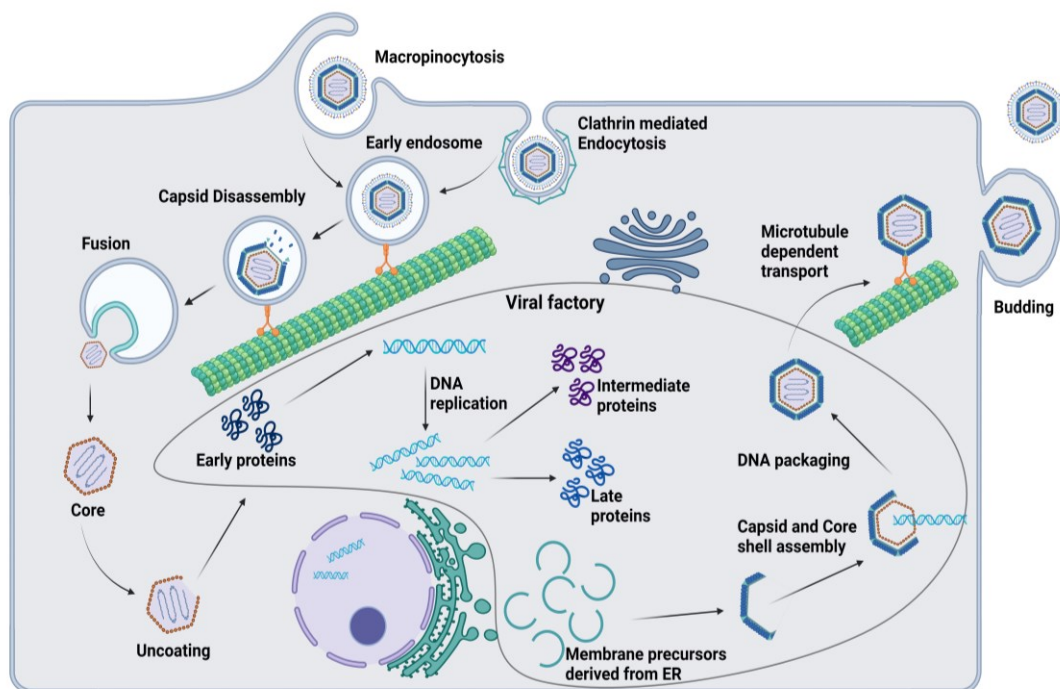
Fig. 3: Replication cycle of ASFV. After virions entered the host cell, the acid environment in endosomes is essential for capsid disassembly. The uncoating process releases immediate and early proteins indispensable for viral DNA replication and is followed by assembly of viral factories. Viral dsDNA and proteins accumulate in the viral factories, enabling assembly of infectious virions. Viral particles migrate along microtubules into cell periphery and are released by budding at the cell surface. Modified from (Galindo & Alonso, 2017; Salas & Andrés, 2013). Created with BioRender.com

2.   Antiviral function of the innate immune system

The innate immune system consists of unspecific humoral and cellular mechanisms against intruding pathogens. Due to its pivotal role, it is localized at vulnerable entry ports of an organism, e.g. the skin or mucosa, to kill invading pathogens at first venue. Simultaneously, it initiates the adaptive immune system for antigen specific defense strategies. Major component of the humoral, antiviral defense mechanism are type I interferons (type I IFNs). Discovered by Isaacs and Lindemann in 1957, type I IFNs represent a large group of secreted cytokines, at which Interferon-α (IFN-α) and Interferon-β (IFN-β) mediate antiviral response in infected cells (Isaacs & Lindenmann, 2015). The IFN-α and IFN-β genes do not exhibit the common exon-intron-structure. In fact, they consist of one exon.

IFN-α comprises several different subtypes regarding to the species. For example, humans express thirteen different IFN-α subtypes, whereas in swine seventeen different subtypes are encoded (Lefevre & La Bonnardiere, 1986; Samuel, 2001; Zanotti et al., 2015). However, for IFN-β only one transcript is described in suidae as well as in humans. Viral infection of human cell lines is associated with elongation of the Poly(A) tail of IFN-β mRNA, resulting in reduced translation of IFN-β (Dehlin et al., 1996; Grafi et al., 1993). Production and secretion of IFN-β is not limited to immune cells. Fibroblasts as well as epithelial cells are capable of IFN-β production and feedback reaction (Kawai & Akira, 2008; McComb et al., 2019). Although activation of IFN-α/β is initiated by various nucleic acid sensing mechanisms (described in chapter *3.1. DNA sensing pathways* and *3.2. RNA sensing pathways*), the downstream transcription factors IFN regulatory factor-3 (IRF-3) and nuclear factor kappa B (NF-κB) coincide between the different pathways (Randall & Goodbourn, 2008). Intensively investigated, it is also known as the classical pathway of IFN-β induction and is further illuminated in the following passages (Haller et al., 2006; Randall & Goodbourn, 2008).

Under physiological conditions NF-κB as well as IRF-3 remain inactive in the cytoplasm. Triggered by an appropriate cell signal, IRF-3 gets phosphorylated (pIRF-3) and undergoes a conformational change, allowing homogenic dimerization and translocation to the nucleus (Dragan et al., 2007; Lin et al., 1998). Phosphorylated IRF-3 plays an indispensable role for induction of IFN-β synthesis, recruiting the transcriptional coactivators p300 and CREB-binding protein in the nucleus (Haller et al., 2006; Hiscott et al., 1999; Lin et al., 1998; Schafer et al.,

1998; Suhara et al., 2002; Wathelet et al., 1998; Yoneyama et al., 1998). Simultaneously, NF-κB migrates into the nucleus, due to disassembly of its natural, cytoplasmic inhibitor (IκB) by proteasomes subsequently to ubiquitination. Although, NF-κB is not essential for IFN-β transcription, it additionally enhances IFN-β production (Ellis & Goodbourn, 1994; Peters et al., 2002).

Secreted IFN-β binds to IFNAR, a specific transmembrane receptor, activating the tyrosine kinases JAK-1 and TYK-2. (Haller et al., 2006; Mogensen et al., 1999; Stark et al., 1998). The kinases phosphorylate the two transcription factors STAT-1 and STAT-2, resulting in heterodimerization and translocation to the nucleus and recruitment of the DNA-binding protein IRF-9 (Haller et al., 2006; Randall & Goodbourn, 2008). This complex is also known as IFN-stimulated gene factor 3 (ISGF-3) that binds to the IFN-stimulated response element (ISRE), enhancing transcription of hundreds of IFN-stimulated genes (ISGs) (de Veer et al., 2001; Der et al., 1998; Frahm et al., 2006; Haller et al., 2006; Randall & Goodbourn, 2008). Most important, initial ISG expression provides the transcription factor IRF-7 essential for IFN-α induction, constituting a switch from "first wave" IFN-β production to predominant IFN-α synthesis (Marié et al., 1998; Sato et al., 1998). Interestingly, both type I IFNs induce the IFNAR pathway via the same receptors, resulting in a positive feedback loop for ISG expression (Mogensen et al., 1999; Sato et al., 1998; Stark et al., 1998). Interplay of the encoded ISGs induces an antiviral state in each cell activated by IFN-α/β, inhibiting establishment of a solid infection in the host organism (Randall & Goodbourn, 2008). Moreover, IFN-α/β are capable to induce a pro-apoptotic state as well as cytosis in infected cells (Clemens, 2003; Maher et al., 2007; Stark et al., 1998). To guarantee recognition of intruding pathogens, eukaryotic cells developed several detection mechanisms. A small selection of nucleic acid sensing strategies is specified in the following chapters.

2.1.   Nucleic acid sensing pathways

Nucleic acid sensing mechanisms are an important tool of the host defense during viral infection. In fact, viruses are reliant to unveil their nucleic acid for transcription as well as for replication in host cells to ensure viral spread and survival. Independent of their genomic identity, viruses can produce double-stranded RNA (dsRNA), a potent inducer of IFN-β production (Marcus, 1983;

Marcus & Sekellick, 1977, 2005). Therefore, detection strategies for double-stranded DNA (dsDNA) as well as dsRNA need to be considered in context with DNA viruses.

2.1.1.   Toll-like receptor 3

Toll-like receptors (TLRs) constitute a family of transmembrane proteins specifically detecting pathogen-associated molecular patterns (PAMPs). They consist of a cytoplasmatic Toll/interleukin-1 receptor (TIR) domain and an extracellular leucin-rich domain, recognizing foreign nucleic acids, lipoproteins, lipopolysaccharides or flagellin (Kawai & Akira, 2008; Moresco et al., 2011). The TIR domain is mainly conserved between the 13 different identified mammalian TLRs and mediates homodimerization as reaction to corresponding ligands (Brikos & O'Neill, 2008; Jin & Lee, 2008). Generated homodimers recruit the downstream adaptor protein MyD88 (myeloid differentiation primary response protein 88) or TRIF (TIR-domain-containing adaptor-inducing IFN-β), depending on the member of the TLR family (Brikos & O'Neill, 2008; Watters et al., 2007). Downstream signaling induces the IFN-α/β pathway as described in chapter 3 *Antiviral function of the innate immune system* (Haller et al., 2006; Randall & Goodbourn, 2008).

TLR3 is expressed in myeloid dendritic cells, macrophages and mast cells, but also in fibroblasts, epithelial cells and neurocytes (Alexopoulou et al., 2001; Cario & Podolsky, 2000; Kulka et al., 2004; Matsumoto et al., 2002; Town et al., 2006). Depending on the cell type, TLR3 is localized in different cell compartments. For example, in macrophages it is associated with lysosomes, whereas in fibroblasts it is attached to the cell surface and endosomes (Fig. 4) (de Bouteiller et al., 2005; Lee et al., 2006; Matsumoto et al., 2002). After dsRNA bound to the TIR domain of TLR3, downstream signaling cascade is initiated by recruiting the cytoplasmic adaptor molecule TRIF (Hoebe et al., 2003; Yamamoto et al., 2003). Subsequent processes contain a complex interplay of different cytoplasmic factors, necessary to activate the two major transcription factors for IFN-β production (as depicted in chapter *3. Antiviral function of the innate immune system*) (Jiang et al., 2004). Therefore, TRIF initiates two distinct pathways by engagement of TRAF6 (tumor necrosis factor receptor-associated factor 6) and RIP1 (receptor interacting protein 1) as well as TRAF3, resulting in recruitment of NF-κB and IRF-3, respectively (Cusson-Hermance et al., 2005; Häcker et al., 2006; Jiang et al., 2004; Meylan et

al., 2004; Oganesyan et al., 2006; Sato et al., 2003).
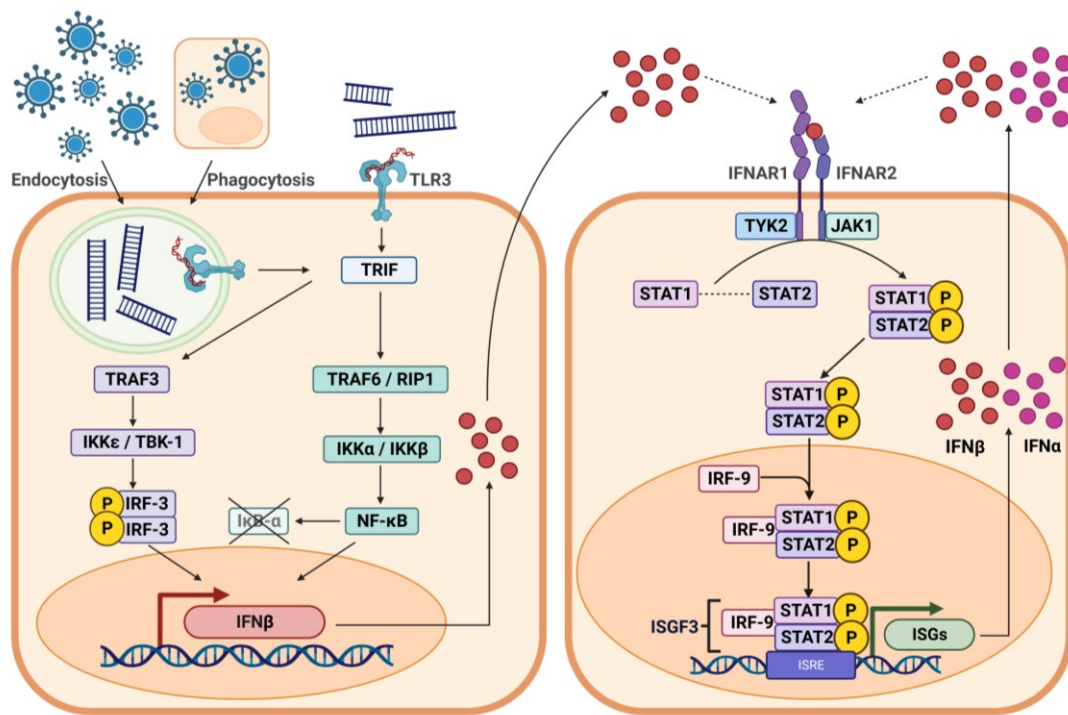
Fig. 4: TLR3 pathway and IFN-β mediated response. Dependent on the cell type, TLR3 is localized at the cell surface as well as in endosomes or lysosomes, detecting dsRNA. Downstream cascade of TLR3 mediates IFN-β production. Secreted IFN-β binds to the IFNAR receptor. Response mechanisms initiate expression of ISGs, which include IFN-α and IFN-β synthesis. Modified from (Haller et al., 2006; Randall & Goodbourn, 2008). Created with BioRender.com

2.1.2.   cGAS-STING

Cytosolic DNA is a potent inducer of IFN-β (Hopfner & Hornung, 2020; Rotem et al., 1963; Stetson & Medzhitov, 2006). The provoked immune response is initiated by the cyclic GMP-AMP synthase (cGAS), constituting another member of the family of pattern recognition receptors (PRRs). Besides its predominant function of pathogen detection, cGAS is verified to initiate signaling upon interaction with intrinsic DNA to guarantee integrity of individual cells in a cell compound (Sun et al., 2013). After DNA is bound to cGAS (Fig. 5), it undergoes a conformational change, enabling production of cyclic GMP-AMP (cGAMP) (Civril et al., 2013; Sun et al., 2013; Wu et al., 2013). The second messenger protein cGAMP activates the cyclic-dinucleotide sensor protein STING (stimulator of interferon genes) (Sun et al., 2013; Wu et al., 2013). STING is a dimeric transmembrane protein, and its inactive form is localized at the endoplasmic reticulum (ER) (Ishikawa & Barber, 2008). The activated adaptor protein migrates from the ER to the Golgi Apparatus.

During translocation, STING interacts with the TANK-binding kinase 1 (TBK1) and the IκB kinase, resulting in phosphorylation of the transcription factors IRF-3 and NF-κB (Ishikawa & Barber, 2008; Liu et al., 2015). Migration of the transcription factors into the nucleus initiates IFN-β production as described in chapter *3. Antiviral function of the innate immune system*.

Fig. 5: cGAS mediated detection of cytosplasmic dsDNA. Activated cGAS initiates synthesis of
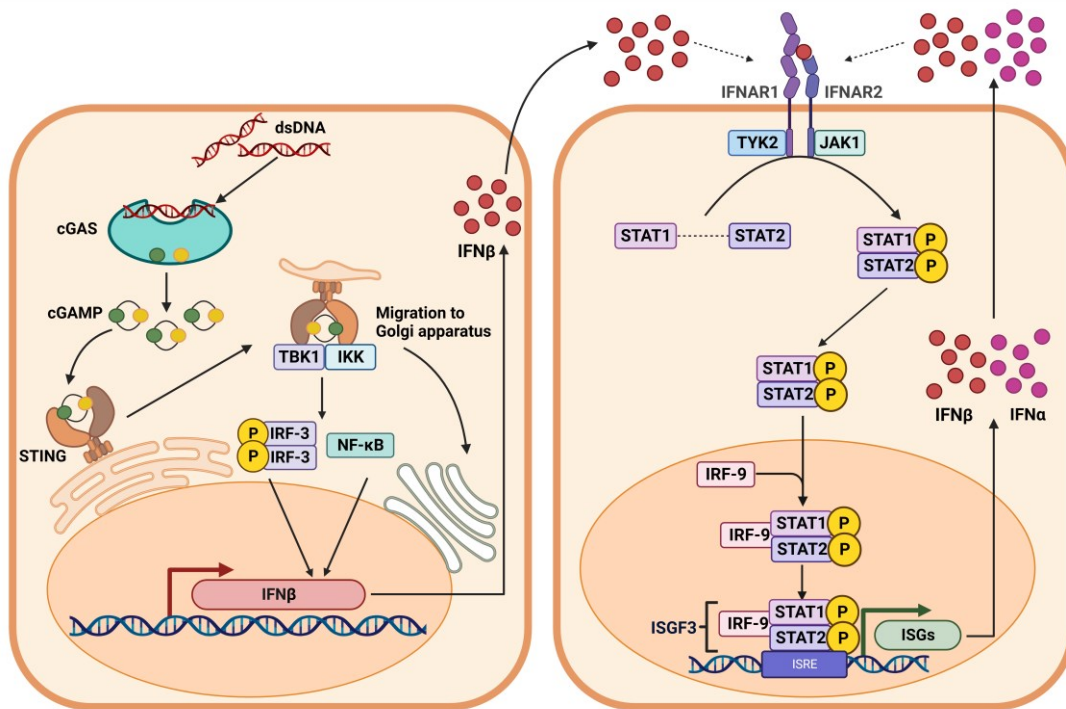
cGAMP. The cytosolic second messenger protein binds to STING, localized at the ER. During migration, STING activates transcription factors important for IFN-β synthesis. IFNAR dependent response to initial IFN-β production includes the same downstream signaling cascade as described previously (chapter *3. Antiviral vundtion of the innate immune response*). Modified from (Chen et al., 2016; Haller et al., 2006; Hopfner & Hornung, 2020; Randall & Goodbourn, 2008). Created with BioRender.com

2.2.   ASFV and modulation of the Interferon-β pathway

Although host immune system developed several defense mechanisms against invading pathogens, viruses evolved different strategies to modulate host immune response to ensure viral replication and survival. ASFV encodes 151 to 167 open reading frames (ORFs), providing numerous possibilities to evade porcine immune system (Arias et al., 2017). ASFV proteins I329L, A238L and DP96R are previously reviewed as inhibitors of the IFN-β pathway, whereas CD2v is especially associated with virus distribution, IFN-β induction and apoptosis in peripheral blood mononuclear cells (PBMCs) (Borca et al., 1994; Chaulagain et al.,

2021; de Oliveira et al., 2011; Revilla et al., 1998; Rodríguez et al., 1993; Wang et al., 2018).

2.2.1.   I329L

The ASFV protein I329L is encoded in the late phase of viral protein expression and is highly conserved between virulent and non-virulent genotypes. Moreover, I329L is a highly glycosylated transmembrane protein, detected at the plasma membrane of the cell surface, early endosomes, golgi apparatus and ER of *in vitro* infected cells via immunofluorescence (Correia et al., 2023; de Oliveira et al., 2011). Intriguingly, bioinformatical studies unveiled sequence homologies between I329L and the ECD as well as the TIR-domain of TLR3 (Correia et al., 2023; de Oliveira et al., 2011). To investigate inhibitory effects of I329L on the TLR3 signaling pathway, human embryonic kidney (HEK-293T) cells, constitutively expressing TLR3 (HEK-TLR3), were transfected with an I329L expression plasmid and a TRIF plasmid vector (de Oliveira et al., 2011). Although the cells were stimulated with Poly(I:C), IFN-β production was remarkably decreased (de Oliveira et al., 2011). Interestingly, recruitment of the downstream factor TRIF as well as dsRNA detection was prevented by dimerization of I329L with TLR3 (Correia et al., 2023; de Oliveira et al., 2011). Furthermore, Correia et al. indicated that I329L is also able to interact with other members of the TLR family, e.g. TLR4, TLR5 and TLR9 (Correia et al., 2023).

2.2.2.   DP96R

Associated with ASFV virulence, the ASFV protein DP96R is highly conserved between different ASFV strains but is missing in the virulent strain Malawi LIL20/1. First deletion experiments revealed that a lack of DP96R expression of the E70 isolate (E70ΔDP96R) could not achieve reduced replication rate in macrophages *in vitro*. Though pigs inoculated with E70ΔDP96R deletion mutants survived infection, due to reduced virulence (Zsak et al., 1998). Predicated on results of Zsak et al., several studies concentrated on attenuation of different virulent ASFV strains to generate possible live attenuated vaccines. Therefore, DP96R was mostly deleted in combination with other virulent factors like NL

(DP71L), MGF360-18R (DP148R) or 9GL and investigated in vaccine experiments challenging with the parental virus after primary infection with the deletion mutant (Abrams et al., 2013; O'Donnell et al., 2017; Qi et al., 2023). Interestingly, dimension of attenuation and protection was dependent of the ASFV strain used in these studies (Abrams et al., 2013; O'Donnell et al., 2017; Qi et al., 2023; Zsak et al., 1998). In 2018, Wang et al. elucidated inhibitory function of DP96R on the cGAS/STING pathway in HEK-293T cells (Wang et al., 2018). Briefly, DP96R significantly reduced IFN-β and NF-κB expression mediated by the cGAS/STING pathway due to inhibition of TBK1 and the TBK1 mediated phosphorylation of IRF-3 (Wang et al., 2018). In summary, DP96R is able to impair IFNβ response of the innate immune system, after detection of viral dsDNA by the cGAS/STING pathway. Considering the necessity of the kinases TBK1 and IKK for downstream signaling of different IFNβ initializing pathways, like TLR3 or RIG-1/mda-5, DP96R might be capable of impeding several distinct nucleic acid sensing mechanisms.

2.2.3.   A238L

In 1997, Yanez et al. described a novel ASFV-protein A238L possessing evident homologies to the ankyrin-repeats of IκB, the physiological inhibitor of NF-κB (Yáñez et al., 1995). The following years intensive research confirmed imitation of IκB function by A238L to prevent NF-κB mediated gene expression and to evade innate immune response (Revilla et al., 1998; Silk et al., 2007; Tait et al., 2000). Interaction of the p65 subunit of NF-κB is most likely mediated by its ankyrin repeats, but it is not able to replace IκB in the heterodimer with NF-κB indicating that A238L is dependent on the degradation of IκB due to activation of the NF-κB pathway to mediate its function (Revilla et al., 1998; Silk et al., 2007; Tait et al., 2000). Intriguingly, A238L did not inhibit translocation of NF-κB, but functions in the cytoplasm as well as in the nucleus of ASFV infected cells *in vitro* (Revilla et al., 1998; Silk et al., 2007). Therefore, the A238L gene encodes two forms of the protein with different molecular weight and different properties (Silk et al., 2007; Tait et al., 2000). The larger 32 kDa form of A238L is a posttranslational modification of the smaller 28 kDa form and is actively transported into the nucleus (Silk et al., 2007).

Virulent ASFV strains encoding A238L significantly decrease expression of

cytokines like IFN-α, Tumor necrosis factor (TNF) α as well as several Interleukins in porcine PBMCs and porcine alveolar macrophages in contrast to ASFV strains with deletion of the A238L gene (Gil et al., 2003; Powell et al., 1996; Salguero et al., 2008).

Furthermore, A238L unveiled multiple distinct mechanisms to evade innate as well as adaptive immune system during ASFV infection. In this context, A238L is described as inhibitor of the NFAT (nuclear factor of activated T cells) transcription pathway by interaction with the calcineurin phosphatase (CaN) in T cells (Miskin et al., 2000). Moreover, A238L impedes expression of several host response genes by interaction with the CBP (CREB-binding protein)/p300 complex and inhibition of Cyclooxygenase 2 (COX2) transcription, respectively (Granja et al., 2006a; Granja et al., 2004; Granja et al., 2008; Granja et al., 2006b; Silk et al., 2007). Remarkably, virulence and replication capacity of ASFV is independent of A238L expression, implying transcription of related viral proteins inheriting mechanisms of A238L in case of malfunction (Neilan et al., 1997; Salguero et al., 2008; Silk et al., 2007).

2.2.4. EP402R / 8-DR / CD2v

The viral protein CD2v is a highly glycosylated transmembrane protein encoded by the EP402R gene (also known as 8-DR gene) in the late phase of viral infection. It comprises an intracellular (or cytoplasmic) and an extracellular domain as well as a transmembrane domain. Intriguingly, each domain allocates multiple properties spinning a complex, and in some cases a paradox, network of protein functions, whereof a selection is outlined in the following passages.

CD2v is well known to provide hemadsorption of infected cells to erythrocytes to accelerate viremia in infected animals (Koltsov et al., 2023). Therefore, the extracellular domain is associated with 15 potential glycosylation sites, at which N-glycosylation of exact two asp residues in the N-terminal (Nt) region of the protein determine the phenomenon of hemadsorption (HAD) (Pérez-Núñez et al., 2023). In former studies ASFV strains were classified into CD2v expressing and non-expressing strains regarding its ability to induce HAD. Pérez-Núñez et al. recently depicted that the non-HAD strain NH/P68 definitely encodes CD2v, but its Nt region is augmented with an inhibitory sequence indicating that CD2v might be expressed during ASFV infection independent of the viral strain (Pérez-Núñez et

al., 2023). Although CD2v functions as haemadsorbing protein at the cell surface, it is predominantly localized within intracellular membranes and is unveiled as potent inducer of IFN-β as well as ISG transcription in porcine kidney (PK15) cells and in porcine blood-derived macrophages (Chaulagain et al., 2021; Goatley & Dixon, 2011). Results of Huang et al. counteracted the IFN-β stimulatory capabilities of the protein, identifying CD2v s as potent inhibitor of IFN-α as well as IFN-β production when co-transfected with cGAS/STING or STING plasmid vectors (Huang et al., 2023). Moreover, it also impaired IFNAR mediated feedback reaction induced by IFN-α, resulting in decreased mRNA expression levels of certain proteins mediating the antiviral state of host cells (Huang et al., 2023).

3.   Modified Vaccinia Virus Ankara (MVA)

3.1.   A short history of MVA

Modified Vaccinia Virus Ankara is well established as vector vaccine for human, veterinary and zoonotic diseases due to its high immunogenicity and safety profile. To gain recent popularity, a long evolutionary process of its ancestor virus, the Chorioallantoic Vaccinia Virus Ankara (CVA), was necessary. Multiple passages of CVA on chicken embryonic fibroblasts (CEF) resulted in attenuation and growth restriction in most mammalian cells due to the deletion of six major genomic regions and several smaller gene loci (Meyer et al., 1991). After comprehensive analysis of the viral genomic structure, naturally occurring deletion sites were utilized to insert foreign DNA sequences into the MVA genome via homologous recombination (Fig. 6). Though any deletion site could be used for insertion, the deletion III region remains as the most popular cloning site of MVA (Volz & Sutter, 2017). Contributing to its potency as viral vector, MVA is still capable of early, intermediate and late gene expression in mammalian cells, leading to high expression levels of inserted genomic sequences (Volz & Sutter, 2017). However, morphogenesis of virions in mammalian cells is inhibited and immature virions are not competent to establish a productive infection in non-permissive cells (Volz & Sutter, 2017), allowing handling of MVA under conditions of biosafety level 1. In 1994, MVA was successfully established as protective vector vaccine against Influenza Virus in a mouse model (Sutter et al., 1994). During this first vaccination experiment, MVA unveiled its high immunogenic potential by generating a strong cytotoxic T cell response and high antibody titers in sera of infected mice (Sutter et al., 1994). Since then, recMVAs were subject to various vaccination experiments, confirming the strong impact onto the host adaptive immunity (Kalodimou et al., 2019; Meyer Zu Natrup et al., 2022; Song et al., 2013). Immunogenic capabilities of MVA were further confirmed, depicting MVA as potent inducer of the innate immune system *in vivo* as well as *in vitro*. During murine lung infection MVA initiated Chemokine expression attracting natural killer cells as well as T cells to the infection site and in human blood-derived macrophages MVA induced strong IFN-β production (Lehmann et al., 2016; Royo et al., 2014). Taken together, MVA represented an attractive vector to analyze expression of indicated ASFV proteins

as well as IFN-β production in porcine cell lines.
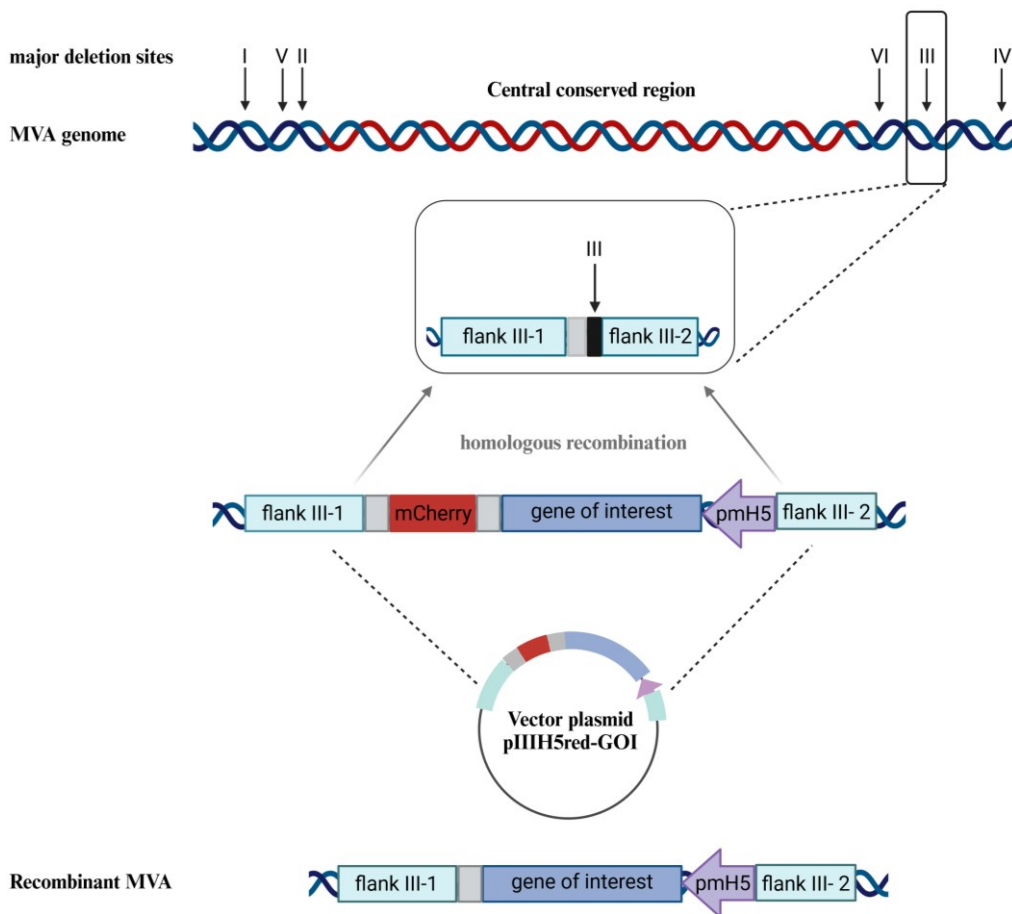
Fig. 6: Generation of recMVAs. To insert the gene of interest (GOI) into the deletion site III of the MVA genome, the target sequence is cloned into a vector plasmid flanked by the appropriate viral genomic sequences on both sides. During homologous recombination, the flank sequences guide the GOI to the determined deletion site. The marker gene mCherry verifies successful insertion of the GOI into the MVA backbone and is removed by intragenomic homologous recombination due to repeated plaque passaging.

3.2.   Taxonomy and replication cycle

Regarding its evolution from Vaccinia Virus Ankara, MVA belongs to the class of Pokkesviricetes, the family Poxviridae, the subfamily Chordopoxvirinae and the genus Orthopoxvirus. The genus of Orthopoxvirus comprises a variety of different species, including Vaccinia Virus Ankara, Variola Virus and Monkeypox Virus. Poxviruses are huge, enveloped viruses with a size of approximately 200 to 400 nm, containing linear double stranded DNA. They are described as "brick shaped" or "ovoid" (Fig. 7), due their appearance in electronic microscopy (Ruska et al., 1939). This unique shape is formed by an inner core, not only containing the linear double stranded DNA, but different virus-coding enzymes enabling the virus to replicate immediately and autonomously in the cytoplasm of infected cells (Westwood et

al., 1964). Exclusive replication in the cytoplasm is unique among DNA viruses and require a RNA-polymerase, an early viral transcription factor, a capping enzyme and a poly(A)-polymerase integrated into the viral core (Condit et al., 2006). To guarantee successful replication as well as establishment of a solid infection, the core is accompanied by lateral bodies, providing different proteins to modulate the host immune system and to create optimal conditions for viral replication (Bidgood et al., 2022; Laliberte et al., 2011). Core and lateral bodies are enveloped by an inner and an outer membrane (Condit et al., 2006).
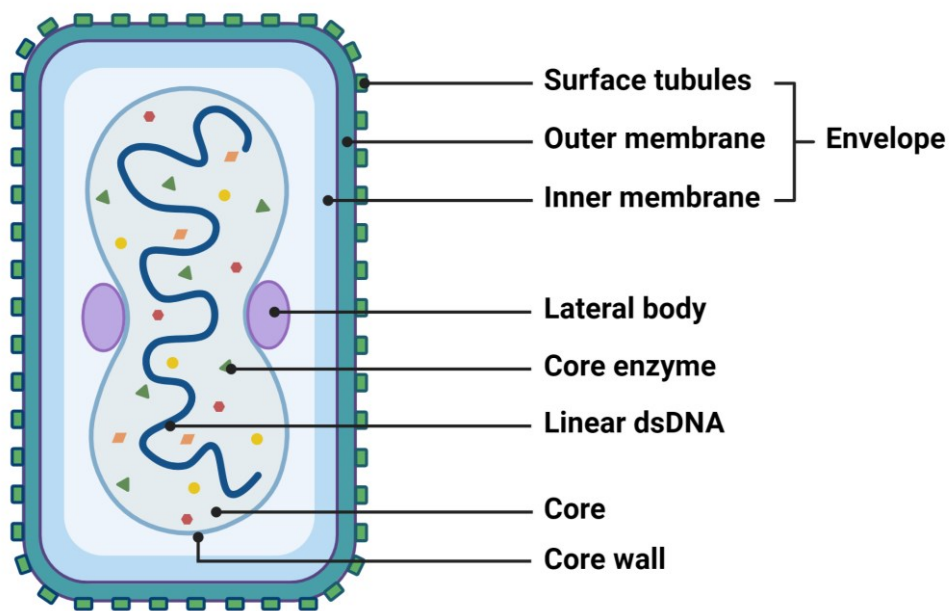
Fig. 7: Morphology of infectious enveloped virions (EV). Poxvirus particles consist of the viral core, which incorporates the nucleoprotein complex as well as viral enzymes. Together with the lateral bodies it is embraced by an envelope consisting of an inner and an outer membrane. The outer membrane includes several different surface tubules mediating viral attachment and fusion. Created with BioRender.com

Once the enveloped virions (EV) attached to the host cell surface, the outer membrane fuses with the host cell membrane, whereupon lateral bodies disassemble and the intact core is released into the cytoplasm (Fig. 8) (Doms et al., 1990; Schmidt et al., 2013). An alternative entry mechanism is provided by macropinocytosis of the host cell, whereupon core and immunomodulatory factors are released of endosomal structures by membrane fusion (Schmidt et al., 2011). The semipermeable core wall remains intact for early transcription and polyadenylated early viral mRNA is discarded into the host cell cytoplasm for translation (Mallardo et al., 2002). To initiate viral replication as well as intermediate and late viral transcription, the linear dsDNA needs to be uncoated (Moss, 2001). To evade nucleic sensing mechanisms of the host cell, the released

dsDNA is immediately enveloped by membranes of the endoplasmic reticulum (ER) (Mallardo et al., 2002; Tolonen et al., 2001). During replication process, these membranes expand enormously generating the characteristic replication factories (Katsafanas & Moss, 2007; Lin & Evans, 2010). With assembly of immature virions (IMV) and encapsidation of viral linear dsDNA, morphogenesis of IMV to mature virions (MV) is initiated and viral particles migrate from replication factories to the golgi apparatus, receiving a bilayer envelope (IEV) (Condit et al., 2006; Cudmore et al., 1995). The IEVs exit the host cell via exocytosis, retaining a monolayer envelope (EV) and establishing productive infection in host organisms (Cudmore et al., 1995; Payne, 1980; Stokes, 1976).

In conclusion, poxviruses encode several genes important for immunoevasion of the host cell to guarantee successful replication. However, MVA lacks several genes important for immunomodulation of the mammalian host cell leading to impaired morphogenesis in most of the mammalian cell lines (Blanchard et al., 1998; Volz & Sutter, 2017). The large genomic deletions and genomic mutations occurred during the 572 serial passages of CVA in CEF cells (Antoine et al., 1998; Volz & Sutter, 2017).
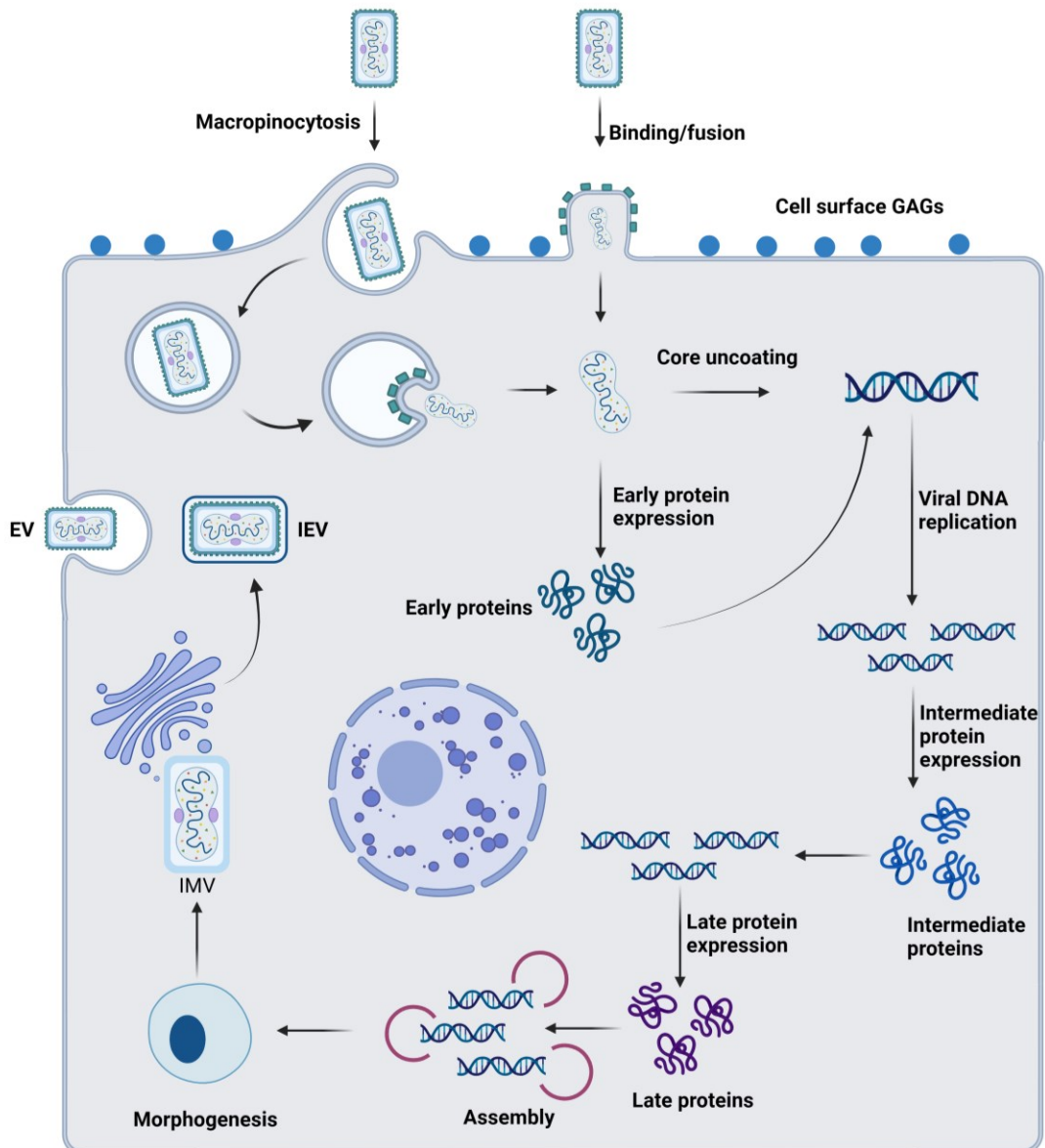
Fig. 8: Poxvirus replication cycle. Intruding extracellular virions (EV) enter host cells by binding to glycosaminoglycans (GAGs) and fusion with the cell membrane or by macropinocytosis. The host cell cytoplasm is venue for early, intermediate and late gene expression as well as viral DNA replication. Viral factories are built during replication cycle are not included in the scheme. The viral replication cycle ends with assembly and morphogenesis of virions. Intracellular enveloped viruses (IEV) are released via membrane fusion. Modified from (McFadden, 2005; Sutter, 2020). Created with BioRender.com

III.   MATERIALS AND METHODS

1.   Materials

1.1.   Bacterial Strains

For amplification of plasmid DNA the commercially available NEB 10-beta competent E. coli (New England Biolabs, Frankfurt, Germany) was used.

1.2.   Cell lines

Cell line	Additional Information	Experiment
CEF	chicken embryo fibroblasts	virus amplification, plaque passage, protein expression, growth kinetics
HaCat	human epidermal ceratinocytes	growth kinetics
LLC-PK1	porcine kidney cells	growth kinetics, protein expression, immunomodulation study
IPEC-J2	porcine jejunal cells	protein expression, immuno-modulation study
3D4/21	porcine alveolar macrophages	protein expression, immuno-modulation study

Table 1: Cell lines

1.3.   Plasmids

Plasmid	Company/Supplier	Characteristics
pc-DNA-DP96R-myc-his	Centro Biología Molecular "Severo Ochoa", Madrid, Spanien	Original sequence of gene of interest; template for modi-fications

Plasmid	Company/Supplier	Characteristics
pc-DNA-DP96R mod.	this work, LMU	Deletion of MVA stop codons; FLAG-tag
pUC-GW-AMP-ASFV I329L	Genewiz, Leipzig	Deletion of MVA stop codons; FLAG-tag
pUC-GW-AMP-ASFV A238L	Genewiz, Leipzig	Deletion of MVA stop codons; FLAG-tag
pIIIH5-ASFV-DP96R	this work, LMU	Gene of interest with strong early and late phase promoter; template for cloning experiments
pIIIH5-ASFV-I329L	this work, LMU	Gene of interest with strong early and late phase promoter; template for cloning experiments
p7.5late-ASFV-A238L	this work, LMU	Gene of interest with weak late phase promoter; template for cloning experiments

Table 2: Plasmids used in this study

1.4. Antibodies

1.4.1. Primary antibodies

Specificity	Company	Host	WB	IFA
Vaccinia virus A27L protein	oriGene, Herford, Germany	Rabbit		1:2,000
FLAG-tag	Sigma-Aldrich, Taufkirchen, Germany	Rabbit	1:3,000	

FLAG-tag	Sigma-Aldrich, Taufkirchen, Germany	Rabbit	1:500	1:150
GAPDH (6C5)	Sigma-Aldrich, Taufkirchen, Germany	Mouse	1:10,000	

Table 3: Primary antibodies

1.4.2.   Secondary antibodies

Specificity	Company	Host	WB	IFA
Anti-Rabbit (HRP-conjugated)	Jackson Immunoresearch, Westgrove, USA	Goat	1:5,000	1:5,000
Anti-Rabbit (Alexa Fluor 488)	Thermo Fisher Scientific, München, Germany	Goat		1:1,000
Anti-Mouse (Alexa Fluor 488)	MoBiTec, Göttingen, Germany	Goat	1:200	

Table 4: Secondary antibodies

1.5.   Oligonucleotides

Oligonucleotides used for control PCRs		
Primer	**Sequence (5' → 3')**	**Product**
MVA-Del I for	CTTCGCAGCATAAGTAGTATGTC	291 bp
MVA-Del I rev	CATTACCGCTTCATTCTTATATTC	
MVA-Del II for	GGGTAAAATTGTAGCATCATATACC	354bp
MVA-Del II rev	AAAGCTTTCTCTCTAGCAAAGATG	
MVA-Del III for	GATGAGTGTAGATGCTGTTATTTTG	446bp

MVA-Del III rev	GCAGCTAAAAGAATAATGGAATTG	
MVA-Del IV for	AGATAGTGGAAGATACAACTGTTACG	502bp
MVA-Del IV rev	TCTCTATCGGTGAGATACAAATACC	
MVA-Del V for	CGTGTATAACATCTTTGATAGAATCAG	603bp
MVA-Del V rev	AACATAGCGGTGTACTAATTGATTT	
MVA-Del VI for	CTACAGGTTCTGGTTCTTTATCCT	702bp
MVA-Del VI rev	CACGGTCAATTAACTATAGCTCTG	
MVA069R-070L for	ATTCTCGCTGAGGAGTTGG	355bp
MVA069R-070L rev	GTCGTGTCTACAAAAGGAG	
DP96R_Insert for	GCCCGCGAAATGACATCATCAG	152bp
DP96R_Insert rev	TGGATGGAGCGCATTAGCGAAC	
A238L_Insert for	TGGAGCAGATCCGACTCAAAA	254bp
A238L_Insert rev	CGCCCACACAGGAACTTTG	
I329L_Insert for	TATCCGCTGCGGGATGAAAA	245bp
I329L_Insert rev	AGAACTGCGGAAGACGCTTT	
mCC_for	GTATGTTGGGGAAATATGAACC	520bp
mCC_rev	GACTACTTGAAGCTGTCCTTCC	
GFP_for	AGCTGACCCTGAAGTTCATCTG	437bp
GFP_rev	GGTGTTCTGCTGGTAGTGGTC	

Table 5: Oligonucleotide primers used for control PCRs

Oligonucleotides used for sequence modification		
Primer	**Sequence (5' → 3')**	**Product**
DP96R_mod for	GGCGGATCCACCATGTCTACACAT GATTGTTCTCTAAAAGAGAAACC	350 bp
DP96R_mod rev	GCCGTCGACGCGGCCGCTTATTACTT GTCGTCATCGTCTTTGTAGTGCGCCAT TATTCTTCTGGATGGAGCGCATTAGC GAACCCTTACC	

Table 6: Oligonucleotide primers used for sequence modification

Oligonucleotides and probes used for qPCRs	
Primer	**Sequence (5' → 3')**
mRNA_IFNb for	TTCTCCACCACAGCTCTTTC
mRNA_IFNb rev	GGACCTCGAAGTTCATCCTATC
mRNA_IFNb probe	AACAGTTGCCTGGGACTCCTCAAT
mRNA_GAPDH for	ATGATTCCACCCACGGCAAG
mRNA_GAPDH rev	AGAAGGGGCAGAGATGATGAC
mRNA_GAPDH probe	CCATCTTCCAGGAGCGAGATCCCGCCA

Table 7: Oligonucleotide primers and probes used for qPCRs

1.6.   Synthetic dsRNA

For stimulation of Interferon beta expression in porcine cell lines, the synthetic dsRNA Poly(I:C) HMW (InvivoGen, San Diego, USA) was used.

2.   Methods

2.1.   Cell Culture

2.1.1.   Passaging, seeding, freezing and thawing of cells

CEF cells were freshly isolated from 10 to 11 day old chicken embryos. The eggs were obtained from a specific pathogen free animal facility. The cells were cultured in MEM with Early Salts and 10% heat inactivated FBS as well as with 1% non-essential amino acid solution.

LLC-PK1 (ACC 637) cells were maintained in DMEM – low glucose with 10% heat inactivated FBS and with 1% non-essential amino acid solution.

IPEC-J2 (ACC 701) cells were cultured in DMEM – high glucose with 10% heat inactivated FBS as well as with 1% non-essential amino acid solution.

3D4/21 (CRL-2843™) cells were maintained in RPMI 1640 with 10% heat inactivated FBS, 1% HEPES solution and 1% non-essential amino acid solution.

For seeding and passaging, cells were washed with PBS and trypsinized for 5 to 15 minutes at 37°C and 5% CO_2. To stop the enzymatic reaction, culture medium was added to the cell suspension. Afterwards, cells were splitted and distributed to new flasks for passaging or diluted with culture medium for seeding. For certain experiments, cells number was determined before seeding and therefore diluted 1:1 with Trypan blue and counted with a Neubauer improved chamber. Cells were incubated at 37°C and 5% CO_2.

In terms of freezing cells, they were handled as described above, until the trypsin reaction was stopped. The cell suspension was then carefully centrifuged and the cell pellet was resuspended in 45% cell culture medium and 45% FBS. As antifreezing compound, 10% DMSO were added slowly and the cell suspension was distributed to cryogenic vials. In first term, cells were frozen at -80°C and after one to two days transferred into liquid nitrogen. For thawing, cryogenic tubes were taken out of the liquid nitrogen and transferred to a water bath with 37°C. The thawed cell suspension was immediately diluted with cell culture medium to avoid cell toxic effects of the DMSO. Cells were centrifuged and the cell pellet resuspended with cell culture medium. Subsequently, cells were transferred into a cell culture flask and incubated at 37°C and 5% CO_2

2.1.2.   Generation of recombinant MVAs

For this study, three different recMVAs were generated, encoding the non-structural protein I329L, DP96R or A238L of the ASFV.

In a first step, the codon of each protein was optimized and stop-codons for the poxviral RNA-polymerase were removed. Therefore, selected nucleic bases of G/C-runs and TTTTTNT regions were exchanged without affecting the amino acid sequence of the target proteins. Moreover, enzyme restriction sites for BamHI and NotI were added to the protein coding sequence, allowing the transfer of the target sequences from the bacterial vector plasmid into the MVA vector plasmid. Due to the lack of ASFV specific antibodies, the sequence of the target genes was additionally enlarged by a c-terminal FLAG-tag coding region, enabling immunostaining of the target protein during protein expression analysis.

The modified genetic sequences for I329L and DP96R were cloned into the MVA vector plasmid pIIIPmH5red, which determined insertion of the GOI at the deletion site III of the MVA genome. The transcription of the target protein was controlled by a strong promoter (PmH5), active during early and late phase of viral protein expression. In contrast, A238L was incorporated into the pIW-73 backbone guiding the GOI to the intergenic region between the essential viral genes MVA069R and MVA070L. Expression of the associated protein was driven by the P7.5 late phase promoter.

In both vector plasmids the GOI is accompanied by a marker gene that is expressed independently from the target gene to verify incorporation of the GOI into the MVA genome during homologous recombination *in vitro*. The marker gene included in the vector plasmid pIIIPmH5red was mCherry and in pIW-73 the marker gene was coding for GFP.

To transfer the GOI into the MVA genome, CEF cells with a confluency of 90-95% were infected with MVA-F6P11GFP or MVA-pLW73mCherry at MOI 0.05 and incubated for one hour at 37°C and 5% CO_2. Subsequently, cells were transfected with 1µg of the expression plasmid. As transfection reagent XtremeGene HP DNA was used, according to the manufacturer´s instructions. After 48 hours incubation time at 37° and 5% CO_2, the success of the cloning experiment was verified under the fluorescence microscope, screening for the transient co-expression of the red marker protein. After several rounds of plaque passaging on CEF cell monolayers, deletion of the marker gene occurred and plaques missing the mCherry signal were

selectively collected and passaged. To obtain large scale stock solutions, recMVAs were amplified on CEF cells in T175 tissue culture flasks and incubated for three days at 37°C and 5% CO2. Flasks were frozen and the whole virus preparation was harvested. The viral stock solution was repeatedly subjected to freeze-thaw circles and to sonication.

The coding sequence for CD2v of ASFV was cloned into the deletion-III site of the MVA-vector system during a former project. The cloning procedure was identical to the experimental approach described above.

2.1.3.   Virus titration/Immunostaining

For virus titration, a tenfold serial virus dilution (10^{-1} to 10^{-8}) was prepared and added to a CEF cell monolayer with a confluence of 90-95%. All dilution steps were performed in duplicates and incubated for 48 hours at 37°C and 5% CO2. Cells were fixed with ice-cold methanol : acetone (1:1) and incubated for 5min. The fixation reagent was discarded and the wells were dried at room temperature for several minutes. As blocking buffer PBS + 3% FBS was used and incubated over night or for one hour at room temperature. Rabbit anti-VACV antibody was diluted in a ratio of 1:2.000 in PBS + 3% FBS and incubated for 1 hour at room temperature. Plates were washed three times with PBS. The secondary goat anti-rabbit antibody was added at a dilution of 1:5.000 in PBS + 3% FBS and incubated for 1 hour at room temperature. Plates were washed three times with PBS. Finally, the TrueBlue Peroxidase Substrate was added to each well and plaques were counted after a significant colour change.

2.1.4.   Multi-step growth kinetic analysis of recombinant MVAs

To investigate the replication deficiency of the obtained recMVAs in eukaryotic cell lines, PK1, HaCat and CEF cells were grown on 24-Well plates. At a confluence of 90-95% cells were infected with MVA-I329L, MVA-DP96R or MVA-A238L at an MOI of 0.05, incubated and frozen at several timepoints post infection (0, 4, 10, 24, 48 and 72 hours). Cells and supernatants were harvested and subjected to three freeze-thaw cycles. After sonication, the different timepoints were titrated on CEF cells as described at chapter *2.1.3 Virus titration/Immunostaining.*

2.1.5. Determination of the MVA infectivity in porcine cell lines

To identify the MOI at which MVA reveals the highest infection rate without severe impairment of the cell vitality, PK1, J2 and 3D4/21 cells were seeded at 24-well tissue plates at a confluence of 85%. Each cell line was infected with MVA-pvgf-eGFP at an MOI of 0.1, 0.5, 1, 2 and 5, respectively. Initial cell vitality was ensured by co-preparation of a non-infected cell control (Mock). After an initial incubation time of 7 hours at 37°C and 5% CO_2, cells were investigated regarding the GFP fluorescence signal by using fluorescence microscopy (Keyence BZ-X700). Subsequently, cells were incubated over night at 37°C as well as 5% CO_2 and reevaluated via fluorescence microscopy after an entire incubation period of 24 hours.

2.1.6. Immunomodulatory Assay

PK1, J2 and 3D4/21 cells were grown on 6-well tissue plates at a confluence of 85%. Cells were then stimulated with Poly(I:C) HMW or infected with MVA F6 / recMVA or infected with MVA-F6 / recMVA and stimulated with Poly(I:C) HMW.

2.1.6.1. Cell stimulation with Poly(I:C) HMW

PK1, J2 or 3D4/21 cell monolayers were transfected with different concentrations of Poly(I:C) HMW (2µg/ml, 1µg/ml, 0.5µg/ml, 0.1µg/ml, 0.05µg/ml, 0.01µg/ml, 0.001µg/ml) and incubated for 6 hours at 37°C and 5% CO_2. As transfection reagent Lipofectamine 2000 was used according to the manufacturer´s instructions. In another preparation, different concentrations of Poly(I:C) HMW (25µg/ml, 10µg/ml, 5µg/ml, 2µg/ml, 1µg/ml, 0.1µg/ml, 0.05µg/ml, 0.01µg/ml) were added into the supernatant without using a transfection reagent. Then the plates were incubated for 6 hours at 37°C and 5% CO_2. After incubation supernatants and cell lysates were collected.

2.1.6.2. Determination of the cell stimulation peak

3D4/21 cell monolayers were transfected with 1µg/ml Poly(I:C) HMW or rather stimulated by 5µg/ml Poly(I:C) HMW added into the supernatant. As transfection reagent Lipofectamine 2000 was used according to the manual. Supernatants and cell lysates were collected after several timepoints post stimulation (0, 2, 4, 6, 8, 10, 12 and 16 hours).

2.1.6.3.   Infection with MVA F6

PK1, J2 and 3D4/21 cells were grown in 6-well tissue plates and infected with the non-recombinant MVA-F6 at a MOI of 5. Cell lysates and supernatants were harvested after 4, 6 or 18 hours.

2.1.6.4.   Infection with recombinant MVAs

3D4/21 cells were grown in a confluent monolayer and infected with MVA-I329L, MVA-CD2v or MVA-DP96R at a MOI of 5. After 18 hours cell lysates and supernatants were harvested.

2.1.6.5.   Infection with MVA-F6 / recMVA and stimulation with Poly(I:C) HMW

3D4/21 monolayers were infected with MVA-F6 or one of the recombinant MVAs (MVA-I329L, MVA-DP96R, MVA-CD2v) at a MOI of 5. After 18 hours of incubation time at 37°C and 5% CO_2, the cells got additionally stimulated by Poly(I:C) HMW. In one preparation the 3D4/21 cells are transfected with 1µg/ml Poly(I:C) HMW and Lipofectamine 2000. In the second preparation, 5µg/ml Poly(I:C) HMW is added into the supernatant. In both cases, supernatants and cell lysates are harvested after 2 or 4 hours.

2.2.   Molecular Biology

2.2.1.   Heat-shock transformation

NEB 10-beta competent E.coli were carefully centrifuged and thawed on ice. Plamid DNA (250-500ng) was added and the tube was gently tapped to mix the components. The vial was chilled on ice for 30 minutes. Subsequently, the preparation was incubated for 30 seconds in a 42°C water bath. Vials were removed from the water bath and immediately placed on ice. Pre-warmed LB-Medium, without antibiotics, was added and the vial was incubated for one hour at 37°C and 225rpm in a shaking incubator. The transformed E.coli were spread on a LB-Agar/Ampicillin plate and grown over night at 37°C. Isolated colonies were collected and amplified in LB/Ampicillin-medium.

2.2.2.   Isolation of plasmid DNA

For characterization studies, amplified plasmid DNA was isolated from the competent E.coli using the PureYield^{TM} Plasmid Miniprep System (Promega, Walldorf, Germany). In a first step, bacteria grown over night in LB/Ampicillin-medium were centrifuged at 13,000 rpm for 30 seconds and the supernatant was discarded. The pellet was lysed and further processed regarding the manufacturer´s instructions. The DNA yield and quality was measured with a PeqLab Nanodrop. Plasmid DNA was stored at -20°C.

After validating the successful transformation, larger yields of plasmid DNA were generated using the Xtra Bond Midi Kit (Macherey-Nagel, Düren, Germany) regarding the manual. Briefly, bacteria were grown in 100mL LB-Ampicillin-Bouillon over night. Bacteria were centrifuged for 30 minutes at 4,500rpm, the supernatant was discarded and the pellet was lysed with RES-Buffer. After several washing and purification steps, plasmid DNA was eluted with 10mM Tris-HCl (pH 8.0). DNA yield and quality was screened with a PeqLab Nano-Drop. Plasmid DNA was stored at -20°C.

2.2.3.   Digestion of plasmid DNA with restriction enzymes

For a first characterization of plasmid DNA, digestion with different restriction enzymes was performed. As enzymes NotI, BamHI, ScaI, HindIII and NcoI were obtained from New England Biolabs, Frankfurt, Germany. According to the manufacturer´s recommendations, the following digestion protocol was established:

> 150-300ng plasmid DNA
> 1µl rCut Smart Buffer (10x)
> 0.1µl enzyme A
> 0.1µl enzyme B
> (0.1µl enzyme C)
> Add H$_2$O up to 10µl

The plasmid digestion was incubated for 2 to 3 hours at 37°C and the digested plasmids were analysed via agarose gel electrophoresis.

To clone the gene of interest into the MVA vector plasmid (pIIIpmH5red), sticky ends were obtained using BamHI and NotI:

> 500-1000ng plasmid DNA
>
> 5µl rCut Smart Buffer (10x)
>
> 0.5µl BamHI
>
> 0.5µl NotI
>
> Add H$_2$O up to 50µl

The preparation was incubated for 2 to 3 hours at 37°C. Digestion success was verified via agarose gel electrophoresis. The opened pIIIpmH5red-plasmid and the gene of interest (GOI) were excised of the agarose gel and eluted with the Wizard® SV Gel and PCR Clean-Up System (Promega, Walldorf, Germany) regarding the manual.

2.2.4.   Ligation reaction

After sticky ends were obtained with BamHI and NotI (*2.2.3 Digestion of plasmid DNA with restriciton enzymes)*, the GOI (ASFV-DP96R, ASFV-I329L, ASFV-A238L) was cloned into the MVA vector plasmid (pIIIPmH5red) by incubation with a T4 ligase (New England Biolabs, Frankfurt, Germany):

> 1µl T4 DNA Ligase Buffer (10x)
>
> x µl Vektor DNA
>
> x µl Insert DNA
>
> 1µl T4 DNA Ligase
>
> Add H$_2$O up to 10µl

Vektor and Insert DNA were added in a molar ratio of 1:3 for the indicated DNA sizes. The ligation reaction was incubated over night at 16°C. For inactivation of the T4 Ligase, the tube was incubated for 10 minutes at 65°C.

2.2.5.   Isolation of viral DNA

For isolation of genomic viral DNA, the DNeasy Blood and Tissue Kit (Qiagen, Hilden, Germany) was used. Briefly, infected cells were harvested after an

incubation time of 48 to 72 hours and centrifuged for 1 minute at 2,000rpm. Supernatant was discarded and the pellet was resuspended in PBS. Cell lysis, washing procedure and elution of the viral DNA was performed as described in the manufacturer´s instructions. DNA yield and quality was determined by a PeqLab Nano-Drop.

2.2.6.   Polymerase Chain Reaction (PCR)

During cloning procedure and virus passaging, specific genomic regions of the plasmid or viral genomic DNA were investigated via PCR. Therefore, two different reaction kits and protocols were used. The oligonucleotide primers are summarized at chapter *1.5 Oligonucleotides*.

2.2.6.1.   Q5® Hot Start High Fidelity 2x MasterMix

This ready to use PCR – mastermix was obtained from New England Biolabs (Frankfurt, Germany) and used for amplifying the MVA deletion sites.

9μl 2x Ready Mix

12,5μl DNAse free H_2O

1,25μl Forward-Primer 10mM

1,25μl Reverse-Primer 10mM

1μl Template (20-40ng DNA)

Step		Temperature	Time
Initial Denaturation		98°C	30sec
Denaturation		98°C	10sec
Annealing	30 cycles	60°C	30sec
Extension		72°C	20-30sec/kb
Final extension		72°C	2min

Table 8: Protocol for the Q5® Hot Start High Fidelty Mix

2.2.6.2.   ReadyMix™ Taq-PCR Reagent Mix

For characterization and amplification of the inserted GOI as well as for verifying the loss of the marker gene during plaque passaging, the Sigma ReadyMix with a

Taq-Polymerase was used.

> 25µl 2x Ready Mix
>
> 22µl DNAse free H2O
>
> 1µl Forward-Primer 10mM
>
> 1µl Reverse-Primer 10mM
>
> 1µl Template (20-40ng)

Step	Temperature	Time
Initial Denaturation	95°C	2min
Denaturation	95°C	30sec
Annealing	55-70°C (regarding Tm° of Primer)	30sec
Extension	72°C	1min/kb
Final extension	72°C	5min

30 cycles (Denaturation, Annealing, Extension)

Table 9: Protocol for the ReadyMix™ Taq-PCR Reagent Mix

2.2.7. Gel electrophoresis

Agarose gel electrophoresis was used to separate PCR products and digested plasmid DNA according to their size. Nucleic acids were mixed with 6x purple Gel loading dye (New England Biolabs, Frankfurt, Germany) and applied to the solid agarose gel. Molecular weight markers were obtained from New England Biolabs (Frankfurt, Germany). As intercalating dye, GelRed® has been used to visualize the applied products with the ChemiDoc™MP Imaging System (Bio-Rad, Munich, Germany).

2.2.8. Sequencing of PCR products

To verify the genetic stability of the recMVAs during plaque passaging and amplifying, PCR products of the DeletionIII - PCR and the I8R-G1L - PCR were analysed by Sanger sequencing. Briefly, the PCR-products were excised after gel electrophoresis and eluted with the Wizard® SV Gel and PCR Clean-Up System (Promega, Walldorf, Germany) regarding the manufacturer´s instructions. For sequencing reaction, the eluted PCR-product and the specific oligonucleotides were

shipped to Eurofins Genomics (Ebersberg, Germany). Sequencing data were analysed with the multiple alignment software MegAlign Pro (DNAstar, Lasergene).

2.2.9.   Generation of cell lysates for protein analysis

CEF, PK1, J2 or 3D4 cells were grown in a monolayer to a confluence of 90-95% or to a confluence of 80-85%. The different monolayers were infected with recMVAs (MVA-I329L, MVA-CD2v, MVA-DP96R, MVA-A238L) or with MVA F6 at a MOI of 5. MVA F6 infection and non-infected cells (Mock) served as controls. The infected monolayers were incubated for 24 hours or regarding kinetic studies for 0,4, 6, 10, 18 and 24 hours at 37°C and 5% CO_2. Supernatant was discarded and the cell layer was carefully washed with PBS. The cells were harvested and centrifuged for 1min at 13,000rpm. The supernatant was discarded and washed a second time with PBS, if required. Cell pellets were resuspended with lysis buffer, based on Triton-X, containing a protease-inhibitor. The cell lysis preparation was incubated for 30 minutes on ice. After centrifugation for 15min at 13,000rpm, supernatants were collected and stored at -80°C.

2.2.10.   Deglycosylation assay

For highly glycosylated ASFV-proteins, like CD2v and I329L, a deglycosylation assay was performed. Cell lysates (description at Chapter *2.2.8 Generation of cell lysates for protein* analysis) were processed with the deglycosylation enzymes PNGase F and EndoH (both obtained from New England Biolabs, Frankfurt, Germany).

2.2.10.1. PNGase F

Deglycosylation reaction with PNGase F was processed in two steps. In a first step, the glycoprotein was denatured regarding the manufacturer´s instructions:

> 1-20µg glycoprotein (cell lysate)
> 1µl Glycoprotein Denaturing Buffer (10x)
> Add H_2O up to 10µl reaction volume

The reaction was incubated at 100°C and immediately chilled on ice after 10 minutes incubation time. In a second step, deglycosylation was obtained and

deglycosylation components were added to the first step reaction regarding the manual:

> 2µl GlycoBuffer (2x)
>
> 2µl NP-40 (10%)
>
> 6µl H_2O
> _____
>
> 1µl PNGase F

The vial was incubated for 1 hour at 37°C and the deglycosylated sample was immediately used for SDS-PAGE or stored at -80°C.

2.2.10.2. Endo H

In a two-step reaction, glycoproteins get denatured and deglycosylated. The denaturing reaction consists of:

> 1-20µg glycoprotein
>
> 1µl Glycoprotein Denaturing Buffer (10x)
>
> Add H2O up to 10µl reaction volume

Subsequently, the vial was incubated under denaturing conditions at 100°C for 10 minutes. Samples were chilled on ice and following deglycosylation mix was added:

> 2µl GlycoBuffer (2x)
>
> 5µl Endo H
>
> 3µl H_2O

For deglycosylation the reaction was incubated at 37°C for 1 hour. The deglycosylated sample was immediately used for SDS-PAGE or stored at -80°C.

2.2.11.   SDS-PAGE and Western Blot

Cell lysates (description at Chapter *2.2.8 Generation of cell lysates for protein analysis*) were carefully thawed on ice. Meanwhile, 4x Laemmli was diluted 1:10 with β-Mercaptoethanol. An aliquot of the thawed lysated was diluted 1:4 with the Laemmli/β-Mercaptoethanol solution. The samples were incubated for 3-5 minutes at 95°C and chilled on ice. Samples as well as the protein standard (Bio-Rad, Munich, Germany) were applied onto a pre-cast, gradient polyacrylamid gel (4-20% gradient, Bio-Rad, Munich, Germany). For decent separation of the proteins,

100V for 1,5 to 2 hours were used. The proteins were transferred onto a nitrocellulose membrane via semidry blotting for 45min. The membrane was incubated with blocking buffer for 1 hour at room temperature. Primary antibodies were applied as described in chapter *1.4 Antibodies* and incubated at 4°C over night. The nitrocellulose membrane was washed in PBS for three times and five minutes each. A matching secondary antibody was diluted as described in chapter *1.4 Antibodies* and incubated for 1 hour at room temperature. After three washing steps with PBS for 5 minutes, the membrane was incubated with another pair of antibodies following the described protocol or Clarity Western ECL Substrate was applied onto the nitrocellulose membrane and incubated for at least 1 minute. Due to visualization, the ChemiDoc[TM]MP Imaging System (Bio-Rad, Munich, Germany) was used.

2.2.12.   Immunofluorescence

PK1, J2 and 3D4/21 cells were grown on cover glasses in 6-Well tissue plates at a confluence of 80%. The monolayers were infected at an MOI of 0.05 with recombinant MVAs (MVA-I329L, MVA-DP96R, MVA-A238L, MVA-CD2v) or with MVA F6 used as infection control. The infected cells were incubated for 16-20 hours at 37°C and 5% CO2. The plates were fixed with ice-cold 4% Paraformaldehyde and incubated for 10 minutes on ice. The fixation reagent was discarded and the monolayer was washed three times with PBS. The preparation was blocked with 0.5% Bovine Serum Albumine in PBS (0.5% BSA-PBS) for 1 hour at room temperature. The anti-FLAG antibody produced in rabbit was diluted 1:150 in 0.5% BSA-PBS and incubated at 4°C over night. The wells were washed three times with PBS for 5 minutes, while rocking gently. As secondary antibody, Goat Anti-Rabbit AlexaFluor[TM]488 was diluted 1:1,000 in 0.5% BSA-PBS and incubated for 1 hour at room temperature and under darkened conditions. The plates were again washed three times with PBS for 5 minutes. As nuclear dye, DAPI was applied as ready to use mix (Invitrogen, Thermo Fisher Scientific, Munich, Germany) onto the cover slides and incubated for at least 1 minute under darkened conditions. Meanwhile, microscope slides were prepared and centrally covered with a single drop of Dako Fluorescence Mounting Medium (Agilent, Waldbronn, Germany). The cover slips were placed onto the microscope slides and sealed with transparent nail polish. For analysis and imaging the Keyence BZ-X700 microscope

was used.

2.2.13. RNA isolation

RNA was isolated from 3D4/21, PK1 and J2 cells grown in 6-well tissue plates with a confluence of 80-85%. Cell monolayers were infected, stimulated with Poly(I:C) or infected and stimulated. The experiment´s procedure is described in detail in chapter *2.1.5. Immunomodulatory Assay*. After a determined incubation time, supernatants were collected and the monolayer was carefully washed with PBS. Cell lysis, gDNA removal, washing steps and elution were performed with the RNeasy Plus Mini Kit (Qiagen, Hilden, Germany) regarding the manufacturer´s instructions. Eluted RNA was strictly kept on ice. The quantity as well as the quality of the isolated RNA was measured with a PeqLab Nano-Drop. Vials were immediately stored at -80°C.

2.2.14. cDNA synthesis

To obtain cDNA in a high quality and in a high scale, the QuantiTect Reverse Transcription Kit from Qiagen (Hilden, Germany) was used regarding the manual. Before thawing the isolated RNA carefully on ice, the mastermix for digestion of remaining genomic DNA was prepared and distributed to different tubes. Thawed RNA was diluted to a concentration of 100ng/µl with RNase free water and 1µg of RNA was added to the prepared gDNA removal mastermix. The vials were incubated for 3 minutes at 42°C and chilled on ice, subsequently. For high-scale cDNA synthesis oligo(dt)-primers were combined with random-primers and the Quantiscript reverse transcriptase, provided by the Reverse Transcription Kit. After the RNA from the gDNA removal preparation was added, the vials were incubated for 30 minutes at 42°C. To stop the synthesis reaction, the vials were incubated at 95°C for 3 minutes. cDNA was stored at -20°C.

2.2.15. Real-Time PCR (qPCR)

Real time PCR was performed for quantitative analysis of interferon beta (IFN-beta) mRNA expression levels in porcine cell lines (PK1, J2 and 3D4/21) obtained to immunomodulatory experiments (description in chapter *2.1.5 Immunomodulatory Assay*). Due to increased stability, cDNA (chapter *2.2.13 cDNA*

synthesis) was used for the mRNA expression studies. Briefly, specific oligonucleotides and probes were added to the Luna® Universal qPCR Mastermix (New England Biolabs, Frankfurt, Germany) containing the reaction buffer, polymerase and dNTPs. The Real-time PCR was designed as a duplex qPCR, relating the IFN-beta expression to the glyceraldehyde 3-phosphate dehydrogenase (GAPDH) expression. Oligonucleotides and probes are listed in Chapter *1.5 Oligonucleotides*. The qPCR was performed regarding the following protocol:

> 10µl Luna Universal Mastermix
>
> 2,8µl DNAse free H_2O
>
> 1,6µl Primer-Probe-Mix 1
>
> 1,6µl Primer-Probe-Mix 2
>
> 4µl Template

Step		Temperature	Time
Initial Denaturation		95°C	1min
Denaturation	42 cycles	95°C	15sec
Annealing/Extension		65°C	1min

Table 10: Protocol for the Luna® Universal qPCR Master Mix

2.3.   Statistical analysis

To detect differences in IFN-β expression between the different porcine cell lines, indicated normalized expression data for IFN-β were analysed using the Kruskal-Wallis test and the post-hoc pairwise Wilcoxon test.

Correlations between the applied Poly(I:C) concentrations and the achieved IFN-β mRNA expression were identified by using Spearman`s correlation coefficient. Calculations were performed with the open-source software R studio (Posit PBC, Boston, MA, USA) whereas graphs were generated by GraphPad Prism 5.0 (GraphPad Software Inc., San Diego, CA, USA).

IV.   RESULTS

1.   Construction and quality control of recombinant MVAs

1.1.   Construction of recombinant MVAs

In collaboration with virological department of the Center for Molecular Biology „Severo Ochoa" in Madrid (Spain), I329L, DP96R, A238L and CD2v were identified as promising candidates to investigate MVA as viral vector for expression analysis of ASFV encoded immunomodulatory proteins.

During *in vitro* experiments, target genes were incorporated into the MVA genome via homologous recombination (as described in chapter *2.1.2 Generation of recombinant MVAs*). The generated recMVAs were investigated regarding their genomic integrity, the proper insertion of the GOI into the determined deletion site and the protein expression in CEF cells as well as in porcine cell lines.

1.2.   Genetic characterization of recombinant MVAs

To depict correct insertion of the target genes into the defined cloning site, oligonucleotide primers spanning the six major deletion sites (Fig. 9) (MVA-Del I to MVA-Del VI as described in chapter *1.5. Oligonucelotides*) and the intergenomic region between MVA069R and MVA070L (Fig. 10) (primer pair I8R-G1L as described in chapter *1.5. Oligonucelotides*) were used, respectively. The molecular weight of each PCR-product was predetermined by sequence data of the MVA genome and the gene of interest. Thus, size of the PCR product was enlarged according to the size of the target gene at the relevant insertion site.

Therefore, PCR-products of the major six deletion sites were compared between non-recombinant MVA F6 and the recMVA-I329L, recMVA-DP96R and recMVA-A238L. The increase of size for recMVA-I329L and recMVA-DP96R in the amount of ~430 bp and ~1.100 bp (Fig. 9) verified the correct insertion of the ASFV-GOI at deletion site III. To confirm the sequence integrity of the target gene and the deletion III region of the MVA genome, PCR products of the Del III – PCR for recMVA-I329L and recMVA-DP96R were sequenced, respectively. Alignment analysis of the sequencing data of the tested recMVAs completely coincided with the sequence of pre-assembled plasmid maps.
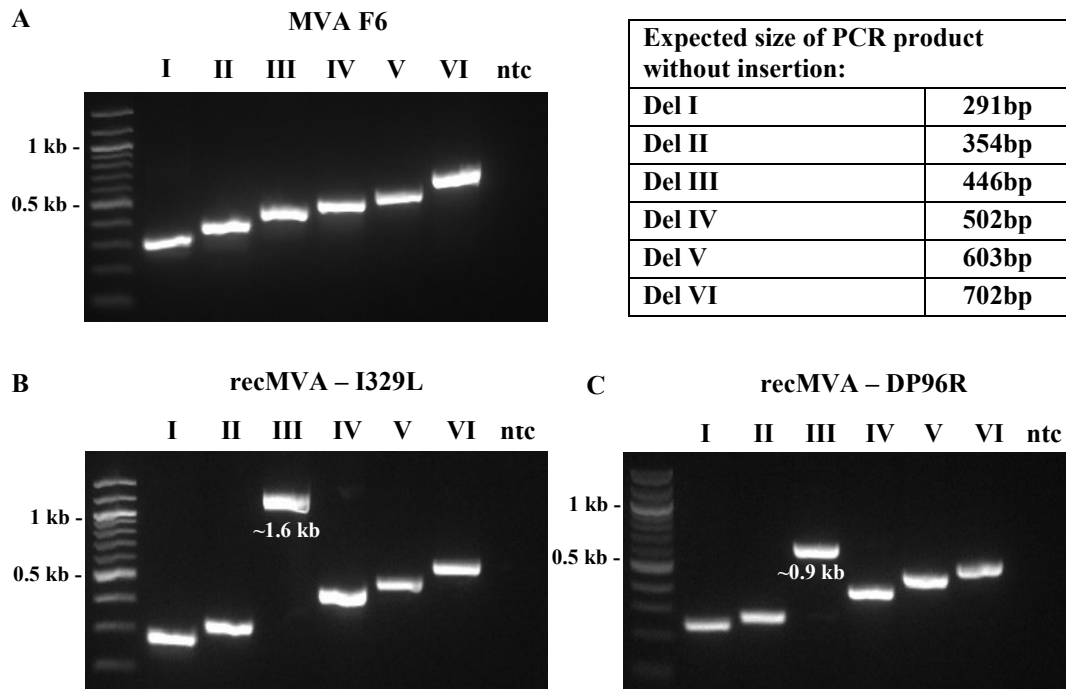
A

B

C

Expected size of PCR product without insertion:	
Del I	291bp
Del II	354bp
Del III	446bp
Del IV	502bp
Del V	603bp
Del VI	702bp

Fig. 9: Correct insertion of I329L and DP96R. Viral DNA was isolated and PCR for the major six deletion site of the MVA genome was performed (I - VI). Separation of the PCR products via agarose-gel electrophoresis verified proper insertion of (B) I329L (~1.6 kb) and (C) DP96R (0.9 kb) into the deletion III site of the MVA genome without affecting other possible insertion sites of (A) MVA.

In contrast, results for the Del III-PCR of recMVA-A238L offer the same molecular weight (446bp) as non-recombinant MVA F6 but depict an increase of size for the I8R – G1L-PCR to the size of 765bp, attesting the insertion of ASFV-A238L at the intended cloning site (intergenomic region between the genes M069R and M070L). Similar PCR results for MVA F6, recMVA-I329L, recMVA-DP96R and recMVA-A238L regarding the non-affected deletion sites confirm the integrity of the genomic regions.
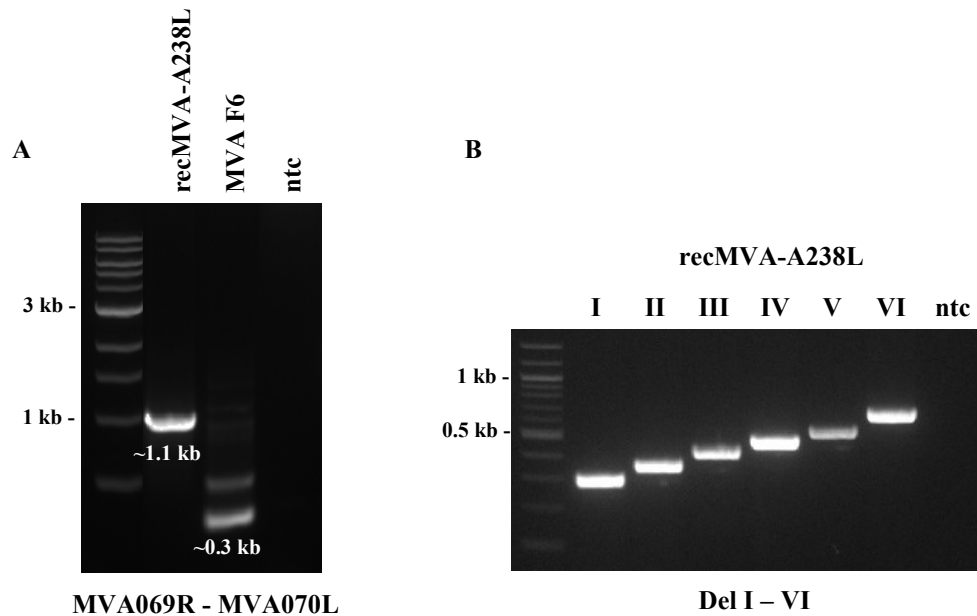
Fig. 10: Correct insertion of A238L. Viral DNA was isolated analysed for correct insertion of the target sequence into the intergenic region between the essential viral genes MVA069R and MVA070L (A) using agarose-gel electrophoresis. The MVA six deletion PCR depicted the genomic integrity of the major six deletion sites (B) of recMVA-A238L.

1.3.   Multi-step growth kinetics of recombinant ASFV-MVAs

To investigate whether replication deficiency of MVA was affected by insertion and expression of the inserted sequence, a multi-step growth analysis was performed on three different cell lines. Therefore, HaCat cells as well as PK1 cells were used as non-permissive, mammalian cell lines to guarantee a steady hazard potential of the biosafety level 1 for the operating staff and the ASFV target species. In terms of experimental control and growth kinetic comparison, CEF cells were incorporated into the studies as representative of MVA-permissive cell line. During the experiment, each cell line was infected with MVA-I329L, MVA-DP96R, MVA-A238L and MVA F6 at a MOI of 0.05 and cells were harvested at different timepoints post infection. To quantify virus titres of the different (recombinant) MVAs at the indicated timepoints, titration of each timepoint was performed on CEF cells independent of the primarily used cell line. For all tested recMVAs as well as for the non-recombinant MVA F6, productive viral replication was only observed in MVA-permissive CEF cells (Fig. 11). Moreover, titres of the ASFV-recMVAs were comparable to those of MVA F6, indicating preservation of replication capabilities for the recMVAs in permissive cell lines.
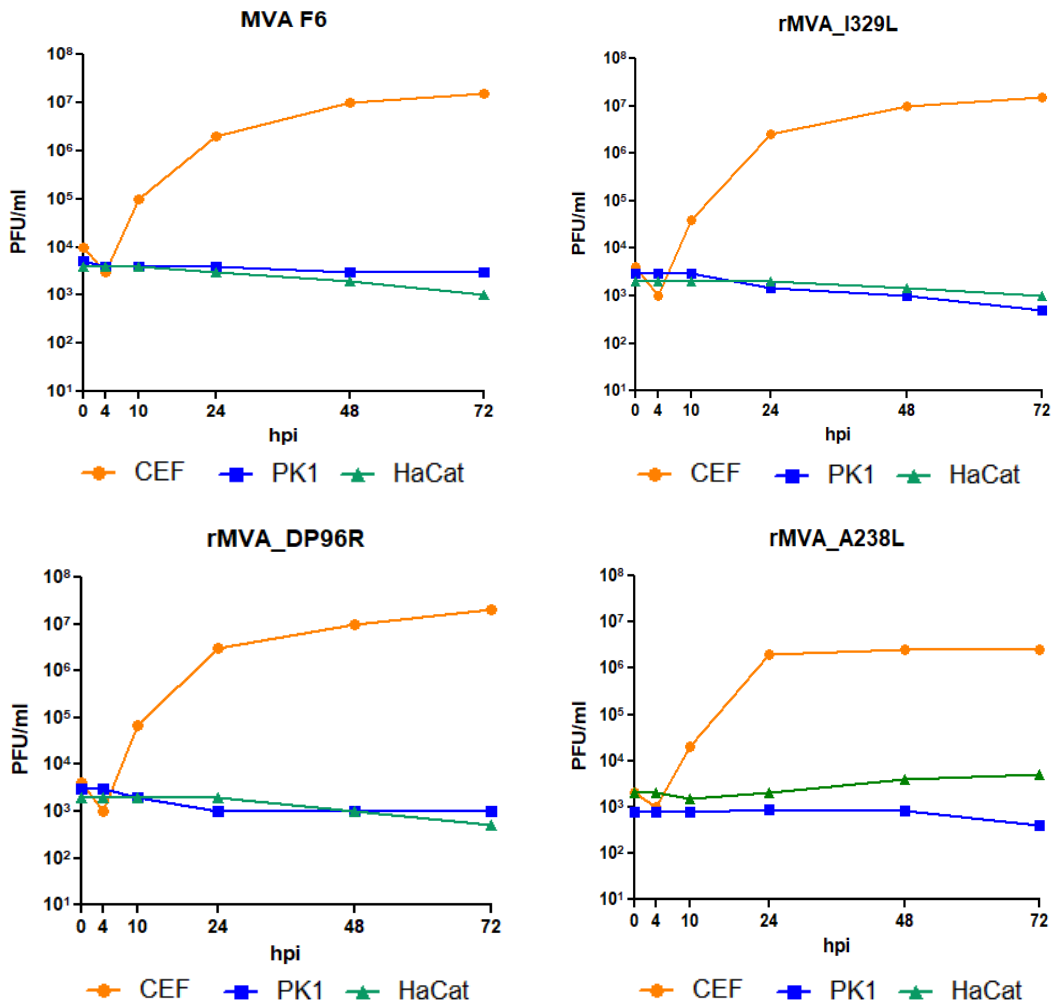
Fig. 11: Multi-step growth analysis of recombinant and non-recombinant MVA. Cells were infected with (recombinant) MVA and collected at determined timepoints. Virus titres were determined by counting plaque-forming units (PFU). MVA F6 as well as ASFV-recMVAs failed to replicate in cell lines with mammalian origin (PK1, HaCat), but were still able to replicate in CEF cells.

1.4.   Analysis of recMVA protein expression

1.4.1.   recMVA Protein expression in CEF cells

Due to the lack of target protein specific antibodies, the FLAG-tag sequence was necessary to evaluate protein expression of recMVAs. CEF cells were infected with a MOI of 5 of recMVA-DP96R, recMVA-I329L, recMVA-A238L and MVA F6, respectively. After 24h incubation time, cells were harvested and proteins were isolated. Immunoblots were performed with an anti-FLAG antibody and results were compared to calculated protein sizes. Additionally, encoded proteins were investigated regarding different protein variants. For all ASFV-recMVAs protein expression was verified and MVA F6 as well as cell control were negative after staining with the anti-FLAG antibody (Figs. 12 – 13).

After infection with recMVA-DP96R, the immunostaining unveiled DP96R as ~17.5 kDa sized protein (Fig. 12a), differing ~5kDa from the calculated protein size of ~12kDa.

For A238L, western blot analysis depicted two different protein variants with ~28kDa and a smaller variant with ~25kDa, spanning the estimated protein size of ~27kDa.
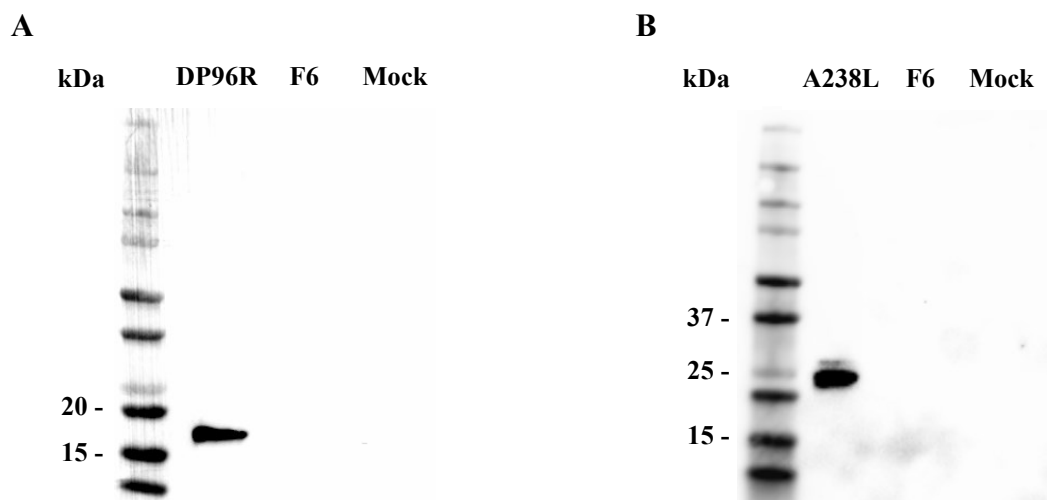

Fig. 12: Target gene expression of recMVA-DP96R and recMVA-A238L CEF cells were infected with recMVA-DP96R, recMVA-A238L or MVA F6 at a MOI of 5, respectively. Cells were harvested after 24h and proteins were separated by SDS-PAGE. The target proteins were stained using an anti-FLAG antibody. Non-infected CEF cells (mock) as well as F6 infected cell served as controls.

Infection with recMVA-I329L resulted in the detection of four different protein variants with a size of ~18kDa, ~30kDa, 55-65kDa and 110-120kDa (Fig. 13).

However, previous calculations showed a protein size of ~37kDa indicating I329L as glycoprotein. Therefore, protein isolates of recMVA-I329L infected CEF cells were incubated with PNGase F and Endo H, respectively (Fig. 13). In addition to the enzyme preparations, a non-digested control as well as a MVA F6 and a cell control were applied for western blot analysis. Endo H digested the variant with the highest molecular weight (110-120kDa) in favour of a variant, which appears to be slightly larger than the ~30kDa variant, whereas peroxidase signalling remains constant for the 55-60kDa variant suggesting that Endo H did not cleave the glycosidic linkage of the latter protein variant. For this reason, digestion of I329L with PNGase F is simultaneously performed in a second preparation. Besides digestion of high mannose and hybrid oligosaccharides, PNGase F cleaves complex oligosaccharides from N-linked glycoproteins. After incubation of I329L with PNGase F, an evident shift from both glycosylated forms to the variant, which is slightly larger than ~30kDa occurs without affecting the ~18kDa form (Fig. 13).
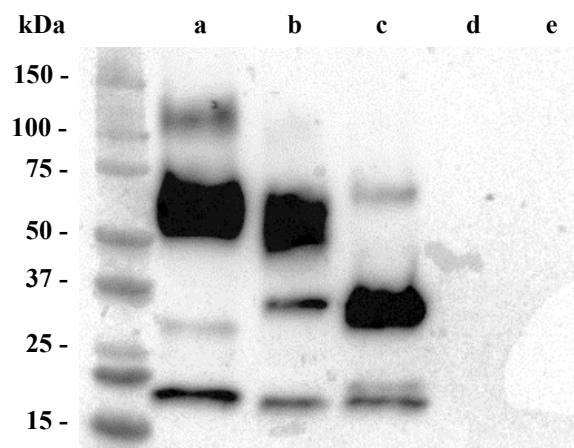

Fig. 13: I329L is a highly glycosylated protein. To investigate glycosylation of I329L, a non-digested protein isolate (a) is applied for SDS-PAGE together with Endo H (b) and PNGase F (c) incubated lysates. The MVA F6 and the cell control are applied in (d) and (e).

To investigate a possible time-dependent occurrence of the different protein variants of I329L, kinetic studies (Fig. 14) were performed on CEF cells. The recMVA-I329L infected cells were harvested at 0h, 4h, 10h, 18h, 24h and 48h. At timepoint 0h, the applied protein isolates were negative for the target protein. Due to the early/late promotor (pmH5) controlled protein expression of recMVA-I329L, first variants have already been detected at 4h post infection. At 10h and 24h p.i. accumulation of the different variants was observed, whereas at 18h and 48h p.i. a decrease of the protein concentration was monitored (Fig. 14). Interestingly, at 4h

p.i. the highly glycosylated variants were detectable, and the smaller variants occured simultaneously to the accumulation of the highly glycosylated variants.
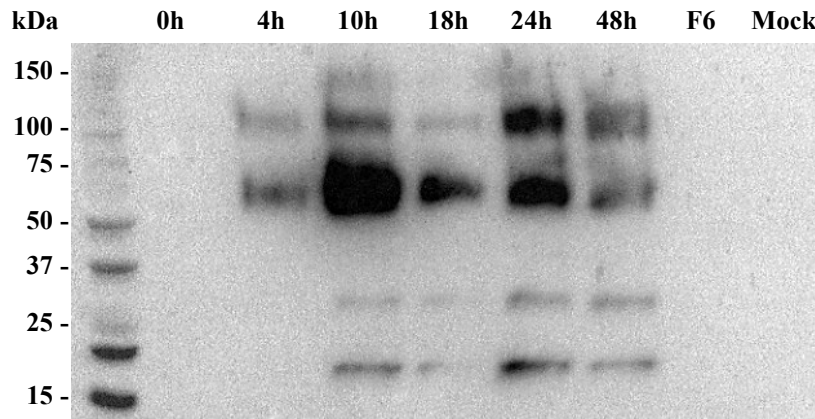

Fig. 14: Kinetic study of I329L. Protein isolates were obtained from recMVA-I329L infected CEF cells after an incubation time of 0h, 4h, 10h, 18h, 24h and 48h. At timepoint 4h p.i. first expression of I329L was detected, lacking the smaller and non-glycosylated variants (~18kDa, ~30kDa). With accumulation of the glycosylated variants (55-60kDa, 110-120kDa) smaller protein variants of I329L were visible.

1.4.2.   recMVA protein expression in porcine cell lines

For further immunomodulatory assays, performed in porcine cell lines, it was essential to verify recMVA protein expression in the non-permissive cell lines 3D4/21, IPEC-J2 as well as LLC-PK1. Therefore, each cell line was infected with recMVA-I329L, recMVA-CD2v, recMVA-DP96R and recMVA-A238L at a MOI of 5. Non-infected cells (Mock) as well as MVA F6 infected cells (MOI 5) served as controls. Cells were harvested after an incubation time of 24h. Isolated proteins were separated by SDS-PAGE and GAPDH as well as FLAG tagged ASFV-proteins were immunostained using appropriate antibodies. Anti-GAPDH immunoprecipitation (37kDa) was positive for all samples, whereas the anti-FLAG immunostaining was only positive for recMVA-CD2v, recMVA-I329L and recMVA-DP96R (Fig. 16). It was not possible to detect recMVA-A238L in porcine cell lines via western blot, contrary to former protein expression analysis of A238L in CEF cells. Interestingly, immunofluorescence microscopy depicted expression of A238L in the cytoplasm of infected J2 cells (Fig. 15a) but was negative for 3D4/21 cells and PK1 cells.
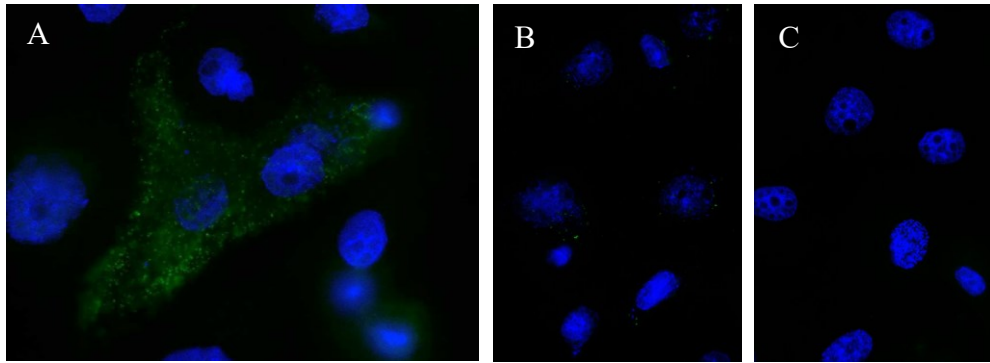
Fig. 15: Localization of A238L in the cytoplasm of J2 cells. RecMVA-A238L infected J2 cells were stained with an anti-Flag antibody and a corresponding conjugate (Alexa Fluor 488). Green fluorescence in the cytoplasm of the infected cells (A) verified expression of A238L. MVA F6 (non-recombinant) infected J2 cells (B) and non-infected J2 cells (C) served as controls.

According to the immunoblot performed for recMVA-DP96R infected CEF cells, DP96R was stably expressed in PK1, J2 and 3D4/21 cell lines with the ascertained size of ~17.5kDa (Fig. 16 a-c). The ASFV protein CD2v was also detected in all 3 porcine cell lines, but the HRP signalling was poor for PK1 cell lysates (Fig. 16c). The glycosylated variant of CD2v coincided with former protein expression studies performed on CEF cells in our lab, unveiling a size of 75-100kDa depicted in one thick band. In PK1 as well as in J2 cells, a glycosylated CD2v variant with a molecular weight of ~100kDa (Fig. 16b) was immunoprecipitated and in 3D4/21 cells two different glycosylated variants with ~75kDa and ~100kDa (Fig. 16b) were distinguished. These results imply that glycosylated variants of CD2v were represented by one thick band in CEF cells due to a strong expression level, which impeded the detection of a ~100kDa and a separate ~75kDa form of CD2v. Furthermore, a smaller variant with a molecular weight of ~25kDa (Fig. 16b) was detected in porcine cell lines, whereas former deglycosylation assays performed with CEF cell lysates resulted in a size 50-55kDa.

For I329L Anti-FLAG immunoblot results were heterogeneous, although Anti-GAPDH immunostaining was positive for all samples. In J2 cells, precipitated protein variants of I329L were mostly identical with the results described for recMVA-I329L infected CEF cell lysates, unveiling forms with the molecular weight of ~18kDa, ~30kDa, 55kDa and 60kDa (Fig. 16a). Apparently, the form with 110-120kDa was not detected in J2 cells and the thick 55-60kDa band monitored after infection of CEF cells (Fig. 13a) could be identified as two different

protein variants (Fig. 16a), one with the molecular weight of ~55kDa and the other with a molecular weight of ~60kDa. In infected PK1 cell lysates the ~18kDa as well
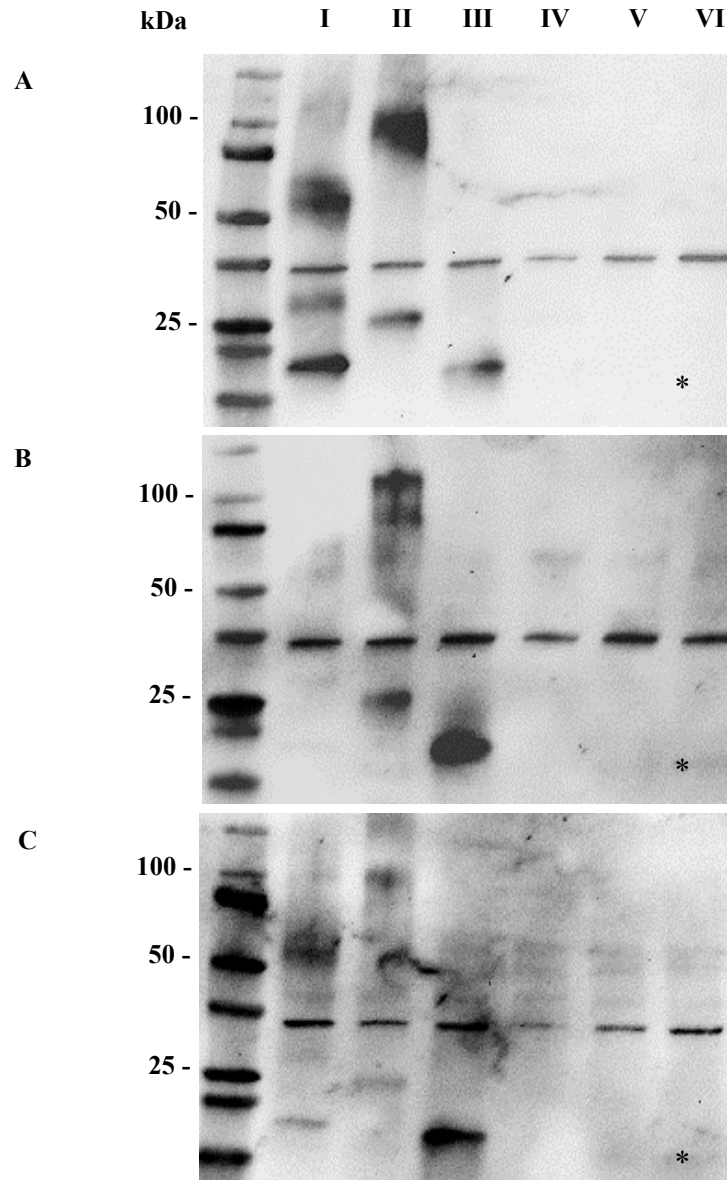
as the 55kDa and 60kDa forms of I329L could be distinguished (Fig. 16c). The immunoblot for I329L in 3D4/21 cells was not evaluable (Fig. 16b).

Fig. 16: Expression of I329L, CD2v and DP96R in porcine cell lines. J2 (A), 3D4/21 (B) and PK1 (C) cells were infected with recMVA-I329L (I), recMVA-CD2v (Kato et al.), recMVA-DP96R (III) or recMVA-A238L (IV). MVA F6 (V) infected, or not infected cells (VI) served as controls. Harvested samples were analysed via western blot. Anti-GAPDH (37kDa*) immunostaining was used to control the quality and quantity of the applied samples.

2.   MVA as viral vector in porcine cell lines

2.1.   Infectivity of MVA in porcine cell lines

To evaluate possible differences in susceptibility of PK1, J2 and 3D4/21 cells towards MVA, each cell line was infected with a recombinant MVA encoding the green fluorescent protein GFP under the control of a pvgf-promoter (MVA-pvgf-eGFP9) at ascending MOIs (0.1, 0.5, 1, 2, 5). Cells were evaluated after an incubation time of 7h and 24h regarding the spread of GFP fluorescence as well as the intensity of the GFP signalling using a fluorescence microscope (Keyence BZ-X700). Aim was an infection rate of at least 50%. Cell vitality was assessed in context with the non-infected cell control (mock). Evident GFP signalling was generated at a MOI of 5 and 24h p.i. in all used porcine cell lines (Fig. 17). With increasing incubation time, impairment of cell morphology is observed compared to non-infected cells. Majority of the infected 3D4/21 cells (Fig. 17a) still showed the characteristic polyglonal morphology and adherence, indicating a vital cell status after an incubation time of 24h at a MOI of 5. In contrast, PK1 cells (Fig. 17b) were strongly affected by the high viral load and long incubation time. However, the majority of the cells was still adherent and showed an intensive GFP signalling. MVA infected J2 cells demonstrated a strong fluorescence signal combined with sustained adherence and the characteristic squamous and cuboidal cell morphology.

In conclusion, MVA depicted a comparable infectivity between the different cell lines and a MOI of 5 was evaluated as optimum viral concentration for infection experiments in porcine cell lines.
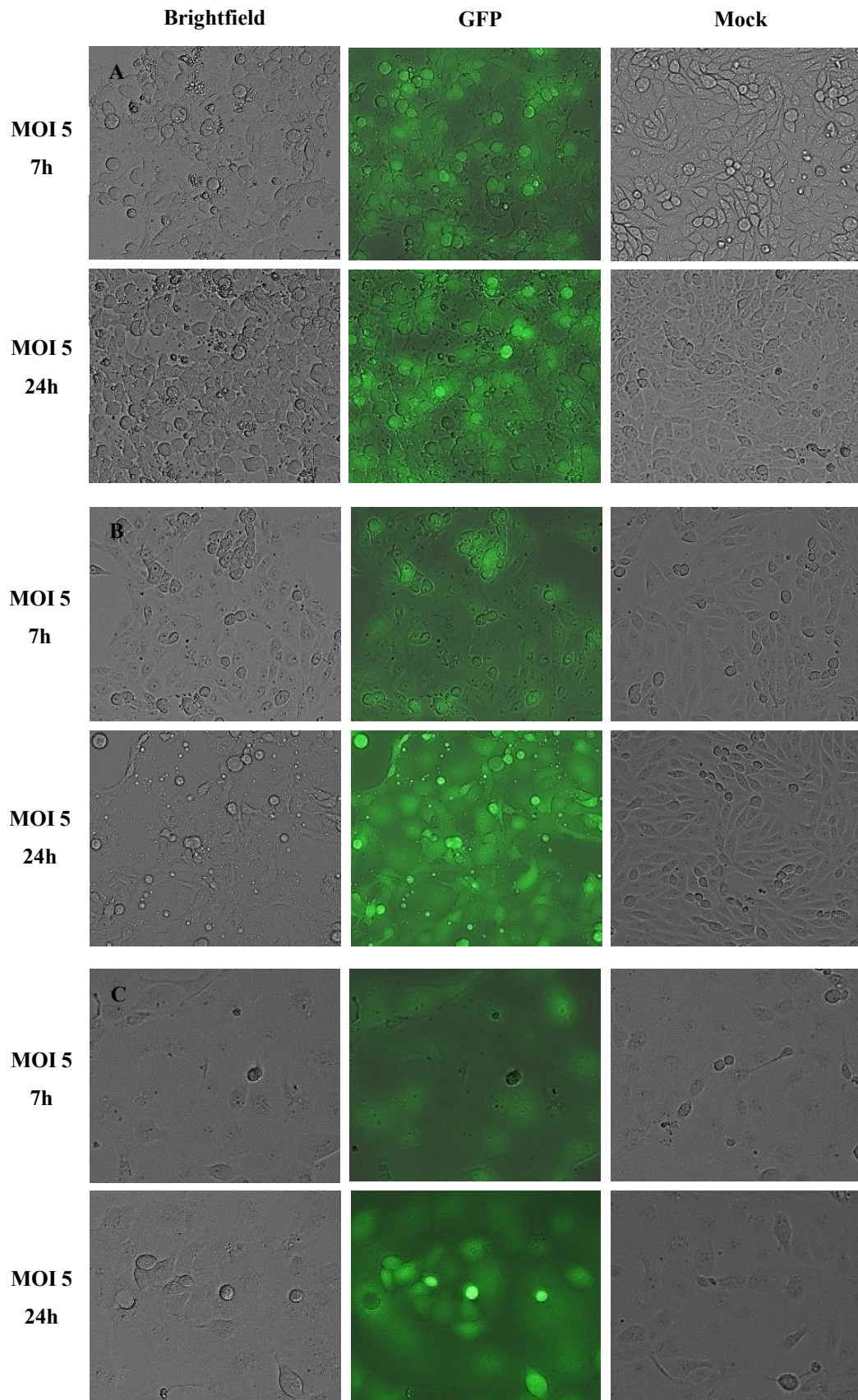
Brightfield	GFP	Mock

Fig. 17: The infectivity of MVA is similar between the porcine cell lines. 3D4 (A), PK1 (B) and J2 (C) cells were infected with MVA-pvgf-eGFP at a MOI of 5, expressing the green-fluorescent pigment GFP under the control of a pvgf-promoter, which provides strong and early transcription of GFP during MVA infection. The GFP signalling was evaluated after 7h and 24h p.i.. The strong expression of GFP 24h p.i. allowed the identification of infected cells.

2.2.   Time dependent target protein expression

After the optimum viral concentration of MVA in 3D4/21 cells has been defined, kinetic studies for the ASFV proteins were performed to identify the expression peak of the target protein in 3D4/21 cells. Therefore, cells were infected with ASFV-DP96R, ASFV-I329L and ASFV-CD2v at a MOI of 5. Cells were harvested at 0h. 4h, 6h, 10h, 18h and 24h p.i. (Fig. 18). Due to the lack of A238L expression in 3D4/21 cells, the protein was not involved into the kinetic studies. In summary, expression of the proteins DP96R (Fig. 18b) and I329L (Fig. 18a) initially occurs at the timepoint 8h p.i., whereas CD2v (Fig. 18c) was already detectable at 4h p.i.. Each ASFV protein reached its maximum after an incubation time of 18h. With increasing incubation time and sustained expression of viral proteins, infected cells were progressively damaged, which is depicted in a decrease of the housekeeping protein GAPDH (37kDa). Consequently, concentrations of the target proteins were impaired except for CD2v infected cells, indicating a moderate cell toxicity of that protein.

Results for the molecular weight as well as for the detected protein variants were comparable to former expression analysis (described in chapter *1.4. Western blot analysis of recMVA protein expression*).
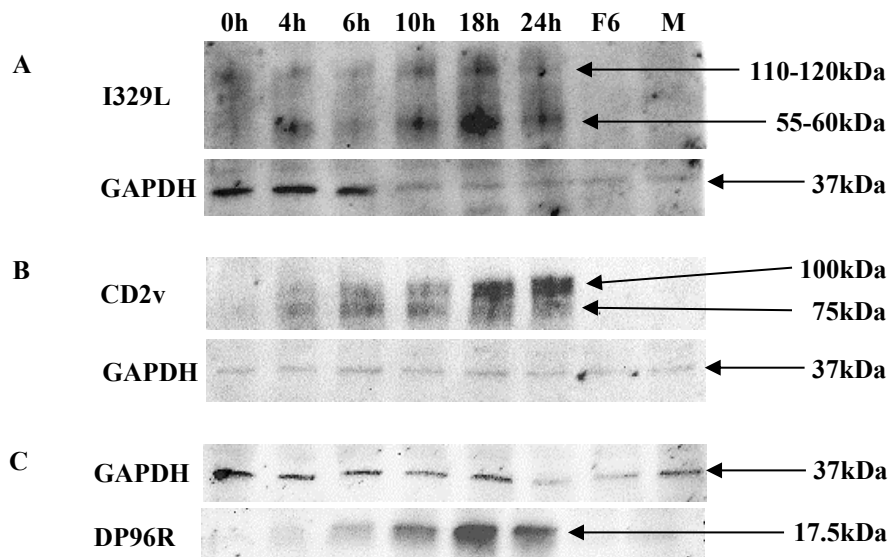

Fig. 18: Maximum expression of the target proteins at 18h p.i. in 3D4/21 cells. The recMVA infected cells were harvested at 0h, 4h, 6h, 10h, 18h and 24h. Immunoblot analysis of the corresponding lysates depicted a time dependent increase of I329L (A), CD2v (B) and DP96R (C) expression until 18h p.i..

2.3.   Distribution of ASFV proteins

3D4/21 cells were infected with each ASFV-recMVA at a MOI of 0.05 and target proteins were detected with an anti-FLAG immunostaining. The specificity of the primary antibody was confirmed by performing the same experiment with non-recombinant MVA (F6) and a Mock infected control, simultaneously. Both controls were negative regarding the detection of Alexa Fluor 488 signalling (Fig. 19d-e). Considering immunofluorescence results for I329L in 3D4/21 cells, slightly highlighted cell membranes are depicted for I329L (Fig. 19a), but CD2v was not detected in the cell membrane (Fig. 19b). However, both ASFV proteins seem to accumulate in an area next to the cell nucleus, whereas the remaining cytoplasm seems less affected by the immunostaining (Fig. 19a-b). DP96R was predominantly localized in the nucleus of 3D4/21 cells (Fig. 19c).
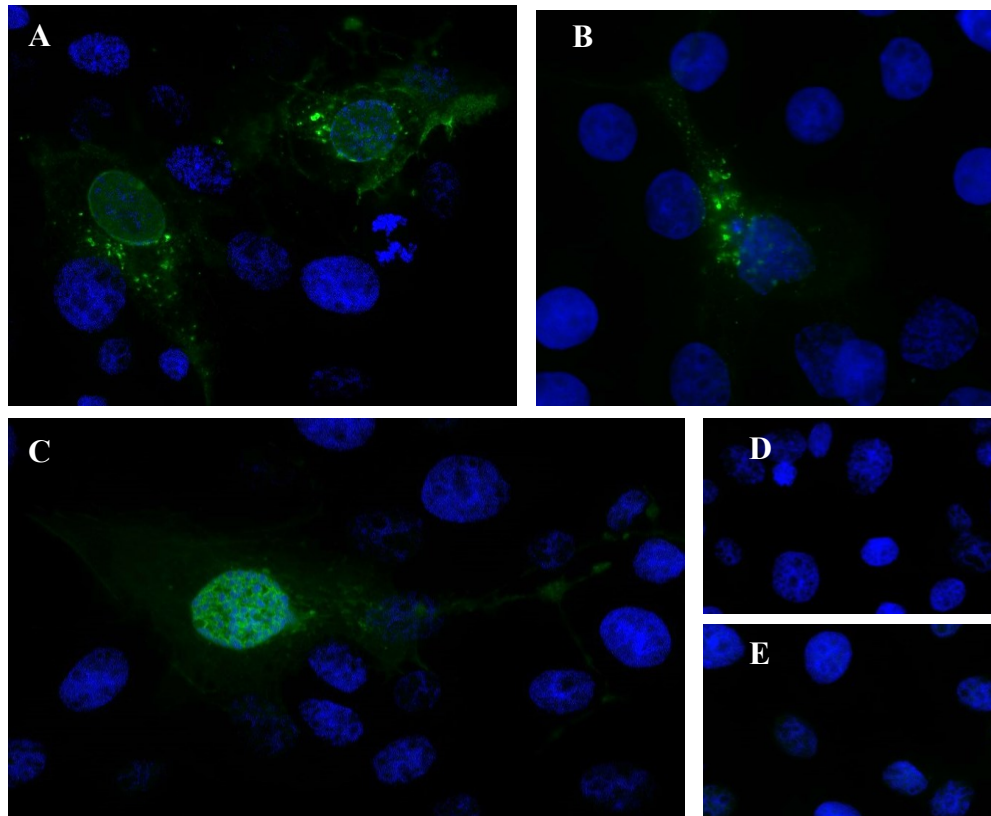

Fig. 19: Localization of ASFV target proteins in 3D4/21 cells. For immunofluorescence analysis, I329L (A), CD2v (B) as well as DP96R (C) were immunostained using an anti-FLAG antibody and DAPI was used as counterstaining. MVA F6 (D) and mock (E) controls were negative regarding the immunostaining.

2.4.   IFN-β production in porcine cell lines

After MVA was established as vector to study the expression of target proteins in porcine cell lines, we asked whether MVA is also an appropriate vector to investigate possible immunomodulatory capabilities of the target proteins on the antiviral response of the porcine innate immune system.

Therefore, different experiments were performed testing the inducibility of IFN-β expression in porcine cell lines as well as possible effects of non-recombinant MVA protein expression on IFN-β production in infected cells. Finally, the impact of recMVA target protein expression on IFN-β production was investigated in 3D4/21 cells.

For each experiment, mRNA expression levels of IFN-β were relatively quantified by probe-based qPCR in technical replicates. Therefore, GAPDH was used as housekeeping gene and normalized expression of IFN-β was calculated by the ΔΔCt-method offering preliminary data.

2.4.1.   MVA does not induce IFN-β expression in porcine cell lines

Experiments verifying MVA as inducer of the innate immune system *in vitro* were mostly performed on human or mouse derived cell lines and a lack of information about the impact of MVA on IFN-β production in porcine cell lines was unveiled. Hypothesizing MVA as possible inducer of IFN-β in porcine cell lines, the virus would be an elegant vector to study possible inhibitory effects of recMVA expressed target proteins on IFN-β production.

Therefore, PK1, J2 and 3D4/21 cells were infected with non-recombinant MVA (F6) at a MOI of 5. A non-infected cell control (Mock) was used to identify basal IFN-β expression in porcine cell lines. Cells transfected with 1µg/ml Poly(I:C) served as a positive experimental control. Intriguingly, mRNA expression levels of IFN-β in MVA infected cells were comparable to those in non-infected cells (Fig. 20). To exclude a negative effect of virus quantity and related cell damage on IFN-β production, the experiment was repeated with infection at a MOI of 1. Results did not differ compared to cells infected with MVA at a MOI of 5, confirming that MVA did not induce a detectable increase of IFN-β mRNA in PK1, J2 and 3D4/21 cells after an incubation time of 6h.

Consequently, Poly(I:C) was included into the protocol as IFN-β stimulant and MVA was used as protein expression vector, providing high levels of target protein

(as depicted in chapters *1.4 Analysis of recMVA protein expression* and *2.2 Time dependent target protein expression*).
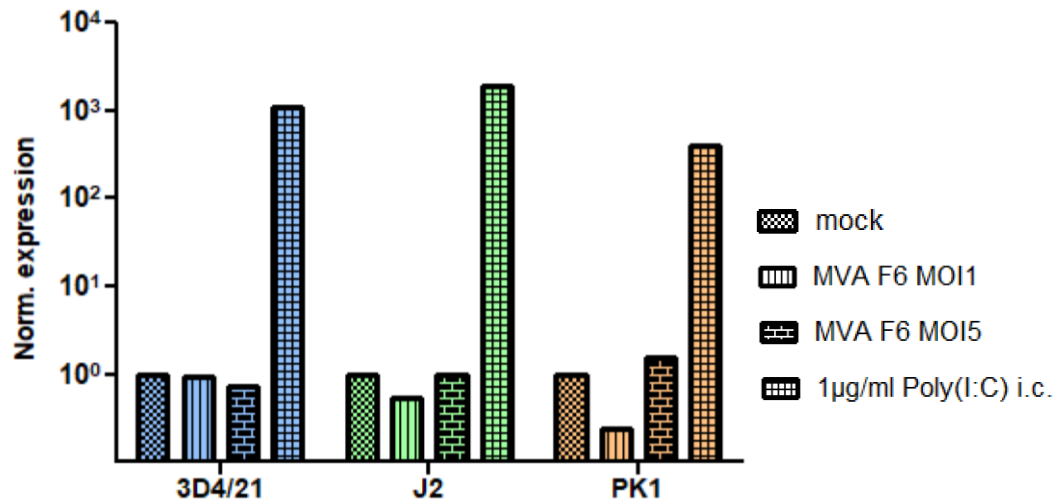

Fig. 20: Analysis of IFN-β expression in porcine cell lines in response to infection with MVA F6. Results for IFN-β expression in response to MVA infection at a MOI of 1 or at a MOI of 5 and stimulation with 1µg/ml intracellular Poly(I:C) are plotted for each cell line.

2.4.2. Poly(I:C) induced IFN-β expression

To elaborate IFN-β stimulatory faculties of Poly(I:C) and to identify the appropriate Poly(I:C) concentration, PK1, J2 as well as 3D4 cells were transfected with ascending amounts of Poly(I:C) (0.1µg/ml, 0.5µg/ml, 1µg/ml, 2µg/ml). In the following referred to as intracellular Poly(I:C) (Fig. 21a). In a second preparation, Poly(I:C) was added into the indicated cell culture media in ascending concentrations (1µg/ml, 2µg/ml, 5µg/ml, 10µg/ml, 25µg/ml) without transfection reagent. In the following referred to as extracellular Poly(I:C) (Fig. 21b).

The maximum IFN-β expression in J2 and PK1 cells was achieved at a concentration of 0.5µg/ml, respectively. For 3D4/21 cells the IFN-β expression peak was depicted at a Poly(I:C) concentration of 1µg/ml. Interestingly, J2 cells generated significantly higher (p-value < 0.001) IFN-β expression levels in response to intracellular Poly(I:C) than PK1 or 3D4/21 cells.

After stimulation with extracellular Poly(I:C), 3D4/21 as well as J2 cells showed increasing IFN-β levels, whereas in PK1 cells normalized expression of IFN-β is significantly lower (p-values < 0.001). Especially in J2 cells a strong positive correlation (r = 0.83, p-value < 0.001) between increasing amounts of extracellular Poly(I:C) and normalized IFN-β expression was verified. In 3D4/21 cells, IFN-β mRNA expression occurred to be constant from 1µg/ml to 10µg/ml extracellular

Poly(I:C) and rapidly increased with 25µg/ml extracellular Poly(I:C). It was not investigated whether concentrations of extracellular Poly(I:C) > 25µg/ml would further increase IFN-β expression in 3D4/21 cells.

In general, comparison of the IFN-β mRNA levels between the different application routes of Poly(I:C) constituted a highly significant IFN-β induction potential (p-value < 0.001) for intracellular Poly(I:C).
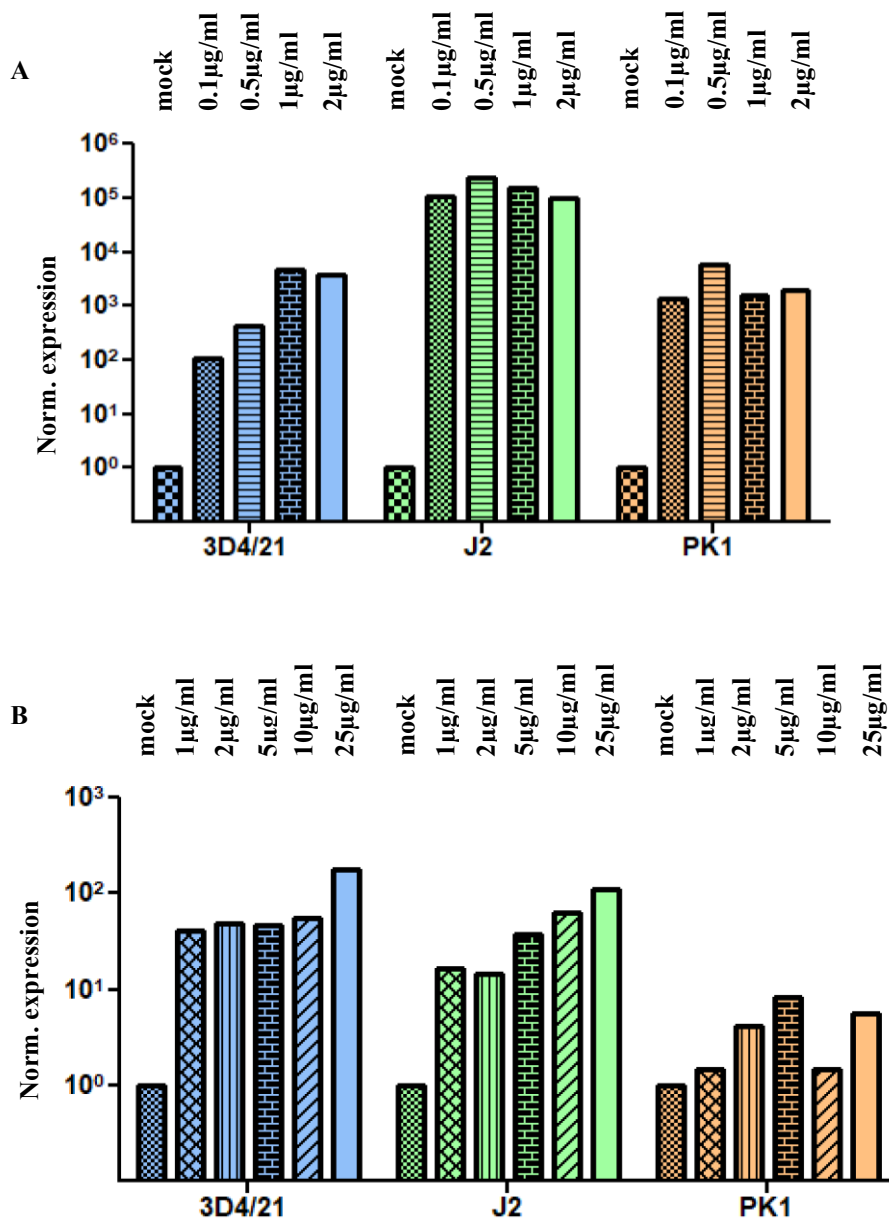

Fig. 21: IFN-β expression after stimulation with intra- or extracellular Poly(I:C) at different concentrations. In (A) IFN-β expression levels in response to intracellular Poly(I:C) are depicted, whereas in (B) results after extracellular Poly(I:C) stimulation are shown. The first bar constitutes the basal IFN-β expression for each cell line and is followed by bars showing the results for IFN-β expression with increasing concentrations of Poly(I:C). For intracellular Poly(I:C), the concentrations counted 0.1µg/ml, 0.5µg/ml, 1µg/ml and 2µg/ml (from left to right). For extracellular stimulation, concentrations of 1µg/ml, 2µg/ml, 5µg/ml, 10µg/ml and 25µg/ml (from left to right) of Poly(I:C) were used. Identical Poly(I:C) concentrations are indicated by replicated column patterns within the Poly(I:C) providing routes (intracellular, extracellular).

2.4.3.   Effects of MVA on Poly(I:C) induced IFN-β expression

To investigate potential impacts of MVA infection on Poly(I:C) induced IFN-β production, 3D4/21 cells were infected with non-recombinant MVA at an MOI of 5 or an MOI of 1 and additionally challenged with intracellular Poly(I:C) (1µg/ml) or extracellular Poly(I:C) (5µg/ml) (Fig. 22). After Poly(I:C) was added, the cells were incubated for 6h. The experiment was broadened by infection controls of MVA at indicated MOIs as well as by positive controls of intracellular and extracellular Poly(I:C) stimulation and a cell control (Mock). Compared to former experiments, results for the IFN-β expression levels in control samples were reproducible.

Interestingly, additional infection of Poly(I:C) stimulated cells with MVA at a MOI of 1 or at a MOI of 5 numbered a 5- to 8-fold reduced IFN-β expression in response to Poly(I:C) application compared to the Poly(I:C) control samples. In contrast, mRNA expression of IFN-β was ~27-fold enhanced when cells were stimulated by extracellular Poly(I:C) (5µg/ml) and additionally infected with MVA at a MOI of 1. After infection of the stimulated cells with MVA at a MOI of 5, the stimulatory effect of extracellular Poly(I:C) was increased by a factor of 7. In summary, MVA depicted IFN-β increasing capabilities combined with application of extracellular Poly(I:C) and showed a tendency to reduce IFN-β expression upon intracellular stimulation of 3D4/21 cells. Moreover, 3D4/21 cells infected at a MOI of 1 and stimulated by Poly(I:C) achieved higher IFN-β expression levels than cells infected with a MOI of 5 and stimulated by Poly(I:C).
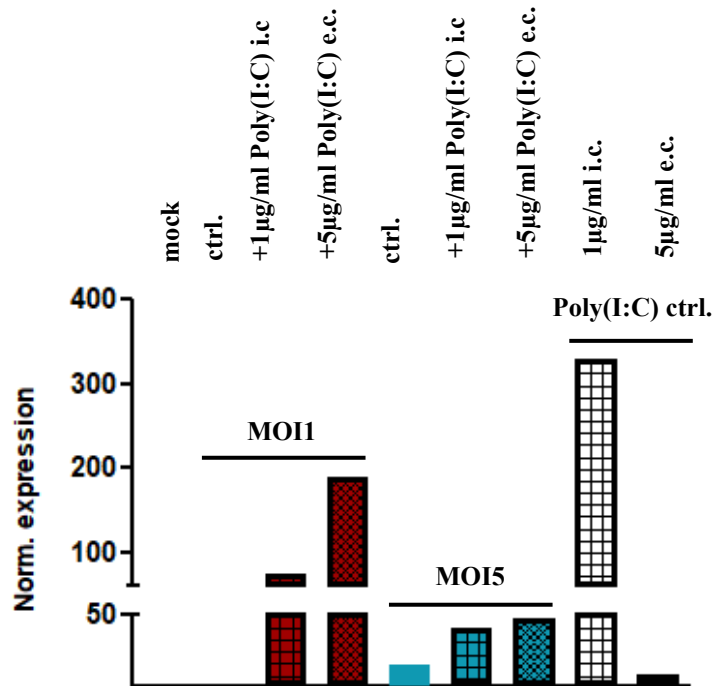
Fig. 22: Effects of MVA F6 on Poly(I:C) induced IFN-β expression. 3D4/21 cells with MVA at a MOI of 5 (blue bars) or at a MOI of 1 (red bars). 18h p.i. the cells were stimulated with Poly(I:C) at a concentration of 1µg/ml intracellularly (i.c.) or 5µg/ml extracellularly (e.c.). The experiment was controlled by a untreated cell control (mock) as well as by Poly(I:C) stimulated cells.

2.4.4.   MVA as vector to study effects of ASFV related proteins on IFN-β production in Poly(I:C) transfected cells

3D4/21 cells were infected with recMVA-I329L, recMVA-DP96R or recMVA-CD2v at a MOI of 5. 18h p.i., the cells were additionally stimulated with 1µg/ml intracellular Poly(I:C) and incubated for 2h. The identical experimental setup was simultaneously performed with non-recombinant MVA (F6) as internal control.

Finally, IFN-β expression levels of recMVA infected and Poly(I:C) stimulated samples were compared to the mock control as well as to Poly(I:C) stimulated control samples at indicated concentrations, application forms and timepoints. To analyse the effects of the target proteins on basal IFN-β production, cells were also infected with recMVAs without Poly(I:C) stimulation.
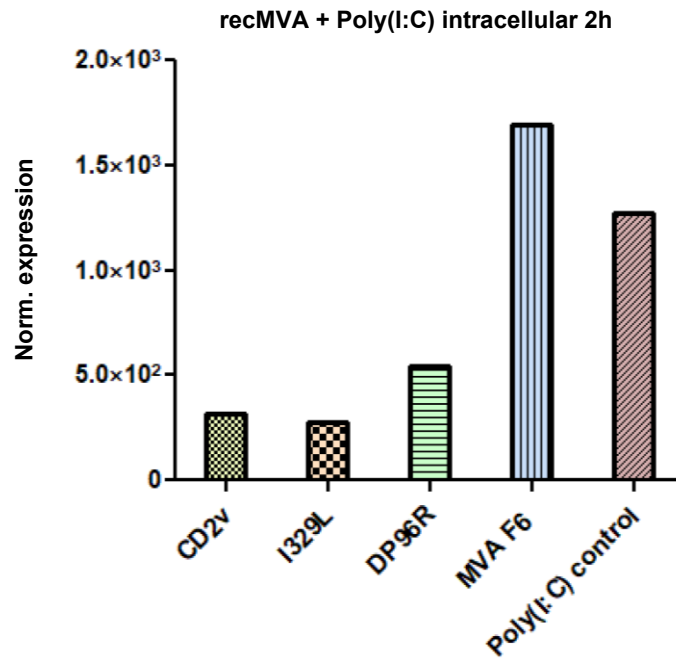
Fig. 23: Infection with recMVAs affected Poly(I:C) induced IFN-β expression. 3D4/21 cells were infected with recMVA-DP96R, recMVA-I329L or recMVA-CD2v. Cellular IFN-β mRNA synthesis was induced by transfection of 1μg/ml Poly(I:C). Cells infected with MVA F6 and stimulated with 1μg/ml intracellular Poly(I:C) as well as cells transfected with 1μg/ml Poly(I:C) served as controls. The quantity of IFN-β mRNA was investigated 2h post transfection.

Results for the IFN-β expression in control samples mostly coincided with former experiments as described previously. Interestingly, after Poly(I:C) transfected cells were incubated for 2h, IFN-β levels for non-recombinant MVA (MVA F6) infected cells were similar to the Poly(I:C) control (Fig. 23), counteracting inhibitory capabilities of MVA F6 after a Poly(I:C) incubation time of 6h (Fig. 22).

After infection with recMVA-I329L and transfection with 1μg/ml Poly(I:C) a ~ 4-fold decrease in the cellular IFN-β production was depicted (Fig. 23), verifying inhibitory faculties of I329L in 3D4/21 cells. Furthermore, I329L did not generate an IFN-β signal without Poly(I:C) stimulus (Fig. 24).

DP96R impaired mRNA expression levels of IFN-β 2h post transfection of 1μg/ml Poly(I:C). Compared to the Poly(I:C) control, DP96R decreased IFN-β expression by a factor of 2 (Fig. 23). IFN-β mRNA levels were comparable to the mock control in recMVA-DP96R infected cells (Fig. 24), missing the Poly(I:C) stimulation. N contrast, CD2v induced a ~320-fold increase of IFN-β mRNA without Poly(I:C) mediated stimulus. Interestingly, IFN-β expression was not exponentiated after intracellular (Fig. 23) or extracellular (Fig. 25) substitution of Poly(I:C).
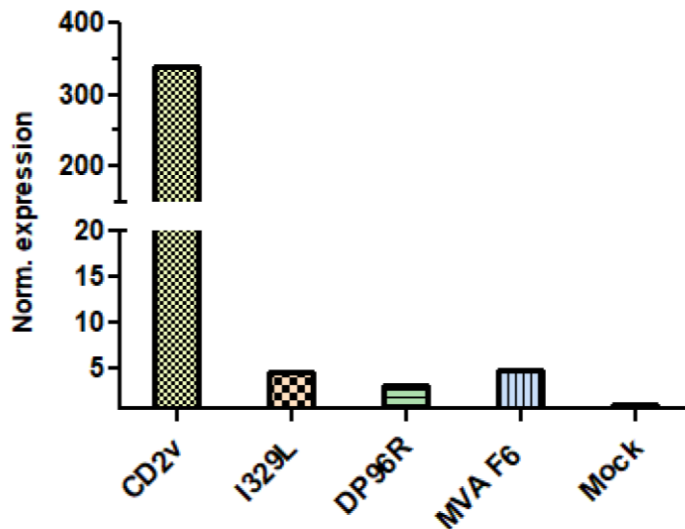
Fig. 24: CD2v induced IFN-β expression. 3D4/21 cells were infected with ASFV-recMVAs and MVA F6 (non-recombinant) at a MOI of 5. CD2v was able to generate an IFN-β response. In contrast, IFN-β expression levels in response to I329L and DP96R were similar to the mock control.

2.4.5.   Extracellular Poly(I:C) mediated IFN-β production is not affected by recMVA protein expression

To investigate possible effects of the Poly(I:C) application route on the experimental setup, recMVA infected 3D4/21 cells were also stimulated with extracellular Poly(I:C) at a concentration of 5µg/ml and incubated for 2h (Fig. 25). After infection with recMVAs at a MOI of 5 and stimulation with 5µg/ml extracellular Poly(I:C) IFN-β mRNA expression levels were comparable to the Poly(I:C) controls (Fig. 25). On the contrary, MVA F6 was able to induce a 5-fold increase of IFN-β expression. The stimulatory capabilities of non-recobinant MVA on extracellular Poly(I:C) induced IFN-β expression were described previously (in chapter *2.4.3. Effects of MVA on Poly(I:C) induced IFN-β expression*).
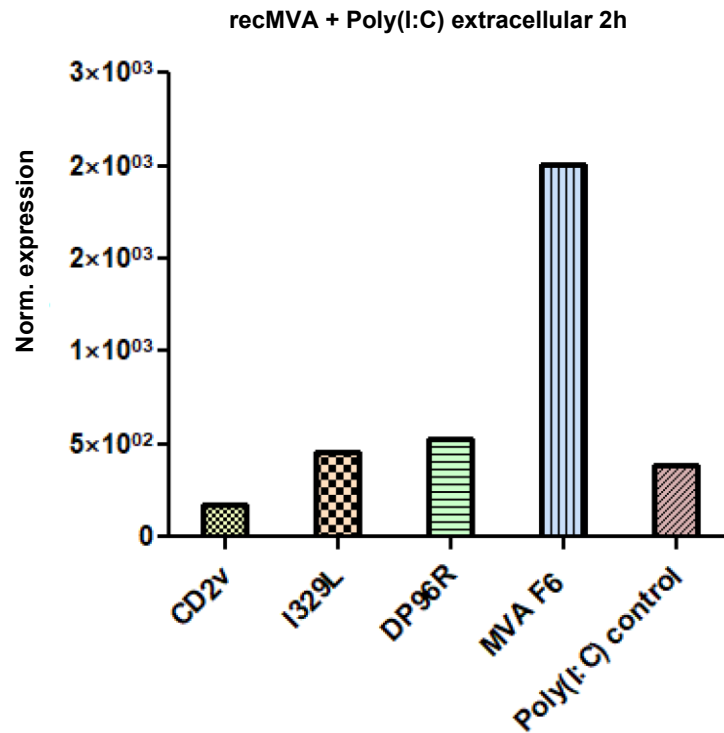
Fig. 25: Unaltered IFN-β expression after infection with recMVAs and stimulation with extracellular Poly(I:C). 3D4/21 cells were infected with recMVA-CD2v, recMVA-I329L and recMVA-DP96R, respectively. 18h p.i. the cells were stimulated with 5µg/ml extracellular Poly(I:C). The experiment was controlled by extracellular Poly(I:C) (5µg/ml) stimulated cells as well as MVA F6 infected and extracellular Poly(I:C) stimulated cells. In contrast to the results after Poly(I:C) transfection, neither DP96R, nor I329L depicted an effect on extracellular Poly(I:C) initiated IFN-β expression in 3D4/21 cells independent of the incubation time.

V. DISCUSSION

ASF is a threatening disease for domestic and wildlife pig populations. Considering the history of ASF outbreaks since its first description in 1921, it is undeniable that ASF is a smoldering disease easily (re)introduced into any country worldwide. Main reasons are global trade and infected wild boar populations in neighboring countries. In contrast to the first intercontinental outbreak in the 1960s, ASF is not eradicated in most countries since its global outbreak in 2018, although multiple trade restrictions are enacted, and different eradication programs are performed. Currently, no effective and safe vaccines against ASFV are available. Consequently, there is a constant pressure on the global pork meat industry. For the development of effective vaccines in the future, the investigation of ASFV protein expression, especially of conserved antigens, as well as the unveiling of protein mediated effects on the host immune system, is most important.

In this study, MVA was evaluated as expression vector for selected ASFV proteins. Genomic sequences of I329L, DP96R, A238L and CD2v were cloned into the MVA vector system. MVA mediated high-level protein expression of the target proteins enabled the analysis of different protein variants in cell lines of avian and porcine origin. Furthermore, the cellular distribution pattern of the ASFV proteins was studied in a porcine alveolar macrophage cell line (3D4/21) via immunofluorescence microscopy.

Finally, effects of the target proteins on cellular IFN-β production as well as modulation of the IFN-β expression upon Poly(I:C) stimulation were investigated in 3D4/21 cells.

Taken together, MVA represents a valuable tool to investigate expression of ASFV proteins and is a promising candidate to study the impact of target protein expression on the innate immune response *in vitro*.

Advantages of using MVA as expression vector

MVA represents a popular viral vector to study protein functions and is commonly used as vaccine platform against human and animal diseases. Besides its strong immunogenic capacities, one of the main advantages of MVA is the high safety record due to the deletion of multiple virulent genes during several hundred passages in the 1960´s (Volz & Sutter, 2017). Therefore, MVA is not able to replicate in human and most mammalian cells and is categorized as risk group 1 by the German central commission for biological safety (ZKBS). The replication deficiency of MVA was sustained after insertion of ASFV related genes into the MVA backbone and allowed the investigation of ASFV encoded proteins under biosafety level 1. In contrast, handling of ASFV deletion mutants would increase hazard of the environment resulting in reservation of ASFV related research to laboratories with biosafety level 3 permissions (African Swine Fever Biological Agent Reference Sheet, EHS – Cornell University).

Moreover, ASFV encodes 151 to 167 ORFs depending on the genotype and some of the proteins are able to compensate a loss of function of related proteins, after genetic sequences have been deleted (Abrams et al., 2008; Dixon et al., 2004; Koltsov et al., 2023). Those compensatory mechanisms might complicate the evaluation of protein functions in experiments using ASFV deletion mutants, whereas constructed recMVAs express a defined target protein in high amounts in permissive and non-permissive cell lines, allowing the isolated investigation of the protein function in different cell lines (Sutter & Staib, 2003). The qualification of MVA as expression vector for ASFV related proteins is further underlined by the phylogenetic relation of poxviruses and asfivirus constituted in similar replication strategies of the DNA-viruses in the cytoplasm of infected cells.

Characterization of recMVA protein expression

For protein expression analysis of DP96R, A238L, I329L and CD2v permissive CEF cells as well as described porcine cell lines were infected with the appropriate recMVAs and results were compared to published data as well as to protein size calculations.

The estimated size of DP96R counted ~12kDa, the actual protein weight in western blot analysis depicted ~17kDa (Fig. 11a). These results were consistent with observations of Zsak et al., who describes DP96R as a theoretically 10.7 kDa sized protein but detect a ~15kDa protein during immunoblot analysis (Zsak et al., 1998).

Remaining differences in size can be ascribed to the additional weight of the FLAG-tag comprising about 1kDa.

The expression of CD2v in porcine cell lines coincided with results of former protein expression studies on CEF cells as well as with published data of Chaulagain et al., depicting variants with ~15kDa, ~25kDa, ~55kDa and a variant that is slightly smaller than 100kDa as well as a variant that is slightly heavier than 100kDa in PK15 cells (Chaulagain et al., 2021).

For the ASFV protein A238L, we found a larger (~28kDa) and a smaller variant (~25kDa) in CEF cells, according to Silk et al. depicting a 28kDa and a 32kDa variant in Vero cells (Silk et al., 2007). The smaller variant is suggested as consistent cytoplasmic form of A238L, possibly binding calcineurin resulting in inhibition of T cell dependent immune response (Silk et al., 2007). The higher molecular mass variant is assumed as predominant nuclear form of A238L, which may inhibit interaction of NF-κB with host cell DNA causing diminished IFN-β production (Silk et al., 2007). However, protein sizes differ from published data ~5kDa for each protein variant (Silk et al., 2007) but with ~25 and ~28kDa western blot analysis overlaps with the assumed protein weight of ~27kDa. Interestingly, in J2 cells distribution of A238L seems to be limited to the cytoplasm indicating that only the smaller cytoplasmic variant was detected or that the nuclear variant of A238L is not expressed in J2 cells.

The ASFV encoded protein I329L is reviewed as highly glycosylated transmembrane protein (Correia et al., 2023; de Oliveira et al., 2011). These observations are confirmed by our western blot data depicting four different protein variants of I329L in CEF cells, whereof two variants were deglycosylated by digestion with Endo H and PNGase F, respectively. With our own performed deglycosylation assays we were able to reconstruct data from de Oliveira et al., unveiling the 55-65kDa variant as a proteoglycan with a complex N-linked oligosaccharide. Moreover, we characterized an additional variant with a molecular weight of 110-120kDa by digestion with Endo H. Considering that Endo H does not cleave complex oligosaccharides as PNGase F, the glycan of 110-120kDa is verified as member of the high mannose and hybrid oligosaccharides. Furthermore, whether PNGase F nor Endo H produced a shift towards the small ~18kDa variant, indicating that the 18kDa form might be a product of protein degradation, an intermediate form of the ~30kDa variant or a splicing variant.

The calculated molecular weight for I329L was ~37kDa, which coincided with the

unglycosylated ~35kDa variant. The remaining difference in size is explained by the flag-TAG constituting about 1kb.

Interestingly, the glycosylated variants of I329L with a molecular weight of 55-65kDa and 110-120kDa were detected during early protein expression of MVA 4h p.i.. According to the continuous expression of the target protein, the cell translation machinery as well as the glycosylation machinery might be saturated, resulting in aggregation of premature polypeptides and protein variants lacking the posttranslational modification. For this reason, it is questionable if the smaller protein variants (~18kDa, ~30kDa) have distinct functions compared to the mature glycosylated forms (55-60kDa, 110-120kDa) or if those forms describe a collateral effect. Furthermore, the protein quantity seemed decreased at 18h and 48 p.i.. Reason for the decreased target protein detection at 18h p.i. might be a difference in the generally applied protein concentration contrary to the other timepoints. In contrast, 48h p.i. CEF cells were already decrepited by the high viral load explaining a reduced protein expression.

The observed accumulation of the target proteins in porcine cell lines is explained by the control of target protein expression by the pmH5 promoter in the viral backbone, providing strong protein transcription during early and late phase of MVA infection. The protein concentration of I329L, DP96R and CD2v reached its maximum 18h p.i.. Interestingly, in 3D4/21 cells I329L was rapidly depleted after its expression peak 18h p.i., resulting in poor results at later timepoints.

In summary, correct protein expression of the ASFV-recMVAs was verified in porcine cell lines and CEF cells, considering published data. Moreover, results regarding target protein expression in CEF cells and porcine cell lines were comparable for the glycosylated ASFV proteins I329L and CD2v and identical for DP96R. The lack of A238L expression in PK1 and 3D4/21 cells remains unclear, but we hypothesize a cell dependent mechanism. Therefore, MVA was repeatedly confirmed as adequate vector for protein expression studies.

Evaluation of target protein distribution in 3D4/21 cells

The plenitude of published data provides a lot of information regarding the cellular distribution of the ASFV proteins I329L, DP96R and CD2v. However, distribution studies of the described proteins are mainly performed in Vero cells, HEK cells, NIH-3T3 or PK15 cells (Chaulagain et al., 2021; Correia et al., 2023; de Oliveira et al., 2011). For this study, a porcine kidney cell line (PK1), a porcine jejunal

epithelium cell line (J2) as well as a porcine alveolar macrophage cell line (3D4/21) was used to investigate possible differences regarding the MVA susceptibility or the target protein expression between the distinct cell lines. An important selection criterion was the competence to express IFN-β (Deng et al., 2020; Liu et al., 2020; Zhou et al., 2020). Moreover, ASFV is verified to have a strong tropism for macrophages, underlining the relevance of 3D4/21 cells to study ASFV related proteins *in vitro* (Gómez-Villamandos et al., 2013).

The predominant distribution of I329L in 3D4/21 cells was mainly consistent with published distribution studies in Vero and NIH-3T3 cells (Correia et al., 2023; de Oliveira et al., 2011). In the latter, I329L is associated with early endosomes, the cell membrane, the endoplasmic reticulum and the golgi apparatus in accordance with its function as inhibitor of the TLR3 pathway of the host cell (Correia et al., 2023; de Oliveira et al., 2011). Localization at the ER and golgi apparatus explained the accumulation of I329L in the perinuclear area of 3D4/21 cells. The main difference was the minor localization of I329L in the cell membrane of 3D4/21 cells.

The same effect was observed for CD2v. Referring to localization studies of Chaulagain et al., CD2v unveiled a strong expression pattern and was detected in the cytoplasm, the perinuclear area and the cell membrane of PK15 cells (Chaulagain et al., 2021). In 3D4/21 cells, the centering of CD2v in the perinuclear region was replicable, but in the remaining cytoplasm only a low fluorescence signal was generated, and the protein was not detected in the cell membrane 18h p.i. Therefore, we hypothesize an impaired transport of glycosylated protein variants from the perinuclear area to the cell membrane in recMVA infected 3D4/21 cells.

Interestingly, MVA was verified to reorganize the cytoskeleton and to accumulate in infected HeLa cells (Gallego-Gómez et al., 2003). However, in PtK2 cells MVA lacked to rearrange the microtubule system compared to wild-type Vaccinia Virus Ankara (Schepis et al., 2006). Taken together, the capability of MVA to impair the intracellular trafficking might be a cell line dependent phenomenon. Consequently, it remains unclear whether MVA is the causing agent for rearrangement of cellular actin filaments and altered endosomal trafficking in non-permissive cells, inhibiting the transport of glycosylated I329L to the cell surface. Furthermore, cell dependent or incubation time dependent mechanisms are suggested, either.

DP96R is unveiled as downregulator of IFN-β production in transfected HEK293T

cells. It functions as inhibitor of the cytoplasmic TBK1 and the subsequent phosphorylation of IRF3. Phosphorylated IRF3 is an essential transcription factor for IFN-β expression, (Lin et al., 1998; Schafer et al., 1998; Wathelet et al., 1998; Yoneyama et al., 1998). Predominant localization of DP96R in the cellular nucleus of 3D4/21 cells might indicate additional functions of the target protein in the nucleus of infected cells during ASFV infection.

MVA mediated modulation of Interferon-β in porcine cell lines

In contrast to former experiments performed in our labaratory, confirming IFN-β stimulating properties of MVA, we failed to induce an IFN-β signal at a MOI of 1 or MOI of 5 in porcine cell lines. Moreover, quantified IFN-β expression tends to be slightly reduced after infection with MVA and subsequent transfection of Poly(I:C). In contrast, we detected an increase of IFN-β production after infection with MVA and subsequent extracellular application of Poly(I:C) in 3D4/21 cells compared to Poly(I:C) stimulated cell controls. While attempting to explain those observations by current literature, we noticed a lack of information about non-recombinant MVA mediated induction of type I interferons in pigs *in vivo* as well as *in vitro*. However, infection of human or mouse-derived cells with non-recombinant MVA induced the IFN-β expression due to activation of the protein kinase R (PKR) and cGAS/STING pathway (Dai et al., 2014; Wolferstätter et al., 2014).

Although MVA deleted large genomic regions coding for immunoevasive proteins, some of the potential virulent factors of its ancestor Vaccinia virus Ankara (VVA) were retained during the serial passages on CEF cells. For example, E3L is an important virulence factor of Vaccinia virus (VV) inhibiting different nucleic acid sensing mechanisms of the host cell to avoid IFN-β induction in infected cells (Marq et al., 2009; Xiang et al., 2002). The functions of E3L during MVA infection are less well understood, but Hornemann et al. verified MVA encoded E3L as indispensable for successful cultivation and viral replication in CEF cells due to inhibition of CEF cell apoptosis and type I IFN production (Hornemann et al., 2003). In human HeLa cells, MVA encoded E3L is also essential for antigen production in the late phase of viral gene expression and appropriate viral replication (Ludwig et al., 2005). In conclusion, MVA encoded E3L interacts with host cell factors to protect viral life cycle in infected cells independent of the host species, but precise mechanisms are not elucidated.

In other experiments, IFN-β production and immunogenicity of MVA was improved in mice after deletion of genes encoding for A46R, A44L and C12L (Holgado et al., 2016).

In summary, the MVA genome still codes for proteins which unveil remaining virulence to ensure viral replication and antigen expression necessary for usage as viral vector. Identification of a certain viral protein, responsible for the lack of IFN-β induction in response to MVA infection in porcine cell lines needs further investigation. We hypothesize a combination of different MVA proteins as well as cell line dependent abnormalities. Unfortunately, there is no clear information about the paradox intensification of IFN-β expression after infection with MVA and extracellular application of Poly(I:C) in literature.

Modulation of IFN-β expression by I329L, DP96R and CD2v

The recMVA expressed protein I329L decreased IFN-β production in 3D4/21 cells after infection with recMVA-I329L and transfection of Poly(I:C). On the contrary, IFN-β expression levels remained unaltered after infection with recMVA-I329L and extracellular application of Poly(I:C). However, comparable experiments in HEK cells unveiled the opposite. De Oliveira et al. depicted an impressive impairment of IFN-β production due to expression of I329L in combination with extracellular application of Poly(I:C) at a concentration of 25µg/ml and an incubation time of 6h (de Oliveira et al., 2011). In contrast, I329L failed to inhibit IFNβ expression in cases Poly(I:C) (0.5µg/ml) was provided intracellularly (de Oliveira et al., 2011). Considering I329L as a homologue to TLR3, we hypothesized a correlation between the application route of Poly(I:C), the initiated cellular pathway and the cellular distribution of I329L to explain I329L mediated results.

As synthetic analogue to dsRNA, Poly(I:C) is detected by different dsRNA sensing mechanisms in challenged cells (Palchetti et al., 2015). Therefore, the application route of Poly(I:C) determines the activation of indicated dsRNA sensing pathways. A common procedure to introduce nucleic acids into targeted cells is provided by Lipofectamine, forming stable lipoplexes with the entrapped nucleic acid. Poly(I:C) delivered by lipofection enters transfected cells mainly via endocytosis and is actively transported towards the nucleus using microtubules (Sauer et al., 2009). During the endosomal pathway, Poly(I:C) is detected by endosomal TLR3 activating the downstream signalling cascade by homodimerization, leading to expression of IFN-β and other chemokines (Bianchi et al., 2017; Palchetti et al.,

2015; Sauer et al., 2009). Interestingly, the majority of transfected Poly(I:C) is entrapped in endosomes up to 24h post transfection, whereas a minority is released into the cytoplasm activating the RIG-1/mda-5 pathway (Matsumoto & Seya, 2008; Palchetti et al., 2015; Sauer et al., 2009).

Due to higher efficiency, Poly(I:C) is mainly transfected in vitro and mechanisms during cell activation with extracellular Poly(I:C) are less precisely elucidated than for intracellular Poly(I:C). Extracellular Poly(I:C) is incorporated into cells by endocytosis and induced TLR3 associated signalling cascades via entering the endosomal pathway (Itoh et al., 2008; Matsumoto & Seya, 2008; Watanabe et al., 2011). However, TLR3 is also localized at the cell surface detecting Poly(I:C) and activating IFN-β transcription (Itoh et al., 2008; Matsumoto et al., 2002; Watanabe et al., 2011). It remains unclear, whether endocytic or surface mediated TLR3 signalling dominated the IFN-β induction in response to extracellular application of Poly(I:C). In accordance to transfected Poly(I:C), extracellular Poly(I:C) is additionally reviewed as activator of the RIG-1/mda-5 pathway (Watanabe et al., 2011).

Comparing the two application routes of Poly(I:C), intracellular Poly(I:C) provided a more efficient induction of IFN-β expression by endosomal activation of TLR3 due to high transfection rates of Lipofectamine (Palchetti et al., 2015). This observation was confirmed by our own data, depicting a massive IFN-β expression in response to Poly(I:C) transfection.

Taken together, I329L is predominantly localized in the perinucear region of 3D4/21 cells and interferes with endosomal TLR3 resulting in a decrease of IFN-β production after transfection of Poly(I:C). In contrast, I329L is poorly detected in the cell membrane of 3D4/21 cells. Therefore, inhibition of TLR3 at the cell surface was not achieved in this experiment. Consequently, IFN-β expression is not impaired after extracellular application of Poly(I:C), indicating that detection of extracellular Poly(I:C) is mainly referred to TLR3 at the cell surface and the endosomal pathway of extracellular Poly(I:C) plays only a minor role. An increased activation of the RIG-1/mda-5 pathway by extracellular Poly(I:C) entering the cell offers another explanation for the lack of IFN-β downregulation, because I329L does not interact with factors of the RIG-1/mda-5 cascade.

As inhibitor of the TBK1 and IKKβ, DP96R was described to impair IFN-β production after activation of the cGAS/STING pathway (Wang et al., 2018).

However, TLR3 as well as RIG-I/MDA5 downstream signalling results in activation of the TBK1, the phosphorylation of IRF-3 and the initiation of IFN-β production by translocated pIRF-3 (Haller et al., 2006). Therefore, DP96R was supposed to impair IFN-β expression independent of the application route of Poly(I:C) and the activated pathway, respectively.

In 3D4/21 cells, DP96R downregulated IFN-β expression 2h post Poly(I:C) transfection confirming interactions of the protein with the TLR3 as well as the RIG-I/MDA5 pathway. Although extracellular Poly(I:C) activates the TLR3 pathway, DP96R did not affect IFN-β expression in response to extracellular Poly(I:C). Considering the significantly reduced efficiency of extracellular Poly(I:C) to induce IFN-β expression compared to intracellular Poly(I:C), extracellular Poly(I:C) might reach significantly less cells than intracellular Poly(I:C). In non-permissive cells the morphogenesis of MVA is inhibited, whereas infected monolayers are growth competent during infection (as depicted in chapter *2.1. MVA infectivity in porcine cell lines*) leading to a discrepancy between recMVA infected cells and cells stimulated with extracellular Poly(I:C). Consequently, the lack of DP96R in extracellular Poly(I:C) stimulated cells is depicted in unaltered IFN-β transcription. Therefore, extracellular application of Poly(I:C) was not suited for the investigation of target protein mediated effects on IFN-β response in 3D4/21 cells.

Consistent with reviewed IFN-β stimulatory capabilities of CD2v (Chaulagain et al., 2021), IFN-β expression was increased in 3D4/21 cells after infection with recMVA-CD2v but did not achieve as high IFN-β levels as Poly(I:C). Intriguingly, IFN-β expression was not further increased in combination with Poly(I:C) stimulation, counteracting the hypothesis that CD2v might cause apoptosis of macrophages during ASFV infection (Chaulagain et al., 2021). However, these findings combine the contrastive published data, concurrently ascribing IFN-β stimulatory as well as IFN-β inhibitory capabilities to CD2v (Chaulagain et al., 2021; Huang et al., 2023; Zhang et al., 2023). We hypothesize that CD2v-associated chemokine expression of infected cells during ASFV infection induces chemotaxis, attracting further target cells of the innate immune system and providing additional infection targets for ASFV. Simultaneously, avoiding premature host cell apoptosis due to IFN-α/β overexpression is important for the viral life cycle and guarantees the release of mature virions at later timepoints of infection.

Limitations of the experimental setup

Although we determined the infectivity as well as the optimum viral load for the maintained porcine cell lines, the main limitation of the experimental setup to evaluate immunomodulatory faculties of the indicated ASFV proteins is the discrepancy between recMVA infection and IFN-β stimulation mediated by (transfected) Poly(I:C). Especially transfection of Poly(I:C) provides an enormous efficiency, resulting in a higher amount of Poly(I:C) stimulated cells than recMVA infected cells. Contrarily, the high efficiency of Lipofectamine mediated transfection is required to increase the probability of simultaneous infection and IFN-β induction. To improve the experimental setup as well as the evaluation of experimental results, flow cytometric analysis is indicated to determine the infectivity of MVA for 3D4/21 cells more exactly.

Effects of the target proteins on IFN-β expression were evaluated upon Poly(I:C) stimulation, defined as activator of TLR3- and RIG-1/mda-5 mediated cascades. Possible interactions of the viral proteins with other IFN-β inducing pathways of the innate immune system were ignored. Considering ASFV as dsDNA virus theoretically able to activate the cGAS/STING mediated pathway, target proteins might offer multiple strategies to evade dsDNA sensing mechanisms. Therefore, it might be indicated to investigate IFN-β expression after infection with recMVAs and stimulation with potent STING agonists, e.g. 2´3´cGAMP or diABZI, in porcine cell lines.

Future perspectives

MVA represents a well-established viral vector and offers multiple possibilities in terms of vaccine development as well as investigation of antigen expression and antigen functions in infected cells. Nevertheless, the lack of IFN-β expression in response to MVA infection unveiled limitations of the MVA immunogenicity and it needs to be further investigated, whether this phenomenon is limited to the cell lines, or it is species dependent.

After further improvement of the experimental setup, MVA represents a valuable tool to analyse functions of certain ASFV proteins regarding the modulation of the cellular innate immune system.

In this manner, recMVAs might contribute to the identification of a subset of potential vaccine candidates providing a reliable security against ASFV infection.

VI.   SUMMARY

ASFV is endemic in sub-Saharan Africa causing a subacute or chronical disease in warthogs and bushpigs, whereas infection of domestic pigs leads to an acute or peracute hemorrhagic disease. The high tenacity of the virus in carcasses as well as in processed pork products combined with global trade is the main reason for epidemic and cross-continental disease outbreaks. The rapid and cross-border viral spread within naive porcine populations complicated political disease management during several outbreaks in the past, emphasizing the necessity of a protective vaccine against ASFV. The complexity of ASFV as well as the large number of immunomodulatory proteins impede the development of protective vaccines. Moreover, not all functions of the over 160 ASFV encoded proteins are fully elucidated.

In this work, MVA was used as well-established viral vector to investigate expression of ASFV encoded, immunomodulatory proteins *in vitro*. Therefore, genetic sequences of I329L, DP96R and CD2v were inserted into the deletion III cloning site of the MVA genome, whereas A238L was cloned into the intergenomic region between the essential viral genes M069R and M070L. The replication deficiency of MVA in human and porcine cell lines was sustained after insertion of the target sequences, allowing protein expression studies under biosafety level 1. High-scale expression levels of I329L, DP96R and CD2v were verified in permissive CEF cells as well as in the non-permissive porcine cell lines LLC-PK1, IPEC-J2 and 3D4/21. Translation of A238L was exclusively confirmed in CEF cells and IPEC-J2 cells. Immunofluorescence analysis of the target proteins in porcine cell lines depicted predominant localization of I329L, CD2v and A238L in the cytoplasm of infected cells, whereas DP96R was detected in the nucleus. To evaluate, whether MVA might be an appropriate expression vector to study effects of the target proteins on the innate immune system in primary target cells of ASFV, 3D4/21 cells were infected with the recombinant MVAs and IFN-β expression was induced with Poly(I:C). Inhibitory functions of I329L and DP96R on cellular IFN-β mRNA production were confirmed and CD2v initiated the IFN-β production in 3D4/21 cells but impaired exponential IFN-β expression after stimulation with Poly(I:C). These data indicate MVA as promising viral vector to investigate expression of ASFV encoded proteins and its effects on IFN-β production *in vitro*, contributing to elucidation of ASFV protein functions, prospectively.

VII. ZUSAMMENFASSUNG

ASPV ist endemisch in afrikanischen Ländern südlich der Sahara. Es verursacht subakute und chronische Verläufe in Busch- und Warzenschweinen, wohingegen die Infektion in domestizierten Schweinen zu einem akuten oder perakuten hämorrhagischen Krankheitsbild führt. Die hohe Tenazität des Virus in Schlachtkörpern, Kadavern und prozessierten Schweinefleischprodukten kombiniert mit globalem Handel ist der Hauptgrund für epidemische und kontinentübergreifende Krankheitsausbrüche. Die rapide und grenzüberschreitende Virusausbreitung innerhalb naiver Schweinepopulationen verkomplizierte das Vorgehen gegen die Seuche während zahlreicher Ausbrüche in der Vergangenheit. Protektive ASP-Impfstoffe wären daher wertvolle Werkzeuge der Tierseuchenbekämpfung. Doch sowohl die Komplexität von ASPV als auch die große Anzahl immunmodulierender Proteine behindern die Entwicklung protektiver Vakzine. Darüber hinaus sind die Funktionen der über 160 Proteine noch nicht gänzlich aufgedeckt.

In dieser Arbeit wurde MVA als umfassend etablierter viraler Vektor verwendet, um die Expression von ASPV kodierten, immunmodulatorischen Proteine *in vitro* zu untersuchen. Dazu wurden die Gensequenzen von I329L, DP96R und CD2v in die Deletion III Klonierungsstelle des MVA-Genoms eingefügt, wohingegen A238L in die intergenomische Region zwischen den essentiellen, viralen Genen M069R und M070L kloniert wurde. Nach der Insertion der Zielsequenzen blieb die Replikationsdefizienz von MVA in humanen und porzinen Zelllinien erhalten, was die Untersuchung der Proteinexpression unter Bedingungen des Biosicherheitslevels 1 erlaubte. Hohe Expressionslevel von I329L, DP96R und CD2v wurden sowohl in permissiven CEF Zellen als auch in den nicht-permissiven porzinen Zelllinien LLC-PK1, IPEC-J2 und 3D4/21 verifiziert. Die Translation von A238L konnte ausschließlich in CEF Zellen und IPEC-J2 Zellen bestätigt werden. Immunfluoreszenzanalysen der Zielproteine in porzinen Zelllinien ergab eine überwiegende Lokalisation von I329L, CD2v sowie A238L im Zytoplasma infizierter Zellen, wohingegen DP96R im Nukleus detektiert wurde. Für die Evaluation, ob MVA ein geeigneter Expressionsvektor ist, um Auswirkungen von Zielproteinen auf das angeborene Immunsystem von primären Zielzellen von ASPV zu untersuchen, wurden 3D4/21 Zellen mit rekombinanten MVAs infiziert und die IFN-β Expression wurde mit Poly(I:C) induziert. Inhibitorische Funktionen

von I329L und DP96R hinsichtlich der zellulären IFN-β Produktion wurden auf mRNA-Ebene bestätigt und CD2v konnte zwar die IFN-β Produktion in 3D4/21 Zellen initiieren, verhinderte jedoch eine überschießende IFN-β Expression nach Poly(I:C) Stimulation. Diese Daten zeigen MVA als vielversprechenden viralen Vektor, um die Expression von ASPV kodierten Proteinen sowie ihre Effekte auf die IFN-β Produktion *in vitro* zu studieren. Damit könnte MVA zukünftig zur Enthüllung der ASPV-Proteinfunktionen beitragen.

VIII.   REFERENCES

Abrams, C. C., Chapman, D. A., Silk, R., Liverani, E., & Dixon, L. K. (2008). Domains involved in calcineurin phosphatase inhibition and nuclear localisation in the African swine fever virus A238L protein. *Virology, 374*(2), 477-486. https://doi.org/10.1016/j.virol.2008.01.005

Abrams, C. C., Goatley, L., Fishbourne, E., Chapman, D., Cooke, L., Oura, C. A., Netherton, C. L., Takamatsu, H. H., & Dixon, L. K. (2013). Deletion of virulence associated genes from attenuated African swine fever virus isolate OUR T88/3 decreases its ability to protect against challenge with virulent virus. *Virology, 443*(1), 99-105. https://doi.org/10.1016/j.virol.2013.04.028

Alejo, A., Matamoros, T., Guerra, M., & Andrés, G. (2018). A Proteomic Atlas of the African Swine Fever Virus Particle. *J Virol, 92*(23). https://doi.org/10.1128/jvi.01293-18

Alexopoulou, L., Holt, A. C., Medzhitov, R., & Flavell, R. A. (2001). Recognition of double-stranded RNA and activation of NF-kappaB by Toll-like receptor 3. *Nature, 413*(6857), 732-738. https://doi.org/10.1038/35099560

Alonso, C., Miskin, J., Hernáez, B., Fernandez-Zapatero, P., Soto, L., Cantó, C., Rodríguez-Crespo, I., Dixon, L., & Escribano, J. M. (2001). African swine fever virus protein p54 interacts with the microtubular motor complex through direct binding to light-chain dynein. *J Virol, 75*(20), 9819-9827. https://doi.org/10.1128/jvi.75.20.9819-9827.2001

Anderson, E. C., Hutchings, G. H., Mukarati, N., & Wilkinson, P. J. (1998). African swine fever virus infection of the bushpig (Potamochoerus porcus) and its significance in the epidemiology of the disease. *Vet Microbiol, 62*(1), 1-15. https://doi.org/10.1016/s0378-1135(98)00187-4

Andrés, G., Alejo, A., Salas, J., & Salas, M. L. (2002). African swine fever virus polyproteins pp220 and pp62 assemble into the core shell. *J Virol, 76*(24), 12473-

12482. https://doi.org/10.1128/jvi.76.24.12473-12482.2002

Andrés, G., García-Escudero, R., Simón-Mateo, C., & Viñuela, E. (1998). African swine fever virus is enveloped by a two-membraned collapsed cisterna derived from the endoplasmic reticulum. *J Virol*, *72*(11), 8988-9001. https://doi.org/10.1128/jvi.72.11.8988-9001.1998

Andrés, G., García-Escudero, R., Viñuela, E., Salas, M. L., & Rodríguez, J. M. (2001). African swine fever virus structural protein pE120R is essential for virus transport from assembly sites to plasma membrane but not for infectivity. *J Virol*, *75*(15), 6758-6768. https://doi.org/10.1128/jvi.75.15.6758-6768.2001

Andrés, G., Simón-Mateo, C., & Viñuela, E. (1997). Assembly of African swine fever virus: role of polyprotein pp220. *J Virol*, *71*(3), 2331-2341. https://doi.org/10.1128/jvi.71.3.2331-2341.1997

Antoine, G., Scheiflinger, F., Dorner, F., & Falkner, F. G. (1998). The complete genomic sequence of the modified vaccinia Ankara strain: comparison with other orthopoxviruses. *Virology*, *244*(2), 365-396. https://doi.org/10.1006/viro.1998.9123

Arias, M., de la Torre, A., Dixon, L., Gallardo, C., Jori, F., Laddomada, A., Martins, C., Parkhouse, R. M., Revilla, Y., & Rodriguez, F. A. J. (2017). Approaches and Perspectives for Development of African Swine Fever Virus Vaccines. *Vaccines (Basel)*, *5*(4). https://doi.org/10.3390/vaccines5040035

Bianchi, F., Pretto, S., Tagliabue, E., Balsari, A., & Sfondrini, L. (2017). Exploiting poly(I:C) to induce cancer cell apoptosis. *Cancer Biol Ther*, *18*(10), 747-756. https://doi.org/10.1080/15384047.2017.1373220

Bidgood, S. R., Samolej, J., Novy, K., Collopy, A., Albrecht, D., Krause, M., Burden, J. J., Wollscheid, B., & Mercer, J. (2022). Poxviruses package viral redox proteins in lateral bodies and modulate the host oxidative response. *PLoS Pathog*, *18*(7), e1010614. https://doi.org/10.1371/journal.ppat.1010614

Blanchard, T. J., Alcami, A., Andrea, P., & Smith, G. L. (1998). Modified vaccinia virus Ankara undergoes limited replication in human cells and lacks several immunomodulatory proteins: implications for use as a human vaccine. *J Gen Virol*, *79 (Pt 5)*, 1159-1167. https://doi.org/10.1099/0022-1317-79-5-1159

Blome, S., Gabriel, C., & Beer, M. (2013). Pathogenesis of African swine fever in domestic pigs and European wild boar. *Virus Res*, *173*(1), 122-130. https://doi.org/10.1016/j.virusres.2012.10.026

Borca, M. V., Carrillo, C., Zsak, L., Laegreid, W. W., Kutish, G. F., Neilan, J. G., Burrage, T. G., & Rock, D. L. (1998). Deletion of a CD2-like gene, 8-DR, from African swine fever virus affects viral infection in domestic swine. *J Virol*, *72*(4), 2881-2889. https://doi.org/10.1128/jvi.72.4.2881-2889.1998

Borca, M. V., Kutish, G. F., Afonso, C. L., Irusta, P., Carrillo, C., Brun, A., Sussman, M., & Rock, D. L. (1994). An African swine fever virus gene with similarity to the T-lymphocyte surface antigen CD2 mediates hemadsorption. *Virology*, *199*(2), 463-468. https://doi.org/10.1006/viro.1994.1146

Breese, S. S., Jr., & DeBoer, C. J. (1966). Electron microscope observations of African swine fever virus in tissue culture cells. *Virology*, *28*(3), 420-428. https://doi.org/10.1016/0042-6822(66)90054-7

Brikos, C., & O'Neill, L. A. (2008). Signalling of toll-like receptors. *Handb Exp Pharmacol*(183), 21-50. https://doi.org/10.1007/978-3-540-72167-3_2

Cackett, G., Sýkora, M., & Werner, F. (2020). Transcriptome view of a killer: African swine fever virus. *Biochem Soc Trans*, *48*(4), 1569-1581. https://doi.org/10.1042/bst20191108

Cario, E., & Podolsky, D. K. (2000). Differential alteration in intestinal epithelial cell expression of toll-like receptor 3 (TLR3) and TLR4 in inflammatory bowel disease. *Infect Immun*, *68*(12), 7010-7017. https://doi.org/10.1128/iai.68.12.7010-7017.2000

Carrasco, L., de Lara, F. C., Martín de las Mulas, J., Gómez-Villamandos, J. C., Pérez, J., Wilkinson, P. J., & Sierra, M. A. (1996c). Apoptosis in lymph nodes in acute African swine fever. *J Comp Pathol*, *115*(4), 415-428. https://doi.org/10.1016/s0021-9975(96)80075-2

Carrasco, L., Núñez, A., Salguero, F. J., Díaz San Segundo, F., Sánchez-Cordón, P., Gómez-Villamandos, J. C., & Sierra, M. A. (2002). African swine fever: Expression of interleukin-1 alpha and tumour necrosis factor-alpha by pulmonary intravascular macrophages. *J Comp Pathol*, *126*(2-3), 194-201. https://doi.org/10.1053/jcpa.2001.0543

Carrascosa, A. L., Sastre, I., & Viñuela, E. (1991). African swine fever virus attachment protein. *J Virol*, *65*(5), 2283-2289. https://doi.org/10.1128/jvi.65.5.2283-2289.1991

Chaulagain, S., Delhon, G. A., Khatiwada, S., & Rock, D. L. (2021). African Swine Fever Virus CD2v Protein Induces β-Interferon Expression and Apoptosis in Swine Peripheral Blood Mononuclear Cells. *Viruses*, *13*(8). https://doi.org/10.3390/v13081480

Chen, Q., Sun, L., & Chen, Z. J. (2016). Regulation and function of the cGAS-STING pathway of cytosolic DNA sensing. *Nat Immunol*, *17*(10), 1142-1149. https://doi.org/10.1038/ni.3558

Civril, F., Deimling, T., de Oliveira Mann, C. C., Ablasser, A., Moldt, M., Witte, G., Hornung, V., & Hopfner, K. P. (2013). Structural mechanism of cytosolic DNA sensing by cGAS. *Nature*, *498*(7454), 332-337. https://doi.org/10.1038/nature12305

Clemens, M. J. (2003). Interferons and apoptosis. *J Interferon Cytokine Res*, *23*(6), 277-292. https://doi.org/10.1089/107999003766628124

Condit, R. C., Moussatche, N., & Traktman, P. (2006). In a nutshell: structure and assembly of the vaccinia virion. *Adv Virus Res*, *66*, 31-124.

https://doi.org/10.1016/s0065-3527(06)66002-8

Correia, S., Moura, P. L., Ventura, S., Leitão, A., & Parkhouse, R. M. E. (2023). I329L: A Dual Action Viral Antagonist of TLR Activation Encoded by the African Swine Fever Virus (ASFV). *Viruses*, *15*(2). https://doi.org/10.3390/v15020445

Costard, S., Mur, L., Lubroth, J., Sanchez-Vizcaino, J. M., & Pfeiffer, D. U. (2013). Epidemiology of African swine fever virus. *Virus Res*, *173*(1), 191-197. https://doi.org/10.1016/j.virusres.2012.10.030

Cudmore, S., Cossart, P., Griffiths, G., & Way, M. (1995). Actin-based motility of vaccinia virus. *Nature*, *378*(6557), 636-638. https://doi.org/10.1038/378636a0

Cuesta-Geijo, M. A., Galindo, I., Hernáez, B., Quetglas, J. I., Dalmau-Mena, I., & Alonso, C. (2012). Endosomal maturation, Rab7 GTPase and phosphoinositides in African swine fever virus entry. *PLoS One*, *7*(11), e48853. https://doi.org/10.1371/journal.pone.0048853

Cusson-Hermance, N., Khurana, S., Lee, T. H., Fitzgerald, K. A., & Kelliher, M. A. (2005). Rip1 mediates the Trif-dependent toll-like receptor 3- and 4-induced NF-{kappa}B activation but does not contribute to interferon regulatory factor 3 activation. *J Biol Chem*, *280*(44), 36560-36566. https://doi.org/10.1074/jbc.M506831200

Dai, P., Wang, W., Cao, H., Avogadri, F., Dai, L., Drexler, I., Joyce, J. A., Li, X. D., Chen, Z., Merghoub, T., Shuman, S., & Deng, L. (2014). Modified vaccinia virus Ankara triggers type I IFN production in murine conventional dendritic cells via a cGAS/STING-mediated cytosolic DNA-sensing pathway. *PLoS Pathog*, *10*(4), e1003989. https://doi.org/10.1371/journal.ppat.1003989

de Bouteiller, O., Merck, E., Hasan, U. A., Hubac, S., Benguigui, B., Trinchieri, G., Bates, E. E., & Caux, C. (2005). Recognition of double-stranded RNA by human toll-like receptor 3 and downstream receptor signaling requires multimerization and an acidic pH. *J Biol Chem*, *280*(46), 38133-38145.

https://doi.org/10.1074/jbc.M507163200

de Oliveira, V. L., Almeida, S. C., Soares, H. R., Crespo, A., Marshall-Clarke, S., & Parkhouse, R. M. (2011). A novel TLR3 inhibitor encoded by African swine fever virus (ASFV). *Arch Virol*, *156*(4), 597-609. https://doi.org/10.1007/s00705-010-0894-7

de Veer, M. J., Holko, M., Frevel, M., Walker, E., Der, S., Paranjape, J. M., Silverman, R. H., & Williams, B. R. (2001). Functional classification of interferon-stimulated genes identified using microarrays. *J Leukoc Biol*, *69*(6), 912-920.

Dehlin, E., von Gabain, A., Alm, G., Dingelmaier, R., & Resnekov, O. (1996). Repression of beta interferon gene expression in virus-infected cells is correlated with a poly(A) tail elongation. *Mol Cell Biol*, *16*(2), 468-474. https://doi.org/10.1128/mcb.16.2.468

Der, S. D., Zhou, A., Williams, B. R., & Silverman, R. H. (1998). Identification of genes differentially regulated by interferon alpha, beta, or gamma using oligonucleotide arrays. *Proc Natl Acad Sci U S A*, *95*(26), 15623-15628. https://doi.org/10.1073/pnas.95.26.15623

Dixon, L. K., Abrams, C. C., Bowick, G., Goatley, L. C., Kay-Jackson, P. C., Chapman, D., Liverani, E., Nix, R., Silk, R., & Zhang, F. (2004). African swine fever virus proteins involved in evading host defence systems. *Vet Immunol Immunopathol*, *100*(3-4), 117-134. https://doi.org/10.1016/j.vetimm.2004.04.002

Dixon, L. K., Chapman, D. A., Netherton, C. L., & Upton, C. (2012). African swine fever virus replication and genomics. *Virus Res*, *173*(1), 3-14. https://doi.org/10.1016/j.virusres.2012.10.020

Dixon, L. K., Sun, H., & Roberts, H. (2019). African swine fever. *Antiviral Res*, *165*, 34-41. https://doi.org/10.1016/j.antiviral.2019.02.018

Doms, R. W., Blumenthal, R., & Moss, B. (1990). Fusion of intra- and extracellular forms of vaccinia virus with the cell membrane. *J Virol*, *64*(10), 4884-4892. https://doi.org/10.1128/jvi.64.10.4884-4892.1990

Dragan, A. I., Hargreaves, V. V., Makeyeva, E. N., & Privalov, P. L. (2007). Mechanisms of activation of interferon regulator factor 3: the role of C-terminal domain phosphorylation in IRF-3 dimerization and DNA binding. *Nucleic Acids Res*, *35*(11), 3525-3534. https://doi.org/10.1093/nar/gkm142

EFSA, E. F. S. A. (2009). *Scientific review on African Swine Fever to EFSA prepared by Sánchez-Viczaíno, J.M.; Martínez-López, B.; Martínez-Avilés, M.; Martins, C.; Boinas, F.; Vial, L. ; Michaud, V.; Jori, F.; Etter, E.; Albina, E.; Roger, F.*

Ellis, M. J., & Goodbourn, S. (1994). NF-kappa B-independent activation of beta-interferon expression in mouse F9 embryonal carcinoma cells. *Nucleic Acids Res*, *22*(21), 4489-4496. https://doi.org/10.1093/nar/22.21.4489

Enjuanes, L., Carrascosa, A. L., & Viñuela, E. (1976). Isolation and properties of the DNA of African swine fever (ASF) virus. *J Gen Virol*, *32*(3), 479-492. https://doi.org/10.1099/0022-1317-32-3-479

Fitzgerald, K. A., McWhirter, S. M., Faia, K. L., Rowe, D. C., Latz, E., Golenbock, D. T., Coyle, A. J., Liao, S. M., & Maniatis, T. (2003). IKKepsilon and TBK1 are essential components of the IRF3 signaling pathway. *Nat Immunol*, *4*(5), 491-496. https://doi.org/10.1038/ni921

Frahm, T., Hauser, H., & Köster, M. (2006). IFN-type-I-mediated signaling is regulated by modulation of STAT2 nuclear export. *J Cell Sci*, *119*(Pt 6), 1092-1104. https://doi.org/10.1242/jcs.02822

Gabriel, C., Blome, S., Malogolovkin, A., Parilov, S., Kolbasov, D., Teifke, J. P., & Beer, M. (2011). Characterization of African swine fever virus Caucasus isolate in European wild boars. *Emerg Infect Dis*, *17*(12), 2342-2345.

https://doi.org/10.3201/eid1712.110430

Galindo, I., & Alonso, C. (2017). African Swine Fever Virus: A Review. *Viruses*, *9*(5). https://doi.org/10.3390/v9050103

Galindo, I., Cuesta-Geijo, M. A., Hlavova, K., Muñoz-Moreno, R., Barrado-Gil, L., Dominguez, J., & Alonso, C. (2015). African swine fever virus infects macrophages, the natural host cells, via clathrin- and cholesterol-dependent endocytosis. *Virus Res*, *200*, 45-55. https://doi.org/10.1016/j.virusres.2015.01.022

Gallego-Gómez, J. C., Risco, C., Rodríguez, D., Cabezas, P., Guerra, S., Carrascosa, J. L., & Esteban, M. (2003). Differences in virus-induced cell morphology and in virus maturation between MVA and other strains (WR, Ankara, and NYCBH) of vaccinia virus in infected human cells. *J Virol*, *77*(19), 10606-10622. https://doi.org/10.1128/jvi.77.19.10606-10622.2003

García-Beato, R., Salas, M. L., Viñuela, E., & Salas, J. (1992). Role of the host cell nucleus in the replication of African swine fever virus DNA. *Virology*, *188*(2), 637-649. https://doi.org/10.1016/0042-6822(92)90518-t

Gaudreault, N. N., Madden, D. W., Wilson, W. C., Trujillo, J. D., & Richt, J. A. (2020). African Swine Fever Virus: An Emerging DNA Arbovirus. *Front Vet Sci*, *7*, 215. https://doi.org/10.3389/fvets.2020.00215

Gil, S., Spagnuolo-Weaver, M., Canals, A., Sepúlveda, N., Oliveira, J., Aleixo, A., Allan, G., Leitão, A., & Martins, C. L. (2003). Expression at mRNA level of cytokines and A238L gene in porcine blood-derived macrophages infected in vitro with African swine fever virus (ASFV) isolates of different virulence. *Arch Virol*, *148*(11), 2077-2097. https://doi.org/10.1007/s00705-003-0182-x

Goatley, L. C., & Dixon, L. K. (2011). Processing and localization of the african swine fever virus CD2v transmembrane protein. *J Virol*, *85*(7), 3294-3305. https://doi.org/10.1128/jvi.01994-10

Gogin, A., Gerasimov, V., Malogolovkin, A., & Kolbasov, D. (2013). African swine fever in the North Caucasus region and the Russian Federation in years 2007-2012. *Virus Res*, *173*(1), 198-203. https://doi.org/10.1016/j.virusres.2012.12.007

Gómez-Villamandos, J. C., Bautista, M. J., Sánchez-Cordón, P. J., & Carrasco, L. (2013). Pathology of African swine fever: the role of monocyte-macrophage. *Virus Res*, *173*(1), 140-149. https://doi.org/10.1016/j.virusres.2013.01.017

Gómez-Villamandos, J. C., Hervás, J., Méndez, A., Carrasco, L., Martín de las Mulas, J., Villeda, C. J., Wilkinson, P. J., & Sierra, M. A. (1995a). Experimental African swine fever: apoptosis of lymphocytes and virus replication in other cells. *J Gen Virol*, *76 (Pt 9)*, 2399-2405. https://doi.org/10.1099/0022-1317-76-9-2399

Grafi, G., Sela, I., & Galili, G. (1993). Translational regulation of human beta interferon mRNA: association of the 3' AU-rich sequence with the poly(A) tail reduces translation efficiency in vitro. *Mol Cell Biol*, *13*(6), 3487-3493. https://doi.org/10.1128/mcb.13.6.3487-3493.1993

Granja, A. G., Nogal, M. L., Hurtado, C., Del Aguila, C., Carrascosa, A. L., Salas, M. L., Fresno, M., & Revilla, Y. (2006a). The viral protein A238L inhibits TNF-alpha expression through a CBP/p300 transcriptional coactivators pathway. *J Immunol*, *176*(1), 451-462. https://doi.org/10.4049/jimmunol.176.1.451

Granja, A. G., Nogal, M. L., Hurtado, C., Vila, V., Carrascosa, A. L., Salas, M. L., Fresno, M., & Revilla, Y. (2004). The viral protein A238L inhibits cyclooxygenase-2 expression through a nuclear factor of activated T cell-dependent transactivation pathway. *J Biol Chem*, *279*(51), 53736-53746. https://doi.org/10.1074/jbc.M406620200

Granja, A. G., Perkins, N. D., & Revilla, Y. (2008). Correction: A238L Inhibits NF-ATc2, NF-κB, and c-Jun Activation through a Novel Mechanism Involving Protein Kinase C-θ-Mediated Up-Regulation of the Amino-Terminal Transactivation Domain of p300. *J Immunol*, *194*(4), 2032. https://doi.org/10.4049/jimmunol.1490049

Granja, A. G., Sabina, P., Salas, M. L., Fresno, M., & Revilla, Y. (2006b). Regulation of inducible nitric oxide synthase expression by viral A238L-mediated inhibition of p65/RelA acetylation and p300 transactivation. *J Virol*, *80*(21), 10487-10496. https://doi.org/10.1128/jvi.00862-06

Guinat, C., Gogin, A., Blome, S., Keil, G., Pollin, R., Pfeiffer, D. U., & Dixon, L. (2016). Transmission routes of African swine fever virus to domestic pigs: current knowledge and future research directions. *Vet Rec*, *178*(11), 262-267. https://doi.org/10.1136/vr.103593

Häcker, H., Redecke, V., Blagoev, B., Kratchmarova, I., Hsu, L. C., Wang, G. G., Kamps, M. P., Raz, E., Wagner, H., Häcker, G., Mann, M., & Karin, M. (2006). Specificity in Toll-like receptor signalling through distinct effector functions of TRAF3 and TRAF6. *Nature*, *439*(7073), 204-207. https://doi.org/10.1038/nature04369

Haller, O., Kochs, G., & Weber, F. (2006). The interferon response circuit: induction and suppression by pathogenic viruses. *Virology*, *344*(1), 119-130. https://doi.org/10.1016/j.virol.2005.09.024

Hernaez, B., & Alonso, C. (2010). Dynamin- and clathrin-dependent endocytosis in African swine fever virus entry. *J Virol*, *84*(4), 2100-2109. https://doi.org/10.1128/jvi.01557-09

Hernaez, B., Escribano, J. M., & Alonso, C. (2006). Visualization of the African swine fever virus infection in living cells by incorporation into the virus particle of green fluorescent protein-p54 membrane protein chimera. *Virology*, *350*(1), 1-14. https://doi.org/10.1016/j.virol.2006.01.021

Hernáez, B., Guerra, M., Salas, M. L., & Andrés, G. (2016). African Swine Fever Virus Undergoes Outer Envelope Disruption, Capsid Disassembly and Inner Envelope Fusion before Core Release from Multivesicular Endosomes. *PLoS Pathog*, *12*(4), e1005595. https://doi.org/10.1371/journal.ppat.1005595

Hiscott, J., Pitha, P., Genin, P., Nguyen, H., Heylbroeck, C., Mamane, Y., Algarte, M., & Lin, R. (1999). Triggering the interferon response: the role of IRF-3 transcription factor. *J Interferon Cytokine Res*, *19*(1), 1-13. https://doi.org/10.1089/107999099314360

Hoebe, K., Du, X., Georgel, P., Janssen, E., Tabeta, K., Kim, S. O., Goode, J., Lin, P., Mann, N., Mudd, S., Crozat, K., Sovath, S., Han, J., & Beutler, B. (2003). Identification of Lps2 as a key transducer of MyD88-independent TIR signalling. *Nature*, *424*(6950), 743-748. https://doi.org/10.1038/nature01889

Holgado, M. P., Falivene, J., Maeto, C., Amigo, M., Pascutti, M. F., Vecchione, M. B., Bruttomesso, A., Calamante, G., Del Médico-Zajac, M. P., & Gherardi, M. M. (2016). Deletion of A44L, A46R and C12L Vaccinia Virus Genes from the MVA Genome Improved the Vector Immunogenicity by Modifying the Innate Immune Response Generating Enhanced and Optimized Specific T-Cell Responses. *Viruses*, *8*(5). https://doi.org/10.3390/v8050139

Hopfner, K. P., & Hornung, V. (2020). Molecular mechanisms and cellular functions of cGAS-STING signalling. *Nat Rev Mol Cell Biol*, *21*(9), 501-521. https://doi.org/10.1038/s41580-020-0244-x

Hornemann, S., Harlin, O., Staib, C., Kisling, S., Erfle, V., Kaspers, B., Häcker, G., & Sutter, G. (2003). Replication of modified vaccinia virus Ankara in primary chicken embryo fibroblasts requires expression of the interferon resistance gene E3L. *J Virol*, *77*(15), 8394-8407. https://doi.org/10.1128/jvi.77.15.8394-8407.2003

Huang, L., Chen, W., Liu, H., Xue, M., Dong, S., Liu, X., Feng, C., Cao, S., Ye, G., Zhou, Q., Zhang, Z., Zheng, J., Li, J., Zhao, D., Wang, Z., Sun, E., Chen, H., Zhang, S., Wang, X., . . . Weng, C. (2023). African Swine Fever Virus HLJ/18 CD2v Suppresses Type I IFN Production and IFN-Stimulated Genes Expression through Negatively Regulating cGMP-AMP Synthase-STING and IFN Signaling Pathways. *J Immunol*, *210*(9), 1338-1350. https://doi.org/10.4049/jimmunol.2200813

Isaacs, A., & Lindenmann, J. (1957). Virus interference. I. The interferon. *Proceedings of the Royal Society of London. Series B-Biological Sciences*, *147*(927), 258-267.

Ishikawa, H., & Barber, G. N. (2008). STING is an endoplasmic reticulum adaptor that facilitates innate immune signalling. *Nature*, *455*(7213), 674-678. https://doi.org/10.1038/nature07317

Itoh, K., Watanabe, A., Funami, K., Seya, T., & Matsumoto, M. (2008). The clathrin-mediated endocytic pathway participates in dsRNA-induced IFN-beta production. *J Immunol*, *181*(8), 5522-5529. https://doi.org/10.4049/jimmunol.181.8.5522

Jiang, Z., Mak, T. W., Sen, G., & Li, X. (2004). Toll-like receptor 3-mediated activation of NF-kappaB and IRF3 diverges at Toll-IL-1 receptor domain-containing adapter inducing IFN-beta. *Proc Natl Acad Sci U S A*, *101*(10), 3533-3538. https://doi.org/10.1073/pnas.0308496101

Jin, M. S., & Lee, J. O. (2008). Structures of TLR-ligand complexes. *Curr Opin Immunol*, *20*(4), 414-419. https://doi.org/10.1016/j.coi.2008.06.002

Jouvenet, N., Monaghan, P., Way, M., & Wileman, T. (2004). Transport of African swine fever virus from assembly sites to the plasma membrane is dependent on microtubules and conventional kinesin. *J Virol*, *78*(15), 7990-8001. https://doi.org/10.1128/jvi.78.15.7990-8001.2004

Kalodimou, G., Veit, S., Jany, S., Kalinke, U., Broder, C. C., Sutter, G., & Volz, A. (2019). A Soluble Version of Nipah Virus Glycoprotein G Delivered by Vaccinia Virus MVA Activates Specific CD8 and CD4 T Cells in Mice. *Viruses*, *12*(1). https://doi.org/10.3390/v12010026

Karger, A., Pérez-Núñez, D., Urquiza, J., Hinojar, P., Alonso, C., Freitas, F. B., Revilla, Y., Le Potier, M. F., & Montoya, M. (2019). An Update on African Swine Fever Virology. *Viruses*, *11*(9). https://doi.org/10.3390/v11090864

Kato, H., Takeuchi, O., Sato, S., Yoneyama, M., Yamamoto, M., Matsui, K., Uematsu, S., Jung, A., Kawai, T., Ishii, K. J., Yamaguchi, O., Otsu, K., Tsujimura, T., Koh, C. S., Reis e Sousa, C., Matsuura, Y., Fujita, T., & Akira, S. (2006). Differential roles of MDA5 and RIG-I helicases in the recognition of RNA viruses. *Nature*, *441*(7089), 101-105. https://doi.org/10.1038/nature04734

Katsafanas, G. C., & Moss, B. (2007). Colocalization of transcription and translation within cytoplasmic poxvirus factories coordinates viral expression and subjugates host functions. *Cell Host Microbe*, *2*(4), 221-228. https://doi.org/10.1016/j.chom.2007.08.005

Kawai, T., & Akira, S. (2008). Toll-like receptor and RIG-I-like receptor signaling. *Ann N Y Acad Sci*, *1143*, 1-20. https://doi.org/10.1196/annals.1443.020

Koltsov, A., Krutko, S., Kholod, N., Sukher, M., Belov, S., Korotin, A., & Koltsova, G. (2023). Deletion of the CD2 Gene in the Virulent ASFV Congo Strain Affects Viremia in Domestic Swine, but Not the Virulence. *Animals (Basel)*, *13*(12). https://doi.org/10.3390/ani13122002

Kulka, M., Alexopoulou, L., Flavell, R. A., & Metcalfe, D. D. (2004). Activation of mast cells by double-stranded RNA: evidence for activation through Toll-like receptor 3. *J Allergy Clin Immunol*, *114*(1), 174-182. https://doi.org/10.1016/j.jaci.2004.03.049

Kuznar, J., Salas, M. L., & Vinuela, E. (1980). RNAs synthesized invitro by purified African swine fever virus. *Archivos de Biologia yMedicina Experimentales*, *13*(4), 465.

Laliberte, J. P., Weisberg, A. S., & Moss, B. (2011). The membrane fusion step of vaccinia virus entry is cooperatively mediated by multiple viral proteins and host cell components. *PLoS Pathog*, *7*(12), e1002446. https://doi.org/10.1371/journal.ppat.1002446

Lee, H. K., Dunzendorfer, S., Soldau, K., & Tobias, P. S. (2006). Double-stranded

RNA-mediated TLR3 activation is enhanced by CD14. *Immunity*, *24*(2), 153-163. https://doi.org/10.1016/j.immuni.2005.12.012

Lefevre, F., & La Bonnardiere, C. (1986). Molecular cloning and sequencing of a gene encoding biologically active porcine alpha-interferon. *J Interferon Res*, *6*(4), 349-360. https://doi.org/10.1089/jir.1986.6.349

Lehmann, M. H., Kastenmuller, W., Kandemir, J. D., Brandt, F., Suezer, Y., & Sutter, G. (2009). Modified vaccinia virus ankara triggers chemotaxis of monocytes and early respiratory immigration of leukocytes by induction of CCL2 expression. *J Virol*, *83*(6), 2540-2552. https://doi.org/10.1128/jvi.01884-08

Lehmann, M. H., Torres-Domínguez, L. E., Price, P. J., Brandmüller, C., Kirschning, C. J., & Sutter, G. (2016). CCL2 expression is mediated by type I IFN receptor and recruits NK and T cells to the lung during MVA infection. *J Leukoc Biol*, *99*(6), 1057-1064. https://doi.org/10.1189/jlb.4MA0815-376RR

Leitão, A., Cartaxeiro, C., Coelho, R., Cruz, B., Parkhouse, R. M. E., Portugal, F. C., Vigário, J. D., & Martins, C. L. V. (2001). The non-haemadsorbing African swine fever virus isolate ASFV/NH/P68 provides a model for defining the protective anti-virus immune response. *J Gen Virol*, *82*(Pt 3), 513-523. https://doi.org/10.1099/0022-1317-82-3-513

Lin, R., Heylbroeck, C., Pitha, P. M., & Hiscott, J. (1998). Virus-dependent phosphorylation of the IRF-3 transcription factor regulates nuclear translocation, transactivation potential, and proteasome-mediated degradation. *Mol Cell Biol*, *18*(5), 2986-2996. https://doi.org/10.1128/mcb.18.5.2986

Lin, Y. C., & Evans, D. H. (2010). Vaccinia virus particles mix inefficiently, and in a way that would restrict viral recombination, in coinfected cells. *J Virol*, *84*(5), 2432-2443. https://doi.org/10.1128/jvi.01998-09

Liu, S., Cai, X., Wu, J., Cong, Q., Chen, X., Li, T., Du, F., Ren, J., Wu, Y. T., Grishin, N. V., & Chen, Z. J. (2015). Phosphorylation of innate immune adaptor

proteins MAVS, STING, and TRIF induces IRF3 activation. *Science*, *347*(6227), aaa2630. https://doi.org/10.1126/science.aaa2630

Ludwig, H., Mages, J., Staib, C., Lehmann, M. H., Lang, R., & Sutter, G. (2005). Role of viral factor E3L in modified vaccinia virus ankara infection of human HeLa Cells: regulation of the virus life cycle and identification of differentially expressed host genes. *J Virol*, *79*(4), 2584-2596. https://doi.org/10.1128/jvi.79.4.2584-2596.2005

Maher, S. G., Romero-Weaver, A. L., Scarzello, A. J., & Gamero, A. M. (2007). Interferon: cellular executioner or white knight? *Curr Med Chem*, *14*(12), 1279-1289. https://doi.org/10.2174/092986707780597907

Mallardo, M., Leithe, E., Schleich, S., Roos, N., Doglio, L., & Krijnse Locker, J. (2002). Relationship between vaccinia virus intracellular cores, early mRNAs, and DNA replication sites. *J Virol*, *76*(10), 5167-5183. https://doi.org/10.1128/jvi.76.10.5167-5183.2002

Marcus, P. I. (1983). Interferon induction by viruses: one molecule of dsRNA as the threshold for interferon induction. *Interferon*, *5*, 115-180.

Marcus, P. I., & Sekellick, M. J. (1977). Defective interfering particles with covalently linked [+/-]RNA induce interferon. *Nature*, *266*(5605), 815-819. https://doi.org/10.1038/266815a0

Marcus, P. I., & Sekellick, M. J. (2005). Interferon induction by viruses. XXV. Adenoviruses as inducers of interferon in developmentally aged primary chicken embryo cells. *Acta Microbiol Immunol Hung*, *52*(3-4), 291-308. https://doi.org/10.1556/AMicr.52.2005.3-4.3

Marié, I., Durbin, J. E., & Levy, D. E. (1998). Differential viral induction of distinct interferon-alpha genes by positive feedback through interferon regulatory factor-7. *Embo j*, *17*(22), 6660-6669. https://doi.org/10.1093/emboj/17.22.6660

Marq, J. B., Hausmann, S., Luban, J., Kolakofsky, D., & Garcin, D. (2009). The double-stranded RNA binding domain of the vaccinia virus E3L protein inhibits both RNA- and DNA-induced activation of interferon beta. *J Biol Chem*, *284*(38), 25471-25478. https://doi.org/10.1074/jbc.M109.018895

Matsumoto, M., Kikkawa, S., Kohase, M., Miyake, K., & Seya, T. (2002). Establishment of a monoclonal antibody against human Toll-like receptor 3 that blocks double-stranded RNA-mediated signaling. *Biochem Biophys Res Commun*, *293*(5), 1364-1369. https://doi.org/10.1016/s0006-291x(02)00380-7

Matsumoto, M., & Seya, T. (2008). TLR3: interferon induction by double-stranded RNA including poly(I:C). *Adv Drug Deliv Rev*, *60*(7), 805-812. https://doi.org/10.1016/j.addr.2007.11.005

McComb, S., Thiriot, A., Akache, B., Krishnan, L., & Stark, F. (2019). Introduction to the Immune System. *Methods Mol Biol*, *2024*, 1-24. https://doi.org/10.1007/978-1-4939-9597-4_1

McFadden, G. (2005). Poxvirus tropism. *Nat Rev Microbiol*, *3*(3), 201-213. https://doi.org/10.1038/nrmicro1099

Mebus, C. A. (1988). African swine fever. *Adv Virus Res*, *35*, 251-269. https://doi.org/10.1016/s0065-3527(08)60714-9

Meyer, H., Sutter, G., & Mayr, A. (1991). Mapping of deletions in the genome of the highly attenuated vaccinia virus MVA and their influence on virulence. *J Gen Virol*, *72 (Pt 5)*, 1031-1038. https://doi.org/10.1099/0022-1317-72-5-1031

Meyer Zu Natrup, C., Tscherne, A., Dahlke, C., Ciurkiewicz, M., Shin, D. L., Fathi, A., Rohde, C., Kalodimou, G., Halwe, S., Limpinsel, L., Schwarz, J. H., Klug, M., Esen, M., Schneiderhan-Marra, N., Dulovic, A., Kupke, A., Brosinski, K., Clever, S., Schünemann, L. M., . . . Volz, A. (2022). Stabilized recombinant SARS-CoV-2 spike antigen enhances vaccine immunogenicity and protective capacity. *J Clin Invest*, *132*(24). https://doi.org/10.1172/jci159895

Meylan, E., Burns, K., Hofmann, K., Blancheteau, V., Martinon, F., Kelliher, M., & Tschopp, J. (2004). RIP1 is an essential mediator of Toll-like receptor 3-induced NF-kappa B activation. *Nat Immunol*, *5*(5), 503-507. https://doi.org/10.1038/ni1061

Miskin, J. E., Abrams, C. C., & Dixon, L. K. (2000). African swine fever virus protein A238L interacts with the cellular phosphatase calcineurin via a binding domain similar to that of NFAT. *J Virol*, *74*(20), 9412-9420. https://doi.org/10.1128/jvi.74.20.9412-9420.2000

Mogensen, K. E., Lewerenz, M., Reboul, J., Lutfalla, G., & Uzé, G. (1999). The type I interferon receptor: structure, function, and evolution of a family business. *J Interferon Cytokine Res*, *19*(10), 1069-1098. https://doi.org/10.1089/107999099313019

Montgomery, E. R. (1921). On A Form of Swine Fever Occurring in British East Africa (Kenya Colony). *Journal of Comparative Pathology and Therapeutics*, *34*, 159-191. https://doi.org/https://doi.org/10.1016/S0368-1742(21)80031-4

Moresco, E. M., LaVine, D., & Beutler, B. (2011). Toll-like receptors. *Curr Biol*, *21*(13), R488-493. https://doi.org/10.1016/j.cub.2011.05.039

Moss, B. (2001). Poxviridae: the viruses and their replication. In B. N. Fields, D. M. Knipe, P. M. Howley, & D. E. Griffin (Eds.), *Fields virology* (4 ed., Vol. 2). Lippincott Williams & Wilkins.

Neilan, J. G., Lu, Z., Kutish, G. F., Zsak, L., Lewis, T. L., & Rock, D. L. (1997). A conserved African swine fever virus IkappaB homolog, 5EL, is nonessential for growth in vitro and virulence in domestic swine. *Virology*, *235*(2), 377-385. https://doi.org/10.1006/viro.1997.8693

O'Donnell, V., Risatti, G. R., Holinka, L. G., Krug, P. W., Carlson, J., Velazquez-Salinas, L., Azzinaro, P. A., Gladue, D. P., & Borca, M. V. (2017). Simultaneous Deletion of the 9GL and UK Genes from the African Swine Fever Virus Georgia

2007 Isolate Offers Increased Safety and Protection against Homologous Challenge. *J Virol*, *91*(1). https://doi.org/10.1128/jvi.01760-16

Oganesyan, G., Saha, S. K., Guo, B., He, J. Q., Shahangian, A., Zarnegar, B., Perry, A., & Cheng, G. (2006). Critical role of TRAF3 in the Toll-like receptor-dependent and -independent antiviral response. *Nature*, *439*(7073), 208-211. https://doi.org/10.1038/nature04374

Oura, C. A., Powell, P. P., & Parkhouse, R. M. (1998). African swine fever: a disease characterized by apoptosis. *J Gen Virol*, *79 (Pt 6)*, 1427-1438. https://doi.org/10.1099/0022-1317-79-6-1427

Palchetti, S., Starace, D., De Cesaris, P., Filippini, A., Ziparo, E., & Riccioli, A. (2015). Transfected poly(I:C) activates different dsRNA receptors, leading to apoptosis or immunoadjuvant response in androgen-independent prostate cancer cells. *J Biol Chem*, *290*(9), 5470-5483. https://doi.org/10.1074/jbc.M114.601625

Parker, J., Plowright, W., & Pierce, M. A. (1969). The epizootiology of African swine fever in Africa. *Vet Rec*, *85*(24), 668-674.

Payne, L. G. (1980). Significance of extracellular enveloped virus in the in vitro and in vivo dissemination of vaccinia. *J Gen Virol*, *50*(1), 89-100. https://doi.org/10.1099/0022-1317-50-1-89

Penrith, M. L., & Vosloo, W. (2009). Review of African swine fever: transmission, spread and control. *J S Afr Vet Assoc*, *80*(2), 58-62. https://doi.org/10.4102/jsava.v80i2.172

Penrith, M. L., Vosloo, W., Jori, F., & Bastos, A. D. (2013). African swine fever virus eradication in Africa. *Virus Res*, *173*(1), 228-246. https://doi.org/10.1016/j.virusres.2012.10.011

Pérez-Núñez, D., García-Belmonte, R., Riera, E., Fernández-Sesma, M. H., Vigara-

Astillero, G., & Revilla, Y. (2023). Signal peptide and N-glycosylation of N-terminal-CD2v determine the hemadsorption of African swine fever virus. *J Virol*, *97*(10), e0103023. https://doi.org/10.1128/jvi.01030-23

Peters, K. L., Smith, H. L., Stark, G. R., & Sen, G. C. (2002). IRF-3-dependent, NFkappa B- and JNK-independent activation of the 561 and IFN-beta genes in response to double-stranded RNA. *Proc Natl Acad Sci U S A*, *99*(9), 6322-6327. https://doi.org/10.1073/pnas.092133199

Powell, P. P., Dixon, L. K., & Parkhouse, R. M. (1996). An IkappaB homolog encoded by African swine fever virus provides a novel mechanism for downregulation of proinflammatory cytokine responses in host macrophages. *J Virol*, *70*(12), 8527-8533. https://doi.org/10.1128/jvi.70.12.8527-8533.1996

Probst, C., Globig, A., Knoll, B., Conraths, F. J., & Depner, K. (2017). Behaviour of free ranging wild boar towards their dead fellows: potential implications for the transmission of African swine fever. *R Soc Open Sci*, *4*(5), 170054. https://doi.org/10.1098/rsos.170054

Qi, X., Feng, T., Ma, Z., Zheng, L., Liu, H., Shi, Z., Shen, C., Li, P., Wu, P., Ru, Y., Li, D., Zhu, Z., Tian, H., Wu, S., & Zheng, H. (2023). Deletion of DP148R, DP71L, and DP96R Attenuates African Swine Fever Virus, and the Mutant Strain Confers Complete Protection against Homologous Challenges in Pigs. *J Virol*, *97*(4), e0024723. https://doi.org/10.1128/jvi.00247-23

Quetglas, J. I., Hernáez, B., Galindo, I., Muñoz-Moreno, R., Cuesta-Geijo, M. A., & Alonso, C. (2012). Small rho GTPases and cholesterol biosynthetic pathway intermediates in African swine fever virus infection. *J Virol*, *86*(3), 1758-1767. https://doi.org/10.1128/jvi.05666-11

Ramiro-Ibáñez, F., Ortega, A., Brun, A., Escribano, J. M., & Alonso, C. (1996). Apoptosis: a mechanism of cell killing and lymphoid organ impairment during acute African swine fever virus infection. *J Gen Virol*, *77 (Pt 9)*, 2209-2219. https://doi.org/10.1099/0022-1317-77-9-2209

Randall, R. E., & Goodbourn, S. (2008). Interferons and viruses: an interplay between induction, signalling, antiviral responses and virus countermeasures. *J Gen Virol*, *89*(Pt 1), 1-47. https://doi.org/10.1099/vir.0.83391-0

Revilla, Y., Callejo, M., Rodrı́guez, J. M., Culebras, E., Nogal, M. L., E., V., & Fresno, M. (1998). Inhibition of Nuclear Factor kB Activation by a Virus-encoded IkB-like Protein. *The Journal of Biological Chemistry*, *273*(9), 5405-5411.

Revilla, Y., Pérez-Núñez, D., & Richt, J. A. (2018). African Swine Fever Virus Biology and Vaccine Approaches. *Adv Virus Res*, *100*, 41-74. https://doi.org/10.1016/bs.aivir.2017.10.002

Rodríguez, J. M., Yáñez, R. J., Almazán, F., Viñuela, E., & Rodriguez, J. F. (1993). African swine fever virus encodes a CD2 homolog responsible for the adhesion of erythrocytes to infected cells. *J Virol*, *67*(9), 5312-5320. https://doi.org/10.1128/jvi.67.9.5312-5320.1993

Rojo, G., García-Beato, R., Viñuela, E., Salas, M. L., & Salas, J. (1999). Replication of African swine fever virus DNA in infected cells. *Virology*, *257*(2), 524-536. https://doi.org/10.1006/viro.1999.9704

Rotem, Z., Cox, R. A., & Isaacs, A. (1963). Inhibition of virus multiplication by foreign nucleic acid. *Nature*, *197*, 564-566. https://doi.org/10.1038/197564a0

Royo, S., Sainz, B., Jr., Hernández-Jiménez, E., Reyburn, H., López-Collazo, E., & Guerra, S. (2014). Differential induction of apoptosis, interferon signaling, and phagocytosis in macrophages infected with a panel of attenuated and nonattenuated poxviruses. *J Virol*, *88*(10), 5511-5523. https://doi.org/10.1128/jvi.00468-14

Ruska, H., Borries, B. v., & Ruska, E. (1939). Die Bedeutung der Übermikroskopie für die Virusforschung. *Archiv für die gesamte Virusforschung*, *1*(1), 155-169. https://doi.org/10.1007/BF01243399

Salas, M. L., & Andrés, G. (2013). African swine fever virus morphogenesis. *Virus Res*, *173*(1), 29-41. https://doi.org/10.1016/j.virusres.2012.09.016

Salas, M. L., Kuznar, J., & Vinuela, E. (1983). *RNA synthesis by African swine fever (ASF) virus.* (Report EUR 8466 EN, Issue.

Salguero, F. J., Gil, S., Revilla, Y., Gallardo, C., Arias, M., & Martins, C. (2008). Cytokine mRNA expression and pathological findings in pigs inoculated with African swine fever virus (E-70) deleted on A238L. *Vet Immunol Immunopathol*, *124*(1-2), 107-119. https://doi.org/10.1016/j.vetimm.2008.02.012

Samuel, C. E. (2001). Antiviral actions of interferons. *Clin Microbiol Rev*, *14*(4), 778-809, table of contents. https://doi.org/10.1128/cmr.14.4.778-809.2001

Sánchez, E. G., Quintas, A., Pérez-Núñez, D., Nogal, M., Barroso, S., Carrascosa Á, L., & Revilla, Y. (2012). African swine fever virus uses macropinocytosis to enter host cells. *PLoS Pathog*, *8*(6), e1002754. https://doi.org/10.1371/journal.ppat.1002754

Sato, M., Hata, N., Asagiri, M., Nakaya, T., Taniguchi, T., & Tanaka, N. (1998). Positive feedback regulation of type I IFN genes by the IFN-inducible transcription factor IRF-7. *FEBS Lett*, *441*(1), 106-110. https://doi.org/10.1016/s0014-5793(98)01514-2

Sato, S., Sugiyama, M., Yamamoto, M., Watanabe, Y., Kawai, T., Takeda, K., & Akira, S. (2003). Toll/IL-1 receptor domain-containing adaptor inducing IFN-beta (TRIF) associates with TNF receptor-associated factor 6 and TANK-binding kinase 1, and activates two distinct transcription factors, NF-kappa B and IFN-regulatory factor-3, in the Toll-like receptor signaling. *J Immunol*, *171*(8), 4304-4310. https://doi.org/10.4049/jimmunol.171.8.4304

Sauer, A. M., de Bruin, K. G., Ruthardt, N., Mykhaylyk, O., Plank, C., & Bräuchle, C. (2009). Dynamics of magnetic lipoplexes studied by single particle tracking in living cells. *J Control Release*, *137*(2), 136-145.

https://doi.org/10.1016/j.jconrel.2009.04.003

Schafer, S. L., Lin, R., Moore, P. A., Hiscott, J., & Pitha, P. M. (1998). Regulation of type I interferon gene expression by interferon regulatory factor-3. *J Biol Chem*, *273*(5), 2714-2720. https://doi.org/10.1074/jbc.273.5.2714

Schepis, A., Schramm, B., de Haan, C. A., & Locker, J. K. (2006). Vaccinia virus-induced microtubule-dependent cellular rearrangements. *Traffic*, *7*(3), 308-323. https://doi.org/10.1111/j.1600-0854.2005.00381.x

Schmidt, F. I., Bleck, C. K., Helenius, A., & Mercer, J. (2011). Vaccinia extracellular virions enter cells by macropinocytosis and acid-activated membrane rupture. *Embo j*, *30*(17), 3647-3661. https://doi.org/10.1038/emboj.2011.245

Schmidt, F. I., Bleck, C. K., Reh, L., Novy, K., Wollscheid, B., Helenius, A., Stahlberg, H., & Mercer, J. (2013). Vaccinia virus entry is followed by core activation and proteasome-mediated release of the immunomodulatory effector VH1 from lateral bodies. *Cell Rep*, *4*(3), 464-476. https://doi.org/10.1016/j.celrep.2013.06.028

Sharma, S., tenOever, B. R., Grandvaux, N., Zhou, G. P., Lin, R., & Hiscott, J. (2003). Triggering the interferon antiviral response through an IKK-related pathway. *Science*, *300*(5622), 1148-1151. https://doi.org/10.1126/science.1081315

Sierra, M. A., Gomez-Villamandos, J. C., Carrasco, L., Fernandez, A., Mozos, E., & Jover, A. (1991). In vivo study of hemadsorption in African swine fever virus infected cells. *Vet Pathol*, *28*(2), 178-181. https://doi.org/10.1177/030098589102800213

Sierra, M. A., Quezada, M., Fernandez, A., Carrasco, L., Gomez-Villamandos, J. C., Martin de las Mulas, J., & Sanchez-Vizcaino, J. M. (1989). Experimental African swine fever: evidence of the virus in interstitial tissues of the kidney. *Vet Pathol*, *26*(2), 173-176. https://doi.org/10.1177/030098588902600211

Silk, R. N., Bowick, G. C., Abrams, C. C., & Dixon, L. K. (2007). African swine fever virus A238L inhibitor of NF-kappaB and of calcineurin phosphatase is imported actively into the nucleus and exported by a CRM1-mediated pathway. *J Gen Virol*, *88*(Pt 2), 411-419. https://doi.org/10.1099/vir.0.82358-0

Song, F., Fux, R., Provacia, L. B., Volz, A., Eickmann, M., Becker, S., Osterhaus, A. D., Haagmans, B. L., & Sutter, G. (2013). Middle East respiratory syndrome coronavirus spike protein delivered by modified vaccinia virus Ankara efficiently induces virus-neutralizing antibodies. *J Virol*, *87*(21), 11950-11954. https://doi.org/10.1128/jvi.01672-13

Stark, G. R., Kerr, I. M., Williams, B. R., Silverman, R. H., & Schreiber, R. D. (1998). How cells respond to interferons. *Annu Rev Biochem*, *67*, 227-264. https://doi.org/10.1146/annurev.biochem.67.1.227

Stetson, D. B., & Medzhitov, R. (2006). Recognition of cytosolic DNA activates an IRF3-dependent innate immune response. *Immunity*, *24*(1), 93-103. https://doi.org/10.1016/j.immuni.2005.12.003

Stokes, G. V. (1976). High-voltage electron microscope study of the release of vaccinia virus from whole cells. *J Virol*, *18*(2), 636-643. https://doi.org/10.1128/jvi.18.2.636-643.1976

Suhara, W., Yoneyama, M., Kitabayashi, I., & Fujita, T. (2002). Direct involvement of CREB-binding protein/p300 in sequence-specific DNA binding of virus-activated interferon regulatory factor-3 holocomplex. *J Biol Chem*, *277*(25), 22304-22313. https://doi.org/10.1074/jbc.M200192200

Sun, L., Wu, J., Du, F., Chen, X., & Chen, Z. J. (2013). Cyclic GMP-AMP synthase is a cytosolic DNA sensor that activates the type I interferon pathway. *Science*, *339*(6121), 786-791. https://doi.org/10.1126/science.1232458

Sutter, G. (2020). A vital gene for modified vaccinia virus Ankara replication in human cells. *Proc Natl Acad Sci U S A*, *117*(12), 6289-6291.

https://doi.org/10.1073/pnas.2001335117

Sutter, G., & Staib, C. (2003). Vaccinia vectors as candidate vaccines: the development of modified vaccinia virus Ankara for antigen delivery. *Curr Drug Targets Infect Disord*, *3*(3), 263-271. https://doi.org/10.2174/1568005033481123

Sutter, G., Wyatt, L. S., Foley, P. L., Bennink, J. R., & Moss, B. (1994). A recombinant vector derived from the host range-restricted and highly attenuated MVA strain of vaccinia virus stimulates protective immunity in mice to influenza virus. *Vaccine*, *12*(11), 1032-1040. https://doi.org/10.1016/0264-410x(94)90341-7

Tabares, E., & Sánchez Botija, C. (1979). Synthesis of DNA in cells infected with African swine fever virus. *Arch Virol*, *61*(1-2), 49-59. https://doi.org/10.1007/bf01320591

Tait, S. W., Reid, E. B., Greaves, D. R., Wileman, T. E., & Powell, P. P. (2000). Mechanism of inactivation of NF-kappa B by a viral homologue of I kappa b alpha. Signal-induced release of i kappa b alpha results in binding of the viral homologue to NF-kappa B. *J Biol Chem*, *275*(44), 34656-34664. https://doi.org/10.1074/jbc.M000320200

Takamatsu, H. H., Denyer, M. S., Lacasta, A., Stirling, C. M., Argilaguet, J. M., Netherton, C. L., Oura, C. A., Martins, C., & Rodríguez, F. (2013). Cellular immunity in ASFV responses. *Virus Res*, *173*(1), 110-121. https://doi.org/10.1016/j.virusres.2012.11.009

Thomson, G. R., Gainaru, M. D., & Van Dellen, A. F. (1980). Experimental infection of warthos (Phacochoerus aethiopicus) with African swine fever virus. *Onderstepoort J Vet Res*, *47*(1), 19-22.

Tolonen, N., Doglio, L., Schleich, S., & Krijnse Locker, J. (2001). Vaccinia virus DNA replication occurs in endoplasmic reticulum-enclosed cytoplasmic mini-nuclei. *Mol Biol Cell*, *12*(7), 2031-2046. https://doi.org/10.1091/mbc.12.7.2031

Town, T., Jeng, D., Alexopoulou, L., Tan, J., & Flavell, R. A. (2006). Microglia recognize double-stranded RNA via TLR3. *J Immunol*, *176*(6), 3804-3812. https://doi.org/10.4049/jimmunol.176.6.3804

Volz, A., & Sutter, G. (2017). Modified Vaccinia Virus Ankara: History, Value in Basic Research, and Current Perspectives for Vaccine Development. *Adv Virus Res*, *97*, 187-243. https://doi.org/10.1016/bs.aivir.2016.07.001

Wang, X., Wu, J., Wu, Y., Chen, H., Zhang, S., Li, J., Xin, T., Jia, H., Hou, S., Jiang, Y., Zhu, H., & Guo, X. (2018). Inhibition of cGAS-STING-TBK1 signaling pathway by DP96R of ASFV China 2018/1. *Biochem Biophys Res Commun*, *506*(3), 437-443. https://doi.org/10.1016/j.bbrc.2018.10.103

Wang, Y., Kang, W., Yang, W., Zhang, J., Li, D., & Zheng, H. (2021). Structure of African Swine Fever Virus and Associated Molecular Mechanisms Underlying Infection and Immunosuppression: A Review. *Front Immunol*, *12*, 715582. https://doi.org/10.3389/fimmu.2021.715582

Watanabe, A., Tatematsu, M., Saeki, K., Shibata, S., Shime, H., Yoshimura, A., Obuse, C., Seya, T., & Matsumoto, M. (2011). Raftlin is involved in the nucleocapture complex to induce poly(I:C)-mediated TLR3 activation. *J Biol Chem*, *286*(12), 10702-10711. https://doi.org/10.1074/jbc.M110.185793

Wathelet, M. G., Lin, C. H., Parekh, B. S., Ronco, L. V., Howley, P. M., & Maniatis, T. (1998). Virus infection induces the assembly of coordinately activated transcription factors on the IFN-beta enhancer in vivo. *Mol Cell*, *1*(4), 507-518. https://doi.org/10.1016/s1097-2765(00)80051-9

Watters, T. M., Kenny, E. F., & O'Neill, L. A. (2007). Structure, function and regulation of the Toll/IL-1 receptor adaptor proteins. *Immunol Cell Biol*, *85*(6), 411-419. https://doi.org/10.1038/sj.icb.7100095

Westwood, J. C., Harris, W. J., Zwartouw, H. T., Titmuss, D. H., & Appleyard, G. (1964). STUDIES ON THE STRUCTURE OF VACCINIA VIRUS. *J Gen*

Microbiol, *34*, 67-78. https://doi.org/10.1099/00221287-34-1-67

Wolferstätter, M., Schweneker, M., Späth, M., Lukassen, S., Klingenberg, M., Brinkmann, K., Wielert, U., Lauterbach, H., Hochrein, H., Chaplin, P., Suter, M., & Hausmann, J. (2014). Recombinant modified vaccinia virus Ankara generating excess early double-stranded RNA transiently activates protein kinase R and triggers enhanced innate immune responses. *J Virol*, *88*(24), 14396-14411. https://doi.org/10.1128/jvi.02082-14

Wu, J., Sun, L., Chen, X., Du, F., Shi, H., Chen, C., & Chen, Z. J. (2013). Cyclic GMP-AMP is an endogenous second messenger in innate immune signaling by cytosolic DNA. *Science*, *339*(6121), 826-830. https://doi.org/10.1126/science.1229963

Xiang, Y., Condit, R. C., Vijaysri, S., Jacobs, B., Williams, B. R., & Silverman, R. H. (2002). Blockade of interferon induction and action by the E3L double-stranded RNA binding proteins of vaccinia virus. *J Virol*, *76*(10), 5251-5259. https://doi.org/10.1128/jvi.76.10.5251-5259.2002

Yamamoto, M., Sato, S., Hemmi, H., Hoshino, K., Kaisho, T., Sanjo, H., Takeuchi, O., Sugiyama, M., Okabe, M., Takeda, K., & Akira, S. (2003). Role of adaptor TRIF in the MyD88-independent toll-like receptor signaling pathway. *Science*, *301*(5633), 640-643. https://doi.org/10.1126/science.1087262

Yáñez, R. J., Rodríguez, J. M., Nogal, M. L., Yuste, L., Enríquez, C., Rodriguez, J. F., & Viñuela, E. (1995). Analysis of the complete nucleotide sequence of African swine fever virus. *Virology*, *208*(1), 249-278. https://doi.org/10.1006/viro.1995.1149

Yoneyama, M., Suhara, W., Fukuhara, Y., Fukuda, M., Nishida, E., & Fujita, T. (1998). Direct triggering of the type I interferon system by virus infection: activation of a transcription factor complex containing IRF-3 and CBP/p300. *Embo j*, *17*(4), 1087-1095. https://doi.org/10.1093/emboj/17.4.1087

Zanotti, C., Razzuoli, E., Crooke, H., Soule, O., Pezzoni, G., Ferraris, M., Ferrari, A., & Amadori, M. (2015). Differential Biological Activities of Swine Interferon-α Subtypes. *J Interferon Cytokine Res*, *35*(12), 990-1002. https://doi.org/10.1089/jir.2015.0076

Zhang, M., Lv, L., Luo, H., Cai, H., Yu, L., Jiang, Y., Gao, F., Tong, W., Li, L., Li, G., Zhou, Y., Tong, G., & Liu, C. (2023). The CD2v protein of African swine fever virus inhibits macrophage migration and inflammatory cytokines expression by downregulating EGR1 expression through dampening ERK1/2 activity. *Vet Res*, *54*(1), 106. https://doi.org/10.1186/s13567-023-01239-w

Zhou, X., Li, N., Luo, Y., Liu, Y., Miao, F., Chen, T., Zhang, S., Cao, P., Li, X., Tian, K., Qiu, H. J., & Hu, R. (2018). Emergence of African Swine Fever in China, 2018. *Transbound Emerg Dis*, *65*(6), 1482-1484. https://doi.org/10.1111/tbed.12989

Zsak, L., Caler, E., Lu, Z., Kutish, G. F., Neilan, J. G., & Rock, D. L. (1998). A nonessential African swine fever virus gene UK is a significant virulence determinant in domestic swine. *J Virol*, *72*(2), 1028-1035. https://doi.org/10.1128/jvi.72.2.1028-1035.1998

IX.   APPENDICES

1.   Chemicals

Chemical	Supplier
2-Propanol ≥ 99,8%	Carl Roth, Karlsruhe, Germany
Acetone	Carl Roth, Karlsruhe, Germany
Albumine, IgG-free	Sigma-Aldrich, Taufkirchen, Germany
Biozym LE agarose	Biozym, Hessisch – Oldendorf, Germany
cOMPLETE, EDTA free	Roche, Basel, Schweiz
DAPI	Thermo Fisher Scientific, Planegg, Germany
Distilled water	In-house production, Oberschleißheim, Germany
DMSO	Sigma-Aldrich, Taufkirchen, Germany
Ethanol 96%	Carl Roth, Karlsruhe, Germany
Fluoresecence Mounting Medium	Agilent Technologies, Waldbronn, Germany
GelRed Nucleic Acid Stain 10 000x	Sigma-Aldrich, Taufkirchen, Germany
Hydrochloric Acid	Carl Roth, Karlsruhe, Germany
Methanol >99,9%	Carl Roth, Karlsruhe, Germany
Neolab water bath stabilizer	Neolab, Heidelberg, Germany
Nonfat dried milk powder	PanReac AppliChem, Darmstadt, Germany
Sodium Chloride	Carl Roth, Karlsruhe, Germany
Tris-Ultrapure	PanReac AppliChem, Darmstadt, Germany
Triton-X100	Sigma-Aldrich, Taufkirchen, Germany
TrueBlue Peroxidase Substrate	Medac Diagnostika, Wedel, Germany
Trypan blue, 0.4%	Sigma-Aldrich, Taufkirchen, Germany
Tween20	Sigma-Aldrich, Taufkirchen, Germany

2.   Commercial Buffers and Solutions

Buffer/Solution	Supplier
Gel loading dye (6x), purple	New England Biolabs, Frankfurt, Germany
Tris/Acetate/EDTA (50x)	Thermo Fisher Scientific, Planegg, Germany
Tris Buffered Saline (10x)	Bio-Rad, Feldkirchen , Germany
Tris/Glycine/SDS (10x)	Bio-Rad, Feldkirchen , Germany

3.   In-house Buffers/Solutions/Agar

LB - Agar	1,5% Agar-Agar in LB-Medium
LB – Medium, pH 7.5	5 g NaCl 5 g Yeast extract 10 g Trypton ad 1l ddH2O
Lysis Buffer	1% Triton X-100 25 mM Tris 1 M NaCl
PBS (1x), pH 7.4	140 mM NaCl KCl $Na_2HPO_4 + 7H_2O$ KH_2PO_4 ad 1 l ddH$_2$O
Transfer Buffer (conc.)	24 g Tris 114,6 g Glycine ad 1l ddH$_2$O
Transfer Buffer (working solution)	80 ml Transfer buffer (conc.) 200 ml Methanol ad 1 l ddH$_2$O

4.   Enzymes, DNA and protein markers

Marker	Supplier
BamHI - HF	New England Biolabs, Frankfurt, Germany
Endo H	New England Biolabs, Frankfurt, Germany
HindIII - HF	New England Biolabs, Frankfurt, Germany
NcoI - HF	New England Biolabs, Frankfurt, Germany
NotI - HF	New England Biolabs, Frankfurt, Germany
DNA ladder, 100bp	New England Biolabs, Frankfurt, Germany
DNA ladder, 1kb	New England Biolabs, Frankfurt, Germany
PNGase F	New England Biolabs, Frankfurt, Germany
Precision plus protein dual color standards	Bio-Rad, Feldkirchen , Germany
SapI - HF	New England Biolabs, Frankfurt, Germany
T4 Ligase	New England Biolabs, Frankfurt, Germany

5.   Media and supplements for cell culture

Medium/supplement	Supplier
DMEM (high glucose)	Sigma-Aldrich, Taufkirchen, Germany
DMEM (low glucose)	Sigma-Aldrich, Taufkirchen, Germany
Fetal bovine serum	Sigma-Aldrich, Taufkirchen, Germany
HEPES solution	Sigma-Aldrich, Taufkirchen, Germany
MEM (early salts)	Sigma-Aldrich, Taufkirchen, Germany
Non-essential amino acids (100x)	Sigma-Aldrich, Taufkirchen, Germany
Opti-MEM, reduced serum medium	Thermo Fisher Scientific, Planegg, Germany
Pathogen-free chicken eggs	VALO BioMedia GmbH, Cuxhaven, Germany
RPMI-1640	Sigma-Aldrich, Taufkirchen, Germany

| Trypsin-EDTA solution | Sigma-Aldrich, Taufkirchen, Germany |

6.   Commercial Kits

Kit	Supplier
BamHI - HF	New England Biolabs, Frankfurt, Germany
Clarity^{TM} Western ECL Substrate	Bio-Rad, Feldkirchen, Germany
DNA ladder, 100bp	New England Biolabs, Frankfurt, Germany
DNA ladder, 1kb	New England Biolabs, Frankfurt, Germany
Endo H	New England Biolabs, Frankfurt, Germany
HindIII - HF	New England Biolabs, Frankfurt, Germany
Luna$^®$ Universal qPCR Mastermix	New England Biolabs, Frankfurt, Germany
Mini-PROTEAN$^®$ TGX Precast Protein Gels	Bio-Rad, Feldkirchen, Germany
NcoI - HF	New England Biolabs, Frankfurt, Germany
NotI - HF	New England Biolabs, Frankfurt, Germany
NucleoBond Xtra Midi	Machery-Nagel, Düren, Germany
PNGase F	New England Biolabs, Frankfurt, Germany
Precision plus protein dual color standards	Bio-Rad, Feldkirchen, Germany
PureYield^{TM} Plasmid Miniprep System	Promega, Walldorf, Germany
Q5$^®$ Hot Start High-Fidelity 2x Master Mix	New England Biolabs, Frankfurt, Germany
QuantiTect Reverse Transcription Kit	Qiagen, Hilden, Germany
QIAmp$^®$ DNA Mini Kit	Qiagen, Hilden, Germany
ReadyMix Taq-PCR master mix	Sigma-Aldrich, Taufkirchen, Germany
RNeasy Plus Mini Kit	Qiagen, Hilden, Germany
SapI - HF	New England Biolabs, Frankfurt, Germany
T4 Ligase	New England Biolabs, Frankfurt, Germany

Wizard® SV Gel and PCR Clean-Up System	Promega, Walldorf, Germany

7.   Consumables

Material	Supplier
6-well tissue culture plates	Sarstedt, Nümbrecht, Germany
24-well tissue culture plates	Sarstedt, Nümbrecht, Germany
Cover glasses	VWR, Ismaning, Germany
CryoPure tube	Sarstedt, Nümbrecht, Germany
Disposal bag	Sarstedt, Nümbrecht, Germany
Filter tips (20µl)	Sarstedt, Nümbrecht, Germany
Filter tips (100µl)	Sarstedt, Nümbrecht, Germany
Filter tips (200µl)	Sarstedt, Nümbrecht, Germany
Filter tips (1000µl)	Sarstedt, Nümbrecht, Germany
Multiply® reaction tubes	Sarstedt, Nümbrecht, Germany
Nitrocellulose Blotting Membrane	GE Healthcare Europe, Freiburg, Germany
SafeSeal reaction tube, 1.5ml	Sarstedt, Nümbrecht, Germany
SafeSeal reaction tube, 2ml	Sarstedt, Nümbrecht, Germany
Serological pipette, 5ml	Sarstedt, Nümbrecht, Germany
Serological pipette, 10ml	Sarstedt, Nümbrecht, Germany
Serological pipette, 20ml	Sarstedt, Nümbrecht, Germany
LABSOLUTE® slides	Th. Geyer, München, Germany
TC Flask 25	Sarstedt, Nümbrecht, Germany
TC Flask 75	Sarstedt, Nümbrecht, Germany
TC Flask 175	Sarstedt, Nümbrecht, Germany
Tube, 15ml	Sarstedt, Nümbrecht, Germany

| Tube, 50ml | Sarstedt, Nümbrecht, Germany |

8. Laboratory equipment

Laboratory equipment	Supplier
ChemiDoc™MP, Imaging System	Bio-Rad, Feldkirchen, Germany
Centrifuge 5424	Eppendorf AG, Hamburg, Germany
Mikroliterzentrifuge, Z 216 MK	Hermle Labortechnik, Wehingen, Germany
Mupid®-One electrophoresis system	Nippon Genetics EUROPE, Düren, Germany
NanoDrop Spectrophometer ND-1000	Peqlab, Erlangen, Germany
Neubauer improved counting champer	Paul Marienfeld, Lauda-Königshofen Germany
KEYENCE BZ-X710 All-in one Fluorescence Microscope	KEYENCE Deutschland GmbH, Hallbergmoos, Germany
Olympus CKX41	Olympus Life Sciences, Hamburg, Germany
Sigma 3-16L	Sigma Zentrifugen, Osterode am Harz, Germany
PeqSTAR 2X Thermocycler	Peqlab, Erlangen, Germany
Sonoplus	Bandelin electronic, Berlin, Germany

9. Software

Software	Supplier
Adobe Reader	Adobe Systems, San Jose, USA
BioRender	BioRender, Toronto, USA
DNASTAR Lasergene	DNASTAR, Inc., Wisconsin, USA
GraphPad prism	GraphPad Software, San Diego, USA
Image Lab 5.0 Software	Bio-Rad, Feldkirchen, Germany
Microsoft Office 365	Microsoft Corp., Redmond, USA

X. DANKSAGUNG

wäre das alles gar nicht möglich gewesen.

Mein Bruderherz **Alex**, vielen Dank für die „gemischtes Hack-Tasse"… Einfach unentbehrlich während dieser Zeit.

Liebe **Heike** und lieber **René** vielen lieben Dank für die vielen lustigen Momente bei gutem Essen und Wein. Nach anstrengenden Tagen und Wochen hat mir eure herzliche Art immer sehr geholfen und mir wieder die nötige Motivation gegeben. Man braucht ja schließlich Projekte…

Und das Beste kommt ja bekanntlich zum Schluss: Lieber **Christian**, du hast mich durch meine komplette Doktorandenzeit begleitet. Die ganzen Höhen und Tiefen sowie meine zugehörigen Launen sind gar nicht mehr aufzuzählen, aber ich glaube, so schnell hält jetzt nichts mehr unser gemeinsames Leben auf.